EVALUATION OF CURING COMPOUND APPLICATION TIME ON THE SURFACE DURABILITY OF CONCRETE

by

Samuel Robert Helgeson

A thesis submitted in partial fulfillment of the

requirements for the degree of

Master of Science

Civil and Environmental Engineering

at the

UNIVERSITY OF WISCONSIN-MADISON

2014

This document is hereby APPROVED as partial fulfillment of the requirements for the degree of Master of Science.

_____

Advisor's Signature

_____ _____

Advisor's Title **Date Signed**

Abstract

The Wisconsin Department of Transportation (WISDOT) has sponsored investigations on the causes of freeze-thaw scaling damage on Portland Cement Concrete (PCC) roadways within the state that are coated with membrane forming curing compounds (MFCCs). Several studies have identified excess bleed water at the time of curing compound application as a potential cause of reduced scaling resistance of concrete pavements. Increasing the delay between concrete finishing steps and MFC application should serve to lessen scaling damage. However, there is currently no literature that sought to quantify a possible linkage between MFCC application time and the scaling resistance.

The primary goal of this research was to evaluate the influence of MFCC application time on the freeze-thaw scaling damage resistance of roadway concrete made with materials native to Wisconsin. A factorial experiment was designed to probe the effect of MFCC application time on scaling damage as measured by ASTM C672. Three emulsion-based curing compounds, Linseed Oil, Wax, and Poly-alpha-methyl-styrene (PAMS) were evaluated at three application times on concrete specimens prepared with one of two sources of coarse aggregate and one of three cementitious materials. An Acrylic solvent-based sealing compound was evaluated at two application times with respect to concrete scaling resistance. Untreated specimens from each mix type were cured in a wet room and tested as controls.

A secondary goal of this project was to evaluate a new method for determining the presence of bleed water on a concrete surface by constructing a device to detect changes in the relative humidity of the air above the concrete surface over time to more reliably determine the cessation of the bleeding than current methods. To achieve this goal, a device was built and its operational capability was tested during the study.

Concrete mixes were designed and specimens were prepared according to WISDOT procedures to provide a good representation of the pavements within Wisconsin. Freeze-thaw scaling damage testing was performed on all specimens and data was recorded following the appropriate testing standard. Properties such as fresh concrete slump, air content, 28-day compressive strength, and curing compound application rates were measured and recorded to ensure compliance with WISDOT standards.

Results in this study indicate that the influence of MFCC application time on the scaling resistance of concrete is dependent upon the compound chosen. The Linseed Oil and Acrylic formulations displayed significantly increased scaling resistance with an increase in application time. The Wax and PAMS formulations did not display significant increases in scaling resistance with an increase in application time. Results from the untreated wet room cured specimens indicate that curing compounds do not promote scaling resistance levels that compare favorably to the humidity control method wet room curing. Scaling resistance was also found to be dependent upon composition of the concrete, especially with respect to the coarse aggregate and cementitious material choice. Elevated levels of ambient relative humidity at the time of specimen manufacture appeared to decrease the scaling resistance, regardless of application time. The device was found not to be reliable for monitoring the presence of bleed water in its current design. Analysis of the data collected by the device showed that future modifications could be made improve its operational capability.

Acknowledgements

I would like to thank the Wisconsin Department of Transportation (WISDOT) and the Wisconsin Highway Research Program (WHRP) for funding the research project used to generate the findings for this thesis (0092-11-05). I am truly appreciative of the opportunity and the support from those at WISDOT who provided it for me.

Thank you to Kevin McMullen at the Wisconsin Concrete Pavement Association. His support and assistance in acquiring materials for this study. I would also like to thank Andrea Breen of Lafarge North America, Inc. for generously donating the cementitious materials used within this study.

I am grateful for the assistance and support from Isabelle Girard and John Newton during the phase of my work at the Biotron facility. Thank you to Chris Worley for being accommodating and supportive during my time at the Water Science and Engineering Laboratory.

Thank you to Jake Effinger, on whose project as an undergraduate I learned how to properly mix concrete. The opportunity he gave me all those years ago set me on the path that led to this document. Thank you to Tom McAdams, Dylan Kissinger, Turner Papendieck, and Jaime Yanez Rojas for their help on this project. I hope that someday the undergraduate researchers that assist them on their thesis projects will be as excellent as they were.

A heartfelt thanks to Bill Lang and Carole Kraak at the Wisconsin Structures and Materials Testing laboratory. Their assistance and guidance ensured that this project could be successful every single day.

A sincere thank you to Ramsey Kropp for every bit of advice, professional help, new idea, and effort you provided for me during the course of this project. We're thesis people now.

Thank you to the Kropp family for the support and enduring our discussions about concrete during my residency with them.

Thank you to my thesis defense committee: Dr. Jose Pincheira, Dr. Gustavo Parra-Montesinos, and especially to my advisor Dr. Steven Cramer. I am eternally grateful for the opportunity Dr. Cramer provided me during my time working on this study. His guidance and direction motivated me to become a better critical thinker, a better scientist, better learner, and a better person for helping me raise my expectations for myself. For these reasons, and more, I am truly thankful.

Thank you to my friends and fellow researchers. Your support, wisdom, kindness, and humor is always greatly appreciated, during the best of times, and the blurst of times.

To my parents, Bob and Joanne Helgeson, and to my family: thank you. I owe everything to you. You mean the world to me. Your unconditional love and support gives me the strength to conquer the challenges that every new day brings, and the perspective to appreciate the road I've travelled. Thank you.

Table of Contents

List of Figures

List of Tables

Chapter 1 Introduction

1.1 Significance

The desire to build and maintain Portland Cement Concrete (PCC) roadways that are both weather resistant and economic to construct has led the Wisconsin Department of Transportation (WISDOT) to sponsor investigations on the causes and remedies for freeze-thaw scaling damage in PCC roadways in Wisconsin. Scaling is a form of surface damage that occurs within the layer of concrete immediately exposed to such weathering factors as seasonal freeze/thaw cycling, deicing salt use, and vehicular traffic. This type of damage is visually evident, where the top ¼" layer of mortar of the PCC surface degrades and eventually separates to expose the aggregates that make up the bulk of the concrete. This premature failure of the concrete surface can accelerate the degradation of the bulk concrete, eventually exposing reinforcing steel to corrosive fluids, and resulting in a reduction of the performance lifetime of the concrete pavement.

Proper curing is necessary for the development of a durable concrete surface layer that is resistant to scaling damage. This requires the presence of enough chemically available water to fully hydrate the cementitious materials within the surface region. However, excess water beyond what is necessary for full hydration can become trapped within the concrete surface microstructure during curing, which can ultimately reduce the durability of the exposed concrete surface.

WISDOT statutory requirements for workability require concrete pavements to be made with a water-to-cement (w/c) by mass ratio of no lower than 0.40, despite the recognized fact that full hydration of the cementitious materials occurs at lower ratios (Taylor 1997). This additional water that does not chemically react will migrate upwards towards the fresh concrete surface as a result of particle settlement; a process called bleeding. Bleed water will form a thin, visible layer

upon the surface of the fresh concrete shortly after placement, where it will evaporate under most environmental conditions.

Scaling commonly occurs in environments where traditional PCC curing methods, such as techniques that employ evaporative and humidity controls, are not feasible. In lieu of these techniques, WISDOT requires that contractors constructing new PCC roadways or overlays to use white pigmented membrane forming curing compounds (MFCC). These compounds are sprayed onto a fresh concrete surface with the intention on providing a continuous hydrophobic membrane that prevents the evaporation of chemically available water at the exposed surface. This is to ensure that there is enough water within the concrete surface to properly cure.

However, it is thought that excess water including bleed water will also become trapped within the concrete surface when the MFCC is applied; potentially reducing the exposed surface's durability. In order to fully form a protective membrane for proper curing, both curing compound manufacturers and the American Concrete Institute (ACI) instruct concrete pavers to apply MFCCs after bleeding has ceased and the surface is free of visible bleed water (ACI Committee 308, 2001). Implementation of this recommendation can be complicated by both highly evaporative conditions and the time length of bleeding, which can result in the concrete surface appearing to be free of bleed water prior to the termination of the bleeding process.

Within recent years, WISDOT has experienced scaling in many PCC roadway and overlay applications despite the use of these MFCCs. It is thought that the application time of MFCCs, especially prior to bleeding cessation, is related to the increased scaling damage observed in these PCC pavements. Despite the ACI recommendation that suggests possible linkages between MFCC application time and concrete durability, there has been no research to date that evaluates a possible relationship. Therefore, the purpose of the research presented here is to evaluate a potential relationship between MFCC application time and concrete scaling resistance.

1.2 Hypothesis

Currently, the impact of MFCC application time on the scaling resistance of PCC pavement has not been evaluated. The primary hypothesis of this research is:

- A Portland cement concrete pavement will suffer more freeze-thaw scaling damage the sooner a curing compound is applied after concrete placement.

This is thought to be the result of two potential factors:

1) Upon application, the MFCC traps within the concrete surface layer excess bleed water. This ultimately reduces the scaling resistance through detrimental changes to the microstructure of the exposed concrete surface.
2) The MFCC in liquid form may be less dense than the bleed water present upon the surface of the concrete. When applied, the MFCC may float on top of the bleed water, resulting in a disassociation of the membrane prior to formation. This prevents the membrane from fully retaining water necessary for curing, which reduces the durability of the concrete surface.

It is thought that because concrete bleeding is a time-dependent process, the scaling resistance of MFCC-coated concrete can be evaluated at application times that correspond to three distinct phases of the bleeding process: during the bleeding phase, after bleeding has stopped and bleed water is no longer present upon the surface, and an intermediate time when the progress of bleeding is unknown. The primary goal of this research was to evaluate the impact that the application time of MFCCs have on the scaling resistance of concretes with materials native to Wisconsin.

The current procedure for determining the termination of the concrete bleeding process by visual inspection is subjective and susceptible to error as a result of environmental conditions. Bleed water is removed from the concrete surface by evaporation. Therefore the secondary hypothesis for this research is:

- An instrument can be developed to reliably detect the presence of bleed water by evaluating changes in relative humidity immediately above the concrete surface over time.

A secondary goal of this research was to evaluate the operational potential of such as device by detecting changes in the relative humidity of the air above a bleeding concrete surface.

1.3 Objectives

This project was funded through the Wisconsin Department of Transportation as part of the Wisconsin Highway Research Program. The primary goal of this research was to evaluate the impact that the application time of MFCC's have on the scaling resistance for PCC pavements containing Wisconsin component materials. This project was broken down into five main tasks:

Task 1: Evaluate current literature on MFCCs, scaling damage, concrete bleeding, and surface microstructural behavior; identifying any relationships or properties that might be useful when crafting the mix matrix and data analysis.

Task 2: Characterize the concrete materials and curing compounds used in this study. This included evaluating the gradation, absorption, percentage of fines, and the air content adjustment factor of the aggregates used within this project.

Task 3: Collect data following the experimental outline of the mix matrix. This included evaluating properties of the fresh concrete such as slump and air content, 28 day

compressive strength, application rate of curing compound, and scaling severity in accordance with the ASTM C672 testing standard.

Task 4: Construct and investigate a thermohygrometer apparatus in an effort to indirectly detect the termination of the bleeding process using relationships between the ambient relative humidity and the relative humidity immediately above the exposed surface of fresh concrete.

Task 5: Complete a statistical analysis of the relevant data, focusing on identifying patterns within the scaling material data.

Analysis of all the relevant data collected in Tasks 1 through 5 was conducted to quantify their effectiveness at evaluating the hypothesis, and therefore the ultimate goal of this research. This evaluation was performed in order to help improve best practices for contractors and WISDOT affiliated organizations associated with the construction and maintenance of MFCC-coated PCC pavements.

1.4 Scope

The main focus of this research is on the freeze-thaw scaling resistance of specimens representing Wisconsin concrete pavements treated with curing compounds. All materials used in the manufacturing of the concrete specimens studied are representative of materials used in PCC pavement projects within Wisconsin. All mix designs used in the manufacturing of the concrete specimens studied within this project were in accordance with the Wisconsin Department of Transportation Grade A, Grade A-S, and Grade A-F mix designs listed in the WISDOT Standard Specifications (WISDOT 2013). Within the specimen manufacture mix matrix, the primary factor separating the mix types was the coarse aggregate; followed by the secondary factor of cementitious material used (Table A-1). Two coarse aggregate types, representative of geology

found in the Northern and Southern regions of Wisconsin were chosen. In addition, one fine aggregate source was used. Finally, three cementitious materials conditions were used: ordinary Portland cement (OPC), OPC and Ground Granulated Blast Furnace Slag (referred to as slag cement or slag), and OPC with Class C Fly Ash. This resulted in a total of six total concrete mix types. All mix types included one brand of air entrainment agent and one brand of water reducer. Chapter 3 contains more detail on both the aggregates used and the mix design.

To evaluate the effect of MFCC application time on scaling resistance, five curing conditions were studied in this research: three curing compounds, one sealing compound, and one untreated, wet room cured condition. Despite differences between sealing and curing compounds, they are all referred to as curing compounds for consistency within this document. Two application times were used for all concrete specimens within this study, 30 Minutes and 4 Hours. At the behest of the funding agency, the agreed upon work plan included a third application time of 2 Hours for three of the compounds only on mixes containing OPC or slag cement. These three times corresponded to stages of the bleeding process: 30 Minutes to represent a time when bleeding was occurring, 4 Hours to represent where both the bleeding process had ended and bleed water was no longer present, and 2 Hours to represent where the bleeding progress was unknown. In total, 66 total mix type-curing compound-application time treatments were evaluated according to ASTM C672 for scaling resistance to assess the hypothesis.

A thermohygrometer apparatus was designed, built, and an operational procedure was developed to assess the feasibility of the secondary goal of this project. The design and operation are presented in further detail in Section 3.6.

Chapter 2 Literature Review

2.1 Membrane Forming Curing Compounds

The curing environments of concrete structures immediately after placement have been known to harbor great impacts on the development of strength, durability, freeze-thaw scaling damage resistance, permeability, aesthetic appearance, and other important properties of the concrete. For high surface area-to-volume structures such as roadway slabs, great efforts must be taken to ensure that the concrete has an adequate curing environment to develop its desired qualities. The fresh concrete comprising these structures is typically poured when exposure to highly evaporative conditions such as solar radiation, wind, high temperature, and low relative humidity are unavoidable due to the seasonal nature of construction. Traditionally, promoting ideal curing environments for exposed fresh concrete surfaces involved labor and time intensive practices such as ponding or covering up with damp burlap (Vandenbossche, 1999). This was necessary to ensure the concrete mix water required for hydration of the cement binder was not exposed to highly evaporative environmental conditions.

Membrane forming curing compounds (MFCCs) were developed to create a similarly effective evaporative barrier that could be sprayed quickly over large swaths of the exposed surface, reducing the labor and time required of previous methods. These compounds typically are solutions containing a solid fraction suspended in a water carrier or an organic solvent. Upon placement, the water or solvent fraction evaporates, depositing the solid fraction on the concrete surface that forms the membrane (Vandenbossche, 1999). If applied properly, curing compounds provide an even, uninterrupted physical membrane that prevents the egress of mix water during curing and the ingress of external chemicals like deicers. Many state DOTs require pigmentation of the MFCCs used on

roadway projects, as they provide the additional benefits of increasing solar radiation reflectance and boosting the aesthetic quality of the surface (Vandenbossche, 1999).

The effectiveness of a curing compound is governed by the integrity of the membrane it forms. Several factors can impact the integrity of the membrane: the quality of the curing compound material (Choi et al., 2012), the amount applied, the application time, the curing compound selected (Kropp et al., 2012), the surface texture (Vandenbossche, 1999), concrete bleeding (Jana, 2007), and environmental conditions (Ye, Shon, Mukhopadhyay, & Zollinger, 2010). Many of these factors can be introduced when poor application procedures are used. American Concrete Institute recommendations stipulate that the optimum time to apply MFCCs is after final finishing, when the concrete surface is free of bleed water (ACI Comittee 308, 2001). This guidance is complicated by evaporative conditions that when too high can prematurely signal the end of bleeding; or when too low extend the period that water appears on the surface. The former condition has been particularly troublesome, as multiple studies have noted that pinholes and cracks can form in the membrane as bleed water can segregates the freshly placed curing compound (Valenza II & Scherer, 2007b; Vandenbossche, 1999). Current application procedures outlined in WISDOT Standard Specification do not provide guidance on how to accurately measure compliance with minimum spray rates (WISDOT 2013). As a result, application has been controlled by subjective visual inspection. If spray nozzle patterns are adequately positioned (Vandenbossche, 1999) and flow rates accurately measured, application rates can be easily obtained as a function of the application cart speed, removing the subjectivity of the operator (Choi et al., 2012). The membrane integrity can also be improved if the application carts have adequate wind shielding to prevent loss of material during application (Vandenbossche 1999; Choi et al. 2012). Moisture retention is an important function of an MFCC, as adequate moisture is required for proper strength and durability development in the concrete surface layer. However, studies have cast doubt on the effectiveness of the current ASTM C 156 procedure

for evaluating the moisture retention of MFCCs and its accuracy for use on actual concrete surfaces (Vandenbossche, 1999; Ye et al., 2010).

2.2 Concrete Surface Formation and Microstructure

The complex chemical and physical behaviors of concrete during the initial curing period have been studied in great detail. The most important process during the curing of concrete is the chemical hydration reaction of the Portland cement in the presence of water. While many hydration reactions occur due to the complexity of Portland cement (H. F. W. Taylor, 1997), the two that are most attributed towards the creation and hardening of the paste that binds the constitutive parts of concrete are the hydration of tricalcium silicate ($3CaO•SiO_2$, or C_3S) and dicalcium silicate ($2CaO•SiO_2$, or C_2S) with water (H_2O) (Mamlouk, 2006); shown as equations (1) and (2) respectively.

$$2C_3S + 6H_2O \rightarrow 3C\text{-}S\text{-}H + 3CH \quad \textbf{(1)}$$

$$2C_2S + 4H_2O \rightarrow 3C\text{-}S\text{-}H + CH \quad \textbf{(2)}$$

The products of these hydration reactions are calcium silicate hydrate ($CaO•SiO_2•3H_2O$, or CSH) and calcium hydroxide ($Ca(OH)_2$, or CH). CSH gel formation is very important not only for its strength and binding properties, but the physical structure of the paste itself can greatly impact the chemical resistance and durability of the concrete surface. To develop an adequate CSH gel network, both of these reactions need water as shown in the hydration equations. This should be provided by proper mix design and adequate curing.

Historically, water-to-cement mass ratio (w/c) has been the primary characteristic of concrete mixtures for balancing concerns of strength, durability, and workability (Abrams, 1920). A (w/c) of

between 0.38-0.42 is thought to be the critical value by which complete hydration can occur without additional water being added during the curing process (Bentz and Stutzman 2006; Taylor 1997). For concrete such as those coated with MFCCs, controlling this ratio is of critical importance in mix design because water is not added during the curing process. Low (w/c) ratios correspond with concretes that have higher strengths (Abrams, 1920), but concerns about fresh concrete workability and drying shrinkage typically require pavement projects to have a (w/c) no lower than 0.4 (Nassif et al., 2003). Chemical admixtures such as water reducers or superplasticizers can be added to improve the workability of fresh concrete without increasing the (w/c) ratio (Valenza & Scherer, 2006).

A fully mature hardened concrete surface requires time for the hydration of the CSH gel layer to form in the presence of enough hydraulically active water. The microstructural development of this layer determines the strength and durability properties of the exposed concrete surface (Snyder & Bentz, 2004). Immediately after placement, the concrete paste can be thought of as a suspension of rigid particles in water (Bentz, 2008). Solid particles such as coarse cement particles, fine and coarse aggregates will migrate towards the bottom of the concrete due to gravity, while mix water will rise, referred to as bleeding once it reaches the surface (Radocea, 1992). Gradients develop within depth of the concrete, with the top layer characterized by a lower density, higher (w/c), and a coarser capillary pore network that is initially filled with water (Bentz, 2008). The ultimate purpose of hydration is to connect the original cement particles into as strong a network of hardened CSH as possible, while disconnecting these original water-filled capillary pores (Bentz and Stutzman 2006). Water is from of the capillary pores during hydration, ultimately hardening into a porous solid of CSH paste combined with aggregates. Autogenous shrinking of the paste occurs as the hydration products occupy less volume than the water consumed during the reactions. While this shrinkage can reduce the size, coarseness, and interconnectivity of the capillary pore network, it can also lead to tensile stresses that eventually result in cracking that reconnect the capillary pore network. If pore space where water was

pulled from empties, the pore becomes a void; which in tandem with resulting nearby unhydrated cement particles, reduces the strength, durability, and density of the surface layer by a process called self-desiccation (Bentz, 2008). The porosity of the hardened paste is ultimately responsible for how permeable the surface is. Decreasing the (w/c) ratio results in poor pore network connectivity, which greatly reduces the permeability and increases the durability of the paste (Bentz and Stutzman 2006). In the introduction of aggregates, both coarse and fine, reduces the paste strength by increasing the porosity by two means: increasing the diameters of the capillary pores (Winslow & Liu, 1990), and the entrapment of voids around the aggregates by 'honeycombing' (Jana, 2007). All sources of porosity can increase the level of permeability, which is a determinant of how resistant the concrete is to ingress of aggressive agents. This ultimately determines the durability of the concrete surface (Song & Kwon, 2007).

2.3 Concrete Bleeding

Bleeding of concrete is an important process that has effects on the microstructural development of the surface layer, and the construction processes of concrete. Research on the subject of concrete bleeding has determined that the primary properties of concrete bleeding are the rate and the total amount of accumulated bleed water. There are many factors that influence these properties: water content of the mix, fineness of the cementing materials,(Radocea, 1992) slab thickness, retarding admixtures, (Jana, 2007) aggregate absorption, aggregate fines, (Topçu & Elgün, 2004) air entrainment, cement composition, and the use of supplementary cementitious materials (SCMs) such as ground granulated blast furnace slag cement or fly ash (Valenza II & Scherer, 2007b). Increased bleeding can reduce surface strength, increase permeability, and delay the onset of finishing operations; while decreased bleeding can increase plastic shrinkage and poor surface hydration (Topçu & Elgün, 2004). These issues related to bleeding have inspired research into identifying the factors that impact bleeding.

Bleeding is a time dependent process, with the highest rates of bleeding in OPC concrete typically occurring early within the first 30 minutes after placement, followed by a steady decline in the rate over the following hour as the concrete begins to harden (Josserand 2004; Josserand et al., 2006). The use of slag and fly ash can result in an increase in the total amount of bleed water by bleeding for longer than typical OPC concrete (Afrani & Rogers, 1994; Wainwright & Rey, 2000). It is hypothesized that this is due to the SCMs requiring longer hydration times that extend the time to initial set, or that water demand is a function of the amount of cement rather than cement plus SCM content; leading to more bleeding in SCM concretes (Valenza II & Scherer, 2007b). Entrained air bubbles used for freeze/thaw resistance reduce bleeding in the paste by adhering to cement particles, preventing downward settlement by increasing buoyancy. The cement particles hydrate and form a hardened network that blocks bleeding channels, reducing the ultimate bleeding amount (Valenza II & Scherer, 2007b).

Construction practices are impacted by a concrete's bleeding behavior. This manifests itself in the ACI guidance for finishing and MFCC use as stated previously. The evaporative environment can mask when the true cessation of bleeding occurs. A reduction in the relative humidity from 80% to 50% can lead to an increase in evaporation of 100%; while increasing the wind speed can increase the evaporation nearly 200% (Topçu & Elgün, 2004). Finishing prior to the cessation of bleeding increases the amount of water in the surface of the paste, which reduces the strength and durability by changing the increasing the (w/c) ratio and microstructure of the gel and air void network as it matures (P. C. Taylor et al. 2004; Bouzoubaâ et al. 2008). This increase in (w/c) ratio of the paste is also thought to occur when curing compounds are applied early, despite the disassociation of the membrane discussed previously (Ye et al., 2010). Because both ACI and WISDOT offer guidance on the construction practices in response to bleeding, determining when bleeding is over along with the absence of bleed water on the surface of the concrete is an important objective for concrete projects.

ASTM C232 is a standardized test for evaluating the amount of mix water that will bleed. However, studies have shown that this standard correlates poorly with the actual bleeding behavior of concrete (Choi et al., 2012) and that it does not account for environmental evaporative conditions even when the ACI-issued nomograph for evaporation conditions is used (Uno, 1998). While several proposed methods show promising results at offering a replacement, practical problems exists within their procedures for implementation on construction sites (Radocea 1992; Josserand et al. 2006; Ye et al. 2010; Choi et al. 2012).

2.4 Concrete Scaling Damage

Concrete surfaces with poor durability that are subjected to freezing and thawing cycles often experience scaling damage when subjected to deicing chemicals. Concrete Scaling is defined by as 'local flaking or peeling away of the near-surface portion of hardened concrete or mortar' (ACI Comittee 308, 2001). Severity of scaling is often identified by visual inspection of the removal of mortar that exposes the near-surface aggregates; or by measuring the depth and mass of the lost material. Extensive research of scaling behavior has revealed that at nearly every stage of concrete's lifecycle and every constitutive part of the designed mix has an impact on the scaling resistance of the concrete. The nature of scaling damage is primarily superficial in that it does not immediately impact the mechanical properties of the bulk concrete. However, the progressive damage accumulation deepens the removed surface, which increases the susceptibility of further chemical ingress into the bulk concrete. This can eventually reduce the strength and stiffness through conventional frost action and expose steel reinforcement to harmful oxidizing chemicals; resulting in a reduced lifespan of the structure (Valenza II & Scherer, 2007b).

In order for concrete freeze-thaw scaling to occur, several conditions must be met prior to accounting for the actual composition and durability of the concrete itself. The first is that water with deicing chemicals must pool on the concrete surface (Valenza II & Scherer, 2007b). Second, no

scaling damage will occur if the minimum temperature is higher than -10°C (14°F) (Valenza II & Scherer, 2007a). Most importantly, scaling damage only occurs when the concentration of the deicing chemical within the pooled water is approximately 3% by mass of the total solution; an amount called the pessimum concentration (Verbeck & Klieger, 1957). The widely adopted Glue Spall method was developed by Valenza and Scherer to explain both the mechanism of scaling and the purpose of the requirement of the pessimum concentration (2006). As pooled water with deicer freezes on a concrete surface, a mechanical bond forms between the layer of ice and the concrete. As the temperature drops further, the thermally expanding ice will crack where there are pockets of deicing brine that weaken the ice. Because the bond between the ice and the roughened concrete surface is stronger than the concrete itself, the crack in the ice will penetrate into the concrete layer (Çopuroğlu & Schlangen, 2008). In successive cycles, the brine that occupies the crack in the concrete will pull out pore water, diluting the solution and allow for further cracking to develop as ice forms. Once the crack reaches the top layer of coarse aggregate, the crack will propagate approximately parallel to the surface of the concrete due to the poor bond between the mortar layer and coarse aggregate at the interfacial transition zone (ITZ) (Ollivier et al., 1995). Similarly-propagating cracks will eventually weaken ITZ bond due to thermal stresses, resulting in the layer removal referred to as scaling (Valenza & Scherer, 2006). The Glue Spall theory uses the strength of the ice to explain the existence of the pessimum concentration, regardless of what deicer is used. Pooled solutions of pure water or less than 3% deicer do not cause scaling because the ice layer is too strong for cracks to form with the ice. For solutions with concentrations higher than 5%, the ice is typically too soft to bond with the concrete and develop fracturing stresses during thermal expansion (Sun & Scherer, 2010; Valenza & Scherer, 2006; Wu, Shi, Gao, Wang, & Cao, 2014). If the depth of the ice layer is large, the tensile cracking forces transferred into the concrete surface are larger, resulting in higher cracking stresses within the concrete surface layer (Çopuroğlu & Schlangen, 2008).

2.5 Scaling Damage Resistance of Concrete

Scaling resistant concrete requires a surface microstructure that is strong, air entrained, and with low permeability. Proper air entrainment is critical for increasing scaling resistance. As the temperature drops, pore water migrates towards entrained air voids where ice nucleation can occur. This has the dual effect of preventing frost action damage due to pore water expansion in the pore network, while also contracting the bulk mortar layer; counteracting the expansive stresses from the bonded ice layer that would result in Glue Spall cracking (Sun & Scherer, 2010; Valenza II & Scherer, 2007b). Air voids should typically be less than 300 μm in diameter, and spaced properly for scaling resistance. A critical spacing factor for air voids in the mortar layer has been identified to correspond well with scaling resistance. Scaling mass loss is roughly proportional to the amount the spacing factor between air voids exceeds the critical amount (Valenza II & Scherer, 2007b). While it has been determined that the compressive and tensile strength of the bulk concrete has little impact on the scaling resistance, (Afrani & Rogers, 1994) it is recommended that the concrete be matured to at least 4000 PSI prior to first exposure of deicing salts (Jana, 2007). A lower (w/c) ratio corresponds with decreased porosity and increased strength, resulting in a more durable surface. At a (w/c) ratio of 0.3, it has been found that no air entrainment in the mortar layer is necessary to prevent scaling due to the density of the microstructure (Valenza II & Scherer, 2007a, 2007b).

Aggregate and SCM use can impact the scaling resistance of concrete. The use of slag or fly ash can result in poor microstructural development by hindering the concrete's ability to entrain air and retain adequate spacing factors between air voids; resulting in increased permeability and scaling susceptibility (Giergiczny, Glinicki, Sokołowski, & Zielinski, 2009; Valenza II & Scherer, 2007b). Carbonation of hydration products in concretes containing slag can destabilize the fresh CSH, ultimately reducing the scaling resistance (Battaglia et al.2010). Aggregates that have high porosity, high absorption, and low moduli of elasticity are particularly susceptible to aggregate popout scaling,

especially when critically saturated as a result of high permeability of the mortar paste. Aggregate popout is a form of scaling where the aggregate underlying the paste fractures due to thermal expansion when saturated with absorbed water during freezing. This results in upwards crack propagation, towards the concrete surface, resulting in localized scaling immediately above the fractured aggregate (Jana, 2007).

There is limited research on the impact that curing compound use has on the ultimate scaling resistance of concrete. Previous research showed that curing compound use results in less scaling resistant concretes when compared to wet burlap or other moist curing methods (Kropp et al. 2012). In addition, curing compounds delayed the onset of scaling damage only slightly, with significant mass loss occurring after only 5 freeze/thaw cycles. It was also hypothesized that the use of curing compounds exacerbated scaling damage by having a stronger bond to the concrete surface than the surface to the bulk concrete. As localized flakes of mortar scaled off, unscaled mortar sections connected to those flakes by the curing compound bond scaled off too due to the compound bond being stronger than the mortar-aggregate bond (Afrani & Rogers, 1994; Jana, 2007). It has been postulated that the application of curing compounds prior to cessation of bleeding can result in a concrete surface that is less scale resistant due to the moisture retained by the curing compound resulting in decreased microstructural properties (Taylor et al. 2004).

ASTM C672 is the standard testing procedure for concrete scaling. This is done by pooling a ¼" layer of 4% by weight sodium chloride (NaCl) and water solution on a concrete surface, subjecting it to freezing and thawing cycles, and measuring the cumulative mass lost by sieve collection and subjective visual inspection. There is significant concern that this testing procedure is inadequate for reproducing accurate and repeatable scaling results between laboratory samples and in-situ slabs. The consensus is that the ASTM C672 procedure significantly overestimates the amount of damage that occurs in laboratory specimens due to the aggressive ponding of water required for the

test (Boyd & Hooton, 2007; Valenza II & Scherer, 2007b). In addition, the visual rating system outlined in ASTM C 672 introduces unacceptable inter-operator variability due to its subjective nature (Taylor et al. 2004; Valenza II and Scherer 2007a; Bouzoubaâ et al. 2008).

Chapter 3 Materials, Methods and Testing Procedures

3.1 Concrete Materials

The concrete tested within this study was prepared following the guidelines of the WISDOT Concrete Grades A, A-FA and A-S for concrete pavements containing cementitious materials consisting of either Ordinary Portland Cement (OPC, and a blend of either OPC and Class C Fly Ash (FA) or Grade 100 Ground Granulated Blast Furnace Slag (GGBFS), respectively. For each mix, the total cementitious material content was 565 lbs/yd^3. In addition to the cementitious material, a coarse aggregate fraction and fine aggregate fraction were used with Madison Municipal tap water for all mixes. A water to cementitious materials ratio (w/c) of 0.40 was used for all mix types, except for three batches of Mix Type 4 where a (w/c) of 0.41 was used to improve workability. The mix designs are provided in Appendix D. Two chemical admixtures were added to each mix: a Low range water reducing agent (WRA) was used to meet the slump requirement of 3±1 inch and an Air Entrainment Agent (AEA) to meet the entrained air requirement of 6±1% (WISDOT 2013).

Two types of coarse aggregate were used to reflect the varying geology of aggregates used in concrete pavements throughout Wisconsin. The first aggregate was a crushed limestone from Waukesha County in the Southeastern part of the state; while the second was a glacial gravel from Eau Claire County. The crushed limestone was angular, homogenous in particle composition, and had an approximate 2:1 to 2.5:1 length to width ratio. The glacial gravel was smoother and rounder, with more particles having a 1:1 length to width ratio. The gravel contained several mineral types and was dustier than the limestone based upon visual observation. Despite this, both aggregates met the WISDOT Standard Specifications for gradation sizes, P200 content, and absorption (WISDOT 2013).

Table 3-1: Coarse Aggregate Properties

Coarse Aggregate Type	Specific Gravity	Absorption	P200
Glacial Gravel	2.658	0.94%	0.50%
Limestone	2.712	1.51%	0.20%

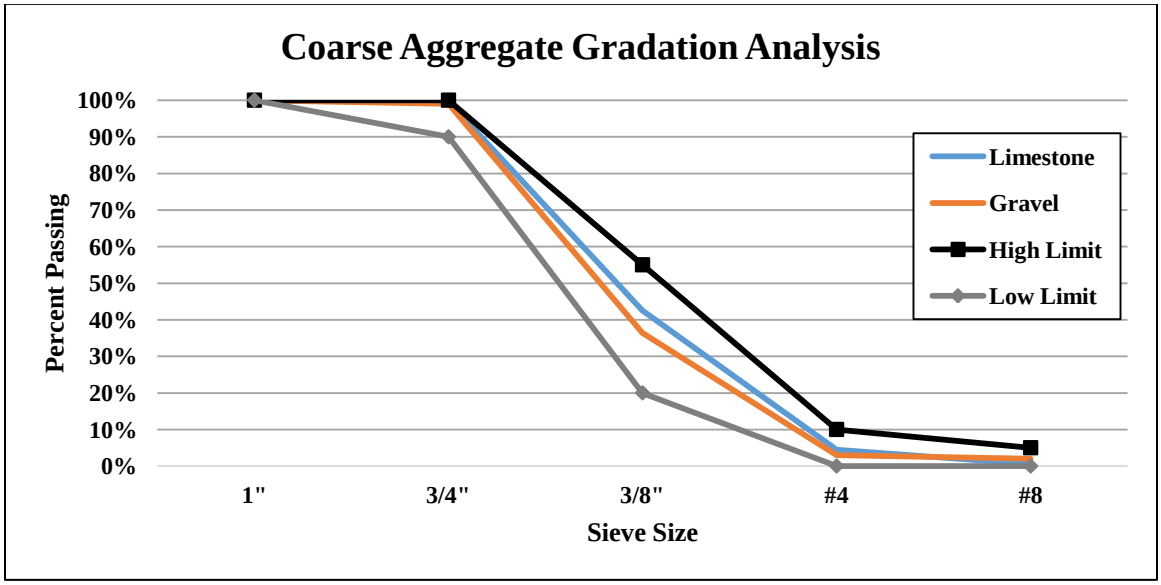

Figure 3-1: Coarse Aggregate Sieve Analysis

A single fine aggregate source from Southern Wisconsin was used for all mixes. It met the WISDOT specifications for gradation, P200 content, and absorption.

Table 3-2: Fine Aggregate Properties

Fine Aggregate Type	Absorption	P200
Sand 1	0.19%	1.17%

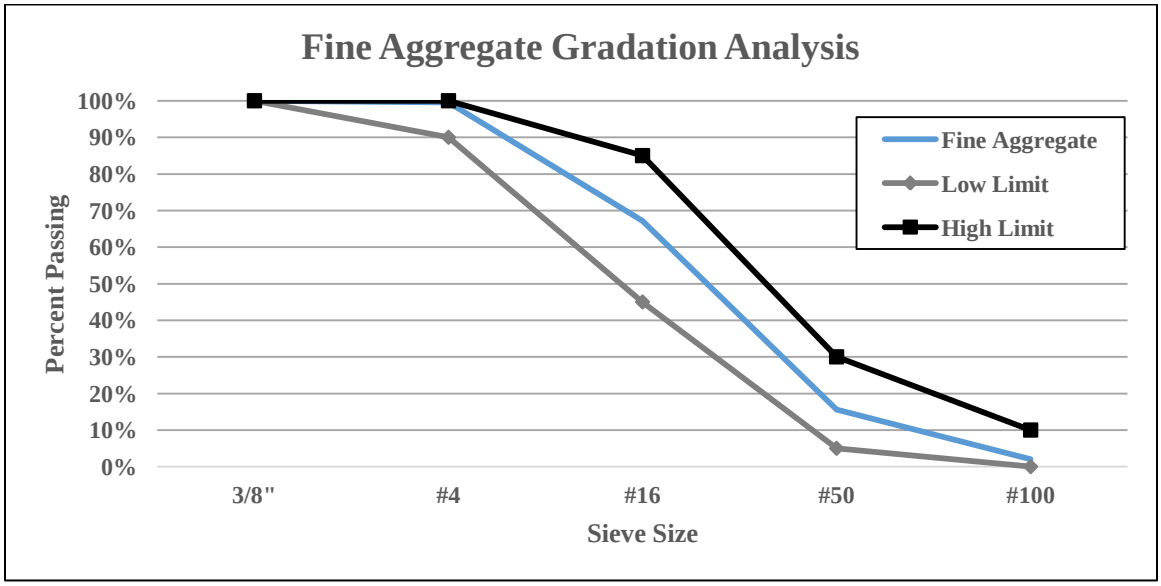

Figure 3-2: Fine Aggregate Sieve Analysis

3.2 Specimen Molds

ASTM C672 requires at least 72 in^2 of exposed concrete surface, with a specimen depth of at least 3 inches. The molds used to fabricate these specimens were created using 12 inch inner diameter Schedule 40 PVC pipe sections, cut into three inch segments. These segments were adhered to a melamine coated particle board with polyurethane construction adhesive. These proved to be durable, reusable, non-absorbent, they allowed for a smooth strike off surface, produced uniformly-sized specimens, and easy to remove with air pressure applied to the non-testing side. Prior to mixing, each mold was coated lightly with a mold release agent to aid in the demolding process.

3.3 Methods

3.3.1 Mixing Procedure and Fresh Concrete Tests

A rotary drum mixer located within a temperature controlled, humidity monitored laboratory environment was used to mix all concrete for this project following the protocol set in ASTM C192. Prior to batches that were used to pour specimens, a butter batch of the same mix components but totaling a concrete volume of 0.66 ft^3 was used to coat the inside of the mixture to prevent concrete loss and to test the slump and air content following the ASTM test protocols C143 and C231 respectively. Calibration of the air content pressure meter was performed with each coarse and fine aggregate mixture to calculate the Air Correction Factor following the procedure in Item 6 of ASTM C143. These are listed in Table 3-3.

Table 3-3: Air Content Correction Factor for Mixes

	Gravel and Sand	Limestone and Sand
Air Content Correction Factor	1.2%	1.1%

Each batch where specimens were poured from were either 2.7 ft^3 or 2.0 ft^3 in volume to allow for the slump, air content test, three 4”x8” compressive strength cylinders, one 3”x4”x16” prism for the ARCHERS test, and nine or six ASTM C672 specimens, respectively. These batches were large so as to ensure that the slump and air content test concrete was not used in specimen manufacture; and that there was additional concrete remaining.

The coarse and fine aggregates were dried in an oven on the day prior to mixing, and portioned out by weight after enough time had passed to allow them to cool to room temperature while covered. The cementitious materials were also weighed out prior to mixing. All mixing tools including the rotary drum were sprayed with water prior to mixing. Recordings of the laboratory

temperature and relative humidity were taken before proceeding with the mix. The batch was weighed out and split into two buckets, so that the WRA and AEA could be dispersed among the batch water independent of one another. The coarse and fine aggregates were added to the rotary mixer; then the water bucket containing the WRA was added. The mixer was turned on, then immediately the cementitious materials were added followed by the remaining water. The concrete mixed for three minutes, then the mixer was stopped for three minutes and covered to prevent evaporation. The mixer was turned on for an additional two minutes, then poured in to a wheelbarrow. Any excess concrete remaining in the mixer was scraped out into the wheelbarrow, where it was mixed for 30 seconds with a hand scoop. The slump and the air content of the fresh concrete were then determined by ASTM C-143 and C-231 respectively. After evaluating that both of these fresh concrete tests fell within their acceptable limits as set out by WISDOT; specimen manufacture began.

The specimen molds were filled by scoop in one layer, and were rodded once per ever two square inches of specimen surface area on the exposed side, per ASTM C-672. The sides of the mold were then tapped with a rubber mallet fifteen times to ensure adequate consolidation; followed by a troweling of the surrounding mold walls to prevent adherence to the wall surface during demolding. Finally, a wood strike off board was used to screed the surface of each mold, using between 12-15 passes in order to ensure a surface level with the height of the mold walls. Once each ASTM C672 specimen was made, three 4” diameter by 8” height 28-day compression cylinders were made using the remaining concrete in accordance with ASTM C192.

3.3.2 Curing Compound Application

Curing compounds were applied for each mix type at three separate times after this screeding effort was complete; unless otherwise noted: 30 minutes, two hours, and four hours. Three replicate specimens for each curing compound application time for each mix type, for a total of nine specimens per batch were made. The curing compounds were sprayed on the specimens using handheld

pressurized nozzle sprayers with the ability to provide even coverage over the specimen. The specimens were placed on an electronic digital scale capable of 0.1 g accuracy. Alternating perpendicular passes over the specimens were used to ensure an even coating of the entire specimen surface. A wooden mask was used to prevent overspray of the mold wall and base. Each specimen was coated with an amount of curing compound as close to the manufacturers recommended spray rate, as is noted in the WISDOT Standard Specifications. Care was taken to ensure that each specimen's surface condition was not disturbed when moving to and from the curing location within the laboratory and the digital scale.

3.3.3 Specimen Preparation

Each specimen was cured for 24 hours in laboratory air, then demolded and labeled. After demolding, each specimen had a 10" inner diameter PVC dam of one inch in height affixed to the sprayed surface with polyurethane construction adhesive. Following the curing time for the construction adhesive, a two part low modulus/low-viscosity sealing epoxy was applied to the non-testing surfaces of the specimens. Once the epoxy had hardened, the edges between the PVC dam and the outside rim of the specimen were sealed with a silicone based caulk to prevent leakage of the deicing solution during testing. After curing for the required amount of time in ASTM C-672, the surface of each specimen was photographed, then taken to the UW-Madison Biotron building where the freeze-thaw cycles could commence.

3.3.4 Compressive Strength

In accordance with ASTM C192, three 28-day compressive strength cylinders were made in each mix where ASTM C672 specimens were made. These cylinders were demolded after 24 hours, placed in a humidity controlled wet room with 100% relative humidity for 28 days. After this curing

time, the cylinders were capped with a sulfur-based capping compound; and tested to failure for compressive strength following the procedure in ASTM C39.

3.4 ASTM C672: Standard Method for Scaling Resistance of Concrete Surfaces Exposed to Deicing Chemicals

After each sample was taken to the Biotron, a picture of the surface was taken to indicate the visual condition of the surface prior to the test. With the dams adhered to the surface of each specimen, a ¼" (approximately 330 mL) deep of 4% by weight sodium chloride (NaCl) and water solution was added to the surface of each specimen. The solution was carefully agitated without harming the surface to prevent settling of undissolved NaCl crystals. The top of the dams of each specimen were covered with a non-restrictive polyethylene sheet to prevent evaporation, and then placed within the Biotron freeze-thaw chamber. Within this chamber, the temperature cycled between 32^{o}C (90^{o}F) for four hours and -16^{o}C (3^{o}F) for twenty hours. Every fifth cycle during the thaw phase, each specimen was taken out of the environmental chamber and the solution was decanted over a #200 sieve. A gentle stream of water was used to rinse off the surface of each specimen. Once the scaled mass for each specimen was collected, the solution was replaced, and the specimen was returned to the freeze-thaw chamber. Any specimens that had noticeable leaking were resealed with three-hour caulk, and returned the same day. Each sample was subjected to 60 cycles, which is to approximate one winters' worth of freeze/thaw cycles. Pictures of each specimen were taken after 30 cycles and 60 cycles, to show visual scaling damage progression at the halfway point and full testing period, respectively.

Once the scaled material had been collected, it was transferred into heat resistant test tubes, then dried out at 80^{o}C (176^{o}F) in a laboratory oven for at least 24 hours. Each sample of scaled

material was then weighed out on a digital balance with a precision of 0.1 grams. The scaled material for each mix type-curing compound-application time set was averaged over three specimen duplicates, and analyzed.

ASTM C672 includes a procedure for assessing the surface damage progression by assigning a number rating based upon visual inspection. The researchers felt that the mass loss evaluation procedure was adequate for the purposes of determining scaling resistance, and that visual inspection by the operator was inherently too subjective to have scientific merit.

3.5 MFCC Types and Specifications

Each curing compound treatment types used on this project either classified as emulsion-based or curing/sealing type. The spray rates for each treatment type were generated based upon the manufacture's recommendation of spray rate, converted from ft^2/gallon to grams/area of specimen based upon the estimated density of the curing compound provided by the manufacturer.

3.5.1 Emulsion MFCCs

The emulsion type MFCCs consist of microscopic spheres or "bubbles" of membrane forming organic compounds and pigment suspended in water. As the water evaporates, the emulsion breaks ("bubbles pop") and deposits the organic fraction onto the surface as a continuous or semi-continuous membrane to prevent evaporation. This organic fraction can be an inert material, reactive with atmospheric oxygen, or autogenically reactive (polymerizing).

3.5.1.1 Linseed Oil Emulsion

The linseed oil based curing compound used in this study was a white-pigmented emulsion of boiled linseed oil and titanium dioxide pigment (1-5% pigment by weight) in water. It met ASTM C-

309 specifications as a Type II Class B curing compound for use on concrete slab work and flat work with a high surface area to mass ratio. The emulsion had a specific gravity between 0.97 and 1.03 g/ml, similar to the water carrier. The manufacturer specified a 40 to 50% solid fraction. This compound had a viscosity greater than water and emitted a mild distinctive odor. As a water emulsion it emitted few volatile organic compounds (VOCs) and requires no special handling. This coating provides a reflectance of 67% and upon application provided a yellowish tint. The spray rate was 14.9 grams/specimen.

3.5.1.2 Wax Emulsion

The wax based curing compound used for this study was a white-pigmented emulsion of refined petroleum wax and titanium dioxide pigment (1-5% pigment by weight) in water. It met ASTM C-309 specifications as a Type II Class A curing compound for use on concrete slab work and flat work with a high surface area to mass ratio. The emulsion has a specific gravity between 0.97 and 1.03 g/ml, similar to the water carrier. The manufacturer specified a 15 to 25% solid fraction. This compound had a viscosity slightly greater than that of water and emitted little odor. As a water emulsion it emitted few VOCs and requires no special handling. The manufacturer did not provide reflectance data. The product was bright white in color. The spray rate was 14.9 grams/specimen.

3.5.1.3 PAMS Emulsion

The polyalphamethylstyrene (PAMS) resin based curing compound used in this study was a white-pigmented emulsion of PAMS resin and titanium dioxide pigment (1-5% pigment by weight) in water. It met ASTM C-309 specifications as a Type II Class B curing compound for use on concrete slab work and flat work with a high surface area to mass ratio. The emulsion has a specific gravity between 0.97 and 1.03 g/ml, similar to the water carrier. The manufacturer provided a solid fraction of 52.5%. This compound has a much higher viscosity than water and has minimal odor. The manufacturer provided a reflectance value of 68%. The product had a yellowish-white appearance. As

a water emulsion it emitted few VOCs and requires no special handling. PAMS resin undergoes cross-linking reactions at sufficient concentration, so as the water carrier evaporates the coating consolidates and seals the surface. The spray rate was 14.9 grams/specimen.

3.5.2 Curing/Sealing type MFCC's

The curing/sealing MFCC used in this study was a solution of membrane forming organic compounds in mixed organic solvents. The organic solvent evaporated during application of this compound and was known to emit VOCs. The curing/sealing compound tested met EPA standards for VOC emissions and contained no pigmentation. It was designed to both form an evaporative barrier and penetrate the porous network of the concrete to a significant degree. This is intended to seal the concrete surface and prevent the ingress of water or deicer solution. Solution type curing/sealing compounds such as this generally have longer shelf lives than emulsion type MFCCs.

3.5.2.1 Clear Acrylic

The acrylic based curing compound used in this study was a clear, colorless copolymer of acrylic and methacrylate resins in an organic solvent mixture (aromatic distillates, trimethylbenzene, cumene, and mixed xylenes). It met ASTM C-309 specifications as a Type I Class A/B curing compound and also ASTM C-1315-95 Type I Class B/C sealing compound. The compound had a specific gravity of 0.91g/ml, lower than water. The manufacturer did not provide a solid fraction, but it was calculated to be 25% based on the MSDS value for the VOC emissions and the density. The compound has a lower viscosity than water and a pronounced odor of organic solvents. There was no pigmentation added to this compound, it provided a surface with a minor shine. The VOC emissions from this coating are very flammable and hazardous, so coating operations generally require adequate ventilation and removal of ignition sources. This compound was a solution of acrylic and methacrylate monomers in an organic solvent. It is designed to cure, seal, and harden concrete by

both forming a surface membrane and penetrating the pore network of the near-surface concrete. From the manufacturer's description, as the organic solvent evaporated the concentration of the monomers increased until a chemical reaction occurred with the pore water and consolidated the membrane. The spray rate was 9.1 grams/specimen.

3.6 Air Reconditioning Concrete Humidity Evaporation Research System (ARCHERS)

An objective of this study was the investigation of a practical, accurate method for determining the termination of the bleeding process of concrete. Currently, ASTM C232 exists as a method for determining the portion of mix water that will bleed by extracting bleed water with a pipette mechanism. This procedure is labor intensive, time consuming, and impractical for most job sites. Other methods have been proposed, but are equally labor and time intensive in their own respects.

The Air Reconditioning Concrete Humidity Evaporation Research System, or ARCHERS, was created as part of this project to indicate the presence of bleed water on a concrete surface over time. The primary operational assumption behind the ARCHERS is that there is detectable gaseous water vapor in the air directly above a liquid due to evaporation. It was hypothesized that the evaporation of liquid bleed water could be evaluated as a change in the relative humidity immediately above the concrete surface. By monitoring the changes in the relative humidity of the air above the concrete over time, it was theorized that the cessation of bleeding could be identified by the gradual reduction in the relative humidity following the final evaporation and dispersion of liquid bleed water.

An enclosed box made of a lightweight, non-absorbent acrylic, containing a hygrometer (humidity probe) and thermocouple were used measure the relative humidity and temperature directly

above the concrete. This is referred to as the contactor in Figure 3-3. The contactor minimized measurement interference from atmospheric conditions such as temperature, solar radiation, wind, or humidity changes. Despite reducing ambient interference, a contactor constructed without an outlet would restrain the evaporated bleed water within, resulting in a constant near-maximum reading of relative humidity. To avoid this problem, a source controllable air flow, treated to operator-set constant temperature would have to replace the air immediately above the concrete surface to obtain a better relative humidity profile above the surface over time.

The ARCHERS layout containing the acrylic contactor is shown in Figure 3-3.The mechanism behind the ARCHERS is a Data Acquisition instrument (DAQ) used to monitor and record the operational process variable of relative humidity, to adjust the primary output: the Fan Duty Cycle (FDC) of the inlet fan in Figure 3-3. This is done through the use of a Proportional-Integral-Derivative (PID) feedback loop within the DAQ software interface on a computer terminal. The DAQ measures a difference in relative humidity before and after a portion of air passes over the concrete surface ΔH, and compares that to a relative humidity difference set point, ΔH_{set}. The error between ΔH and ΔH_{set} is evaluated through the PID logic, changing the output of the FDC in the following time step. The value of the FDC versus time is continually plotted over time, visible to the operator on a graph on the computer terminal. This plot is used by the operator to determine the stage of the bleeding process by evaluating the FDC over time.

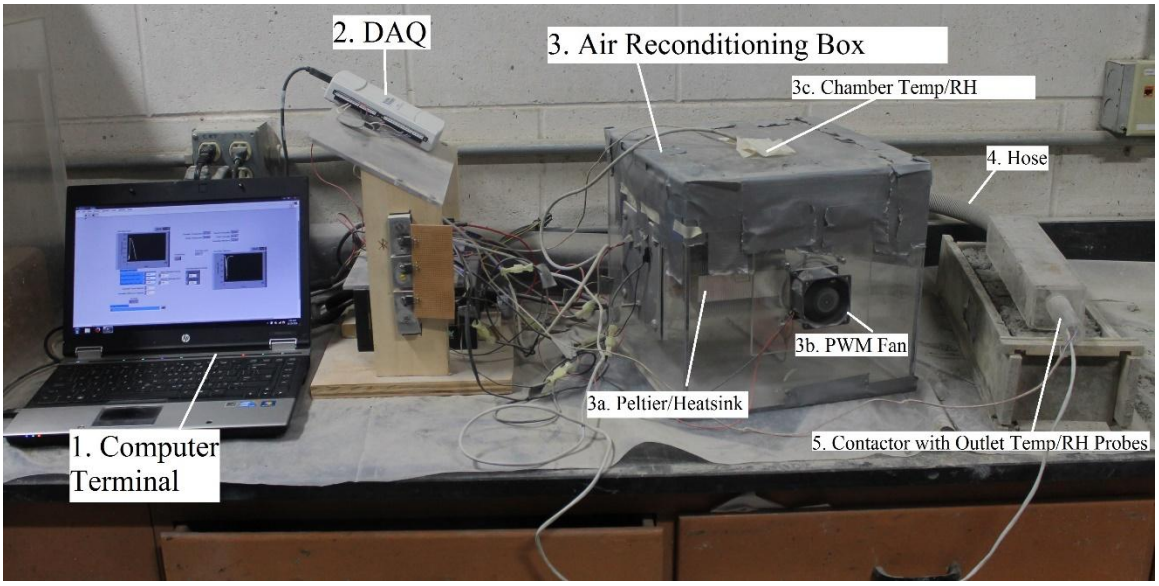

Figure 3-3: ARCHERS Layout

The full operational procedure of the ARCHERS contains the following actions:

A. The computer running the DAQ software (1), DAQ (2), and Air Reconditioning Box (ARB) (3) are turned on. This includes power to the temperature and humidity probes.

B. Within the LABVIEW program, a ΔH_{set}, a temperature of the reconditioned air T_{set}, PID parameters, FDC limits and a time step for averaging readings is set by the operator.

C. Once the concrete is poured and the contactor (5) lightly positioned upon the concrete surface, the data logging procedure is turned on. This turns on the Peltier Thermoelectric Chip which is attached to a heat sink outfitted with a fan to disperse heat (3a) and inlet fan attached to the ARB (3b). This fan pushes the treated air to through a hose (4) to the contactor past the outlet temperature and humidity probes (5).

D. Temperature, Relative Humidity, and the FDC readings are collected within the DAQ and recorded to the computer. An output of the FDC versus time is plotted on the Computer.

E. The difference in humidity between the outlet humidity reading and the humidity within the ARB, ΔH (H_{Out}-H_{In}) is compared to the ΔH_{set}. PID logic within the LABVIEW control system evaluates the different between ΔH and ΔH_{set}:

   I. If $\Delta H > \Delta H_{set,}$ the FDC is increased by the PID gains, unless the FDC is already at its maximum limit

   II. If $\Delta H < \Delta H_{set}$, the FDC is decreased by the PID gains, unless the FDC is already at its minimum limit

   III. If $\Delta H = \Delta H_{set}$, the FDC remains constant

F. The system will continue to run for the duration of the curing period. As the amount of bleed water decreases, the FDC will eventually drop to the minimum limit, and is expected to stay there. After the FDC has remained at the minimum limit for an appropriate amount of time, the operator shuts off the program, concluding the test. A spreadsheet of the recorded data is then saved.

While the theory and construction of the ARCHERS remained the same, parameters within the logic in the DAQ software were continually adjusted to mitigate operational problems found in both the tuning phases and during actual bleed water testing on concrete mixes. Figure 3-4 shows a screenshot of the operational interface of the ARCHERS, followed by explanation of the operator inputs.

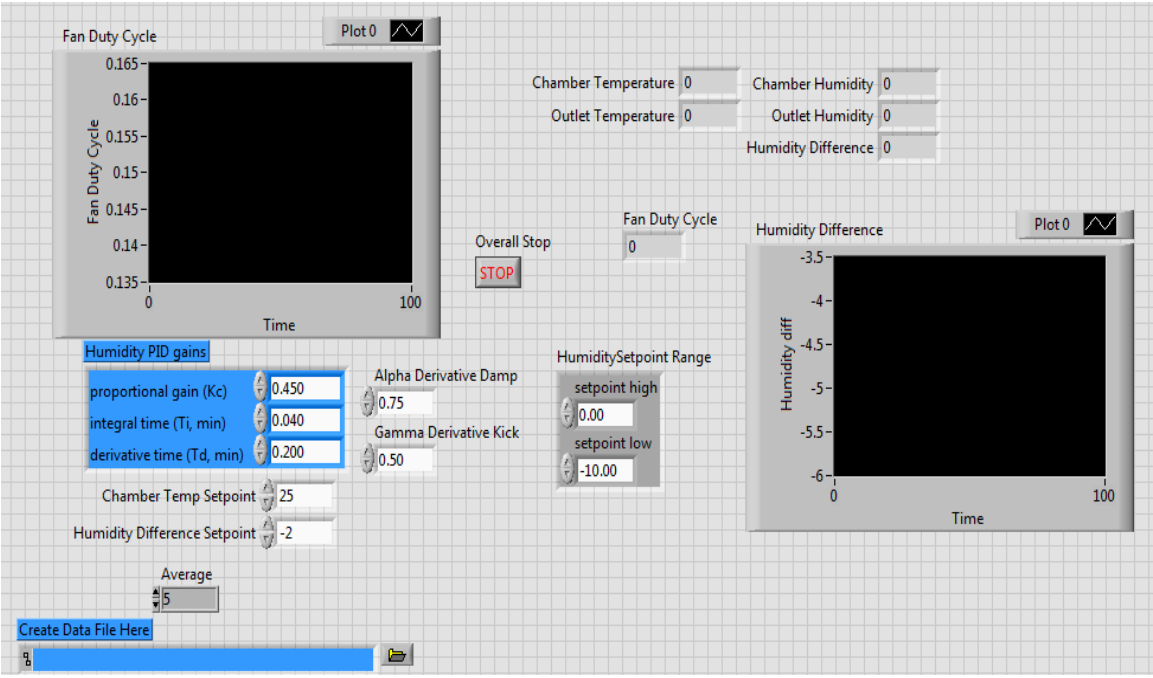

Figure 3-4: ARCHERS Computer Interface

- Humidity Difference Set Point: The process variable that drove the PID to change the FDC. This could be adjusted to react to environmental conditions and technical issues.
- Humidity PID Gains: These are values that govern FDC response to a difference in the humidity difference and the set point. These can be tuned manually or by established tuning methods to idealize the response of the system.
- Derivative Damp/Kick: Limits the instantaneous impact of the derivative term on PID output. It is helpful for reducing the response that individual spikes in the process variable may have on the FDC
- Temperature Set point: This controlled the Peltier heating chip to heat or cool off the air in the ARB based upon thermocouple readings
- Humidity Set Point Range: With the one humidity set point value, the response of the system would frequently ‘ring’ or oscillate around this set point. This range works in

tandem with the set point value by providing an upper limit slightly more than the set point. For example: if the set point humidity was 8% and the limits were from 0 to 10%, the FDC would not increase until the humidity was larger than 10%. This greatly eliminated perturbations in the data that would cause ringing.

- Average: Samples were acquired from the DAQ once every second. This parameter allows the operator to choose the period of averaging the data before it is plotted. Five second running averages were used for this project.
- Create Data File: Once the test had concluded, the operator could name a file and save it for further analysis.

Alterations to the various program parameters could be made with relative ease to tune the operational capacity of the ARCHERS to achieve better performance, or to notify the operator of potential problems with the device. Results and recommendations for the improvement of system performance are discussed in Section 4.5.3.

Chapter 4 Results

4.1 Fresh Concrete Properties

Five concrete batches per mix type were created corresponding to the five curing conditions examined in this study. Table 4-1 displays the fresh concrete properties averaged over the five batches per mix type. Complete fresh concrete properties are given in Appendix B. Each batch was designed to have a (w/c) ratio of 0.4; with the exception of Mix Type 4. This particular mix type created difficulties meeting the low end of the 3±1 inch slump requirement, even with the inclusion of large amounts of High Performance Water Reducer Admixture. As a result, the (w/c) ratio was increased to 0.41. Average air content of the fresh concrete did fall within the 6±1% amount as mandated for WISDOT pavement projects. Mixes 4-6 were poured at times where the relative humidity within the laboratory was heightened, despite near constant temperature. Finally, all mixes prepared for this project exceeded 5000 PSI average 28-days compressive strength.

Specimens were labeled with a four digit identification number, with the first two being most important for the purpose of this data analysis. The first digit (1-6) indicated both the coarse aggregate and supplementary cementitious material (SCM) used, the second digit (A-E) identified the curing compound used. These are listed in Table 4-1 and Table 4-2, respectively. The third digit and fourth digits indicated the application time and replicate number, respectively.

Table 4-1: Fresh Concrete Mix Properties

Mix Type Number	Coarse Aggregate	Cementitious Material (by weight)	w/cm Ratio	Average Slump (inches)	Average Air Content (%)	Ambient Relative Humidity (%)	Compressive Strength (PSI)
1	Crushed Limestone	OPC	0.4	1.25	6.5%	24%	6200
2	Crushed Limestone	30% Slag	0.4	1.50	6.4%	27%	6110
3	Crushed Limestone	30% Fly Ash	0.4	2.50	6.2%	31%	5813
4	Glacial Gravel	OPC	0.41	1.50	6.4%	38%	5348
5	Glacial Gravel	30% Slag	0.4	1.25	5.8%	53%	6129
6	Glacial Gravel	30% Fly Ash	0.4	2.75	5.9%	52%	5817

Table 4-2: Curing Compound Designations

Wet Room	Emulsion			Curing/Sealing
None	Linseed	Wax	PAMS	Acrylic
A	B	C	D	E

4.2 ASTM C672 Results by Individual Mix Type and Curing Compound

The amount of scaling damage was measured by collecting and drying the mass of the scaled material that was collected on a #200 sieve every five freeze-thaw cycles, per ASTM C672. The scaled material was then divided by the exposed area of the specimen and converted to a grams per square meter value. For each mix type-curing compound-application time, the scaled material per square meter value was generated by averaging three replicate specimens. Scaling damage accumulation curves were compiled by summing these average damage values over the 60 cycles of the ASTM C672 test.

Complete scaling damage data is located within Appendix C. Tables are included alongside scaling accumulation charts in this section that include the relative humidity at the time of specimen manufacture, the total amount scaled at 30 and 60 cycles, the percent of damage occurring within the first 15 cycles, and the percent change in scaling damage between the 30 Minute specimens and the 2 and 4 Hour specimens.

4.2.1 Effect of Application Time on Mix Type 1: Crushed Limestone and Ordinary Portland Cement

Mix Type 1 batches were made with crushed limestone aggregate and Ordinary Portland Cement. For all charts in this section, a scale up to 700 g/m^2 was used.

4.2.1.1 Wet Room Cured

Table 4-3 shows that the wet room cured specimens for Mix Type 1 suffered an average of 17.1 g/m^2 in scaling damage. In Figure 4-1, no significant scaling accumulation was detected from 15 cycles to 45 cycles. This set was predicted to have the least amount of scaling of all specimens sets from Mix Type 1 by virtue of being cured in an ideal 100% relative humidity environment prior to freeze-thaw exposure.

Table 4-3: Mix 1-A Scaling Data

Mix 1-A Wet Room Cured			
Relative Humidity	Scaled Mass at 30 Cycles (g/m^2)	Scaled Mass at 60 Cycles (g/m2)	Damage Occuring in First 15 Cycles (%)
27%	2.0	17.1	12%

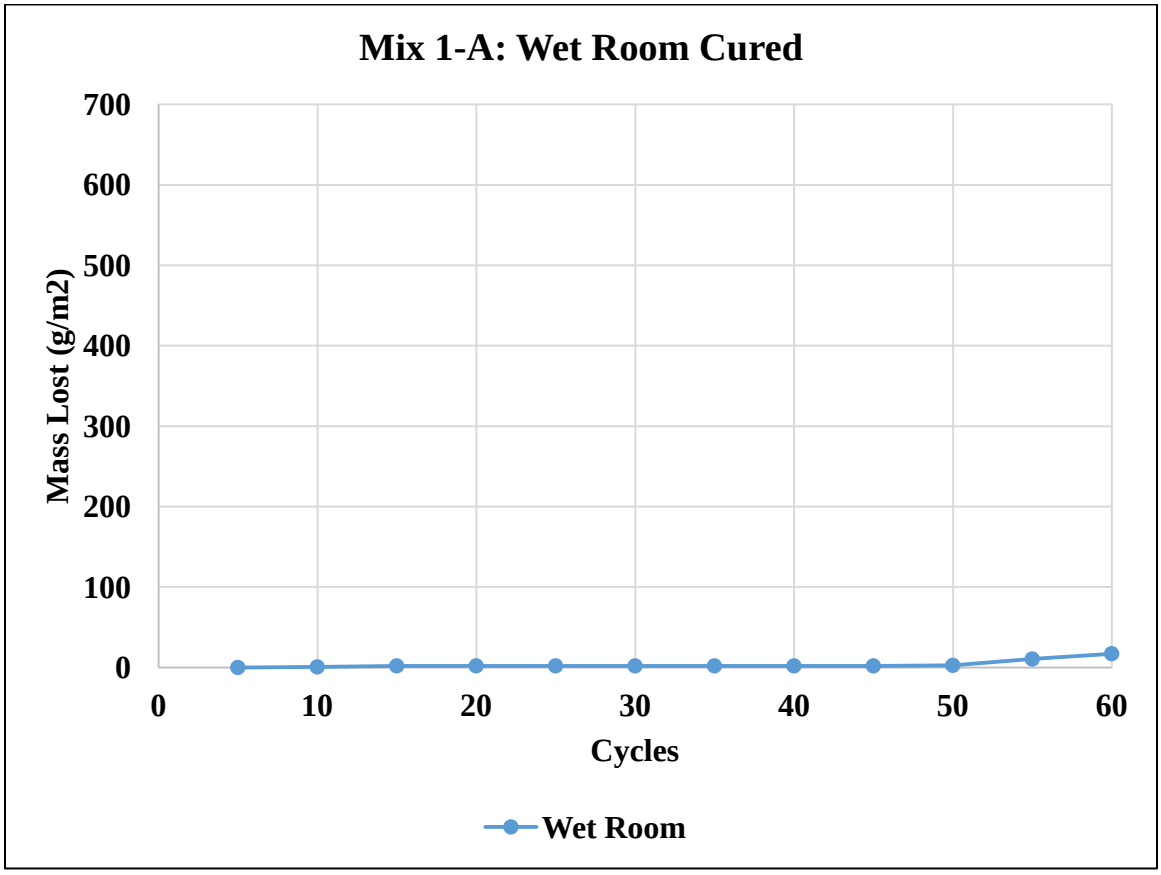

Figure 4-1: Mix 1-A Cumulative Scaling

4.2.1.2 Linseed Oil

The scaling data for Mix 1-B specimens is located in Table 4-4 and the damage accumulation curves are shown in Figure 4-2. For the 30 Minute and 2 Hour specimens, the mass loss rate was very low initially, then accelerated during the last 40 cycles. The 4 Hour application time also possessed low initial scaling, but delayed the increase in mass loss rate until after 30 cycles. Lower amounts of total scaling were exhibited in specimens with longer application times.

Table 4-4: Mix 1-B Scaling Data

Mix 1-B Linseed Oil						
Relative Humidity	Specimens	Scaled Mass at 30 Cycles (g/m^2)	Change in Scaling Amount from 30 Minutes (%)	Scaled Mass at 60 Cycles (g/m2)	Change in Scaling Amount from 30 Minutes (%)	Damage Occuring in First 15 Cycles (%)
21%	30 Minutes	149.3	-----	479.5	-----	4%
	2 Hours	135.5	-9%	446.0	-7%	7%
	4 Hours	30.3	-80%	344.0	-28%	4%

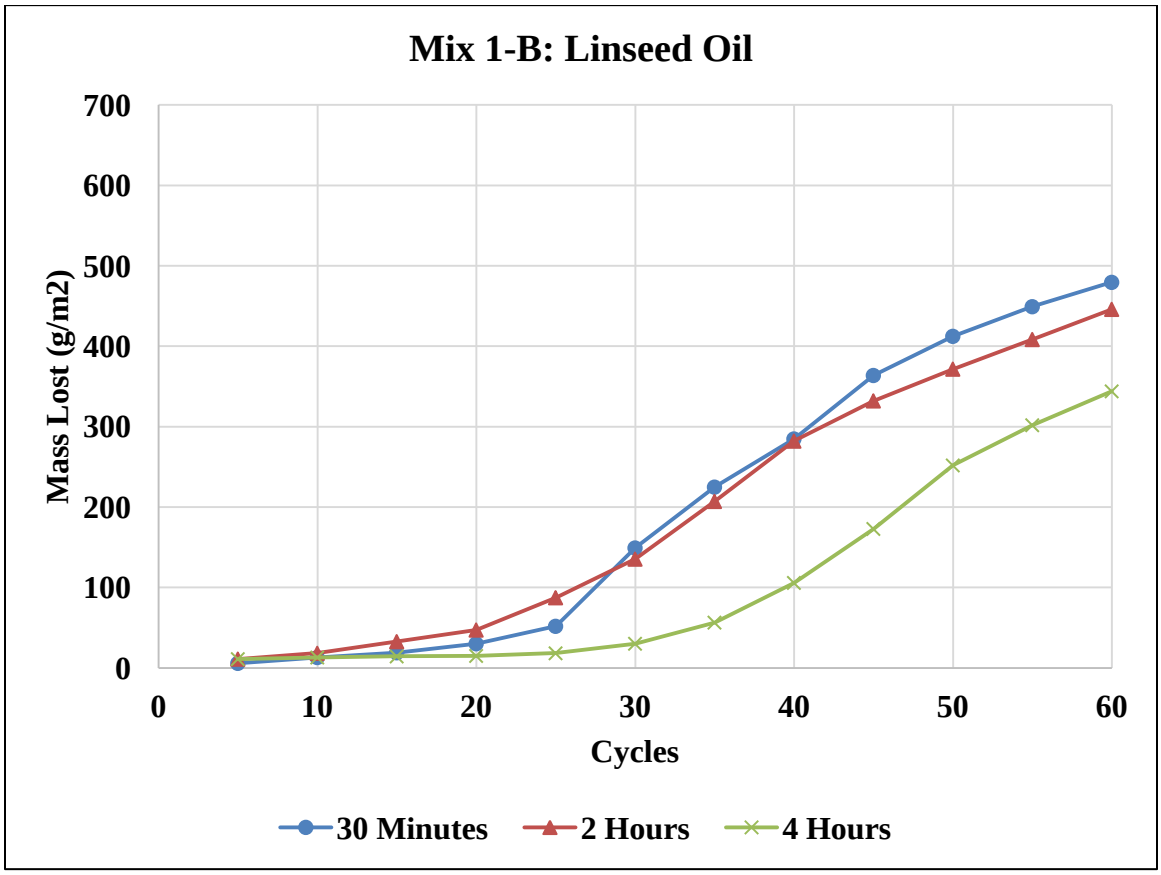

Figure 4-2: Mix 1-B Cumulative Scaling

4.2.1.3 Wax

The damage accumulation curves for Mix 1-C in Figure 4-3 indicate that specimens at all three application times scaled very slowly for the first 45 cycles, then rapidly lost mass during the final 15 cycles. In Table 4-5, the 4 Hour specimens exhibited marginal reductions in scaling damage

as compared to the 30 Minutes specimens. However, the 2 Hour specimens suffered over twice the amount of total scaling damage after 60 cycles as the 30 Minutes specimens. Possible reasons as for why the 2 Hour specimens possessed decreased scaling resistance relative to the 30 Minute and 4 Hour specimens are discussed in 4.4.2.

Table 4-5: Mix 1-C Scaling Data

Mix 1-C Wax						
Relative Humidity	Specimens	Scaled Mass at 30 Cycles (g/m^2)	Change in Scaling Amount from 30 Minutes (%)	Scaled Mass at 60 Cycles (g/m2)	Change in Scaling Amount from 30 Minutes (%)	Damage Occuring in First 15 Cycles (%)
25%	30 Minutes	53.9	-----	301.9	-----	15%
	2 Hours	105.2	95%	621.6	106%	9%
	4 Hours	56.6	5%	259.8	-14%	13%

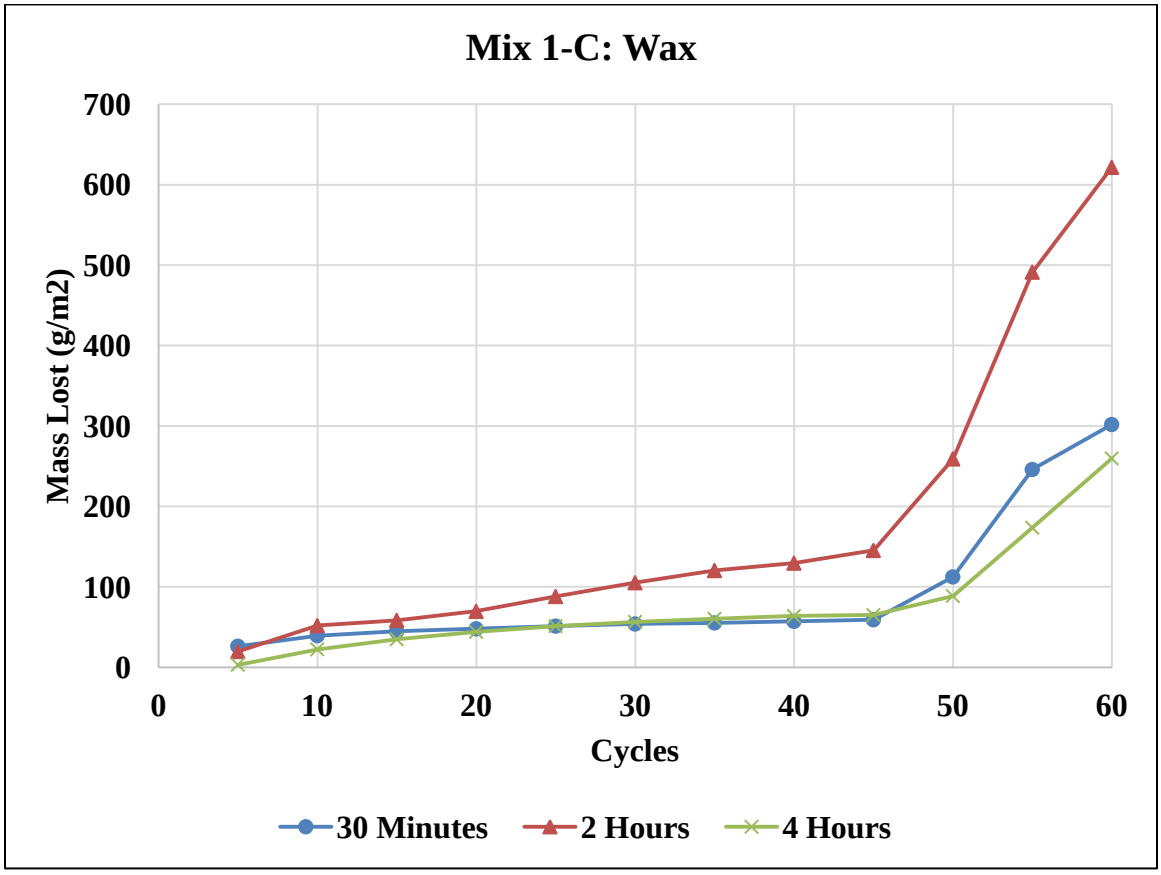

Figure 4-3: Mix 1-C Cumulative Scaling

4.2.1.4 PAMS

The scaling accumulation curves in Figure 4-4 indicated that an increase in the application time led to an increase in scaling damage for Mix 1-D specimens. Table 4-6 shows that all three specimen sets exhibited the majority of the damage they would sustain during the first 15 cycles, with damage rates slowing down for the remainder of the test to near flat line levels. Possible reasons for why the application time scaling patterns were reversed are discussed in 4.4.4.

Table 4-6: Mix 1-D Scaling Data

Mix 1-D PAMS						
Relative Humidity	Specimens	Scaled Mass at 30 Cycles (g/m^2)	Change in Scaling Amount from 30 Minutes (%)	Scaled Mass at 60 Cycles (g/m2)	Change in Scaling Amount from 30 Minutes (%)	Damage Occuring in First 15 Cycles (%)
21%	30 Minutes	46.0	-----	53.9	-----	68%
	2 Hours	83.5	81%	87.5	62%	85%
	4 Hours	121.7	164%	133.5	148%	80%

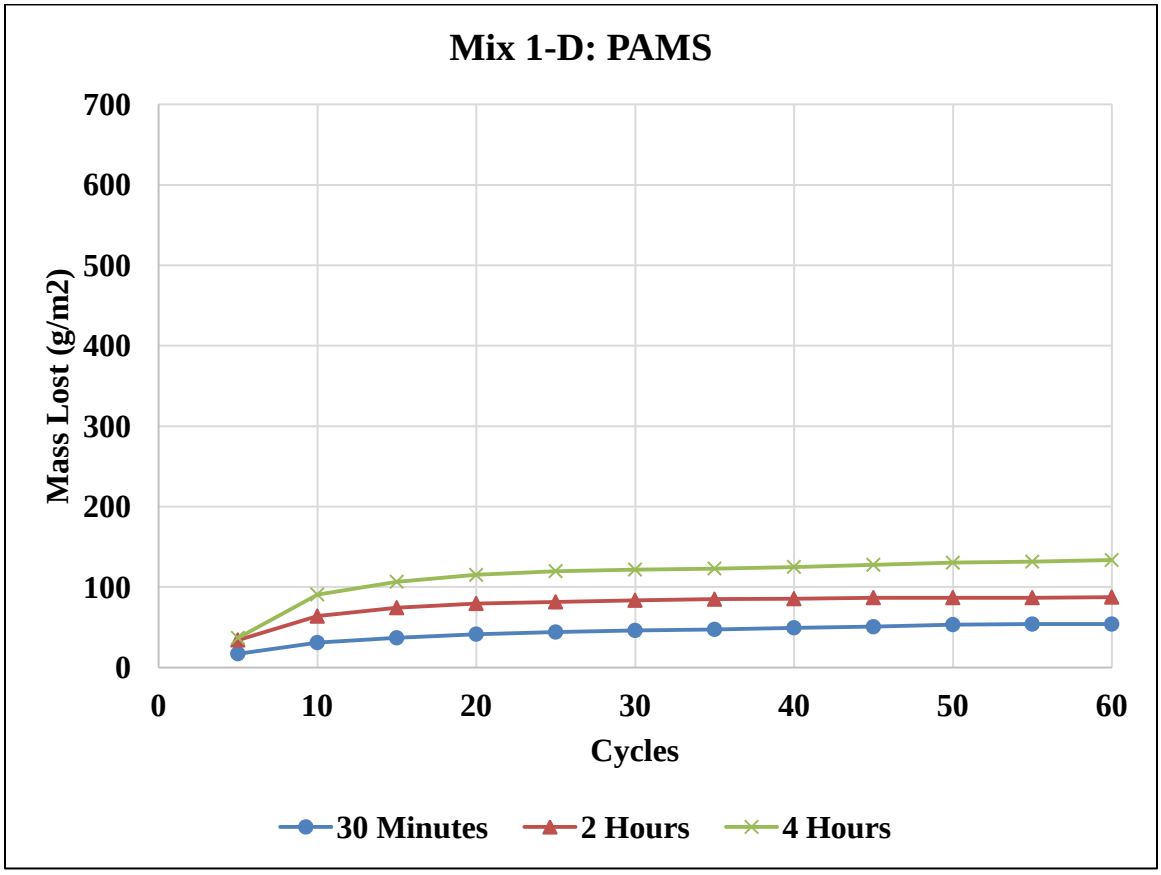

Figure 4-4: Mix 1-D Cumulative Scaling

4.2.1.5 Acrylic

In Figure 4-5, both the 30 Minute and 4 Hours specimen sets of Mix 1-E scaled at approximately the same amount per every five cycles; the main difference was that the 30 Minutes specimens had a higher amount of initial scaling. Results in Table 4-7 indicate the 4 Hour specimens accumulated approximately half the scaling damage of the 30 Minute specimens. It is important to note that the total amount of scaling for the 30 Minutes at the end of 60 Cycles did not exceed 150 g/m^2.

Table 4-7: Mix 1-E Scaling Data

Mix 1-E Acrylic						
Relative Humidity	Specimens	Scaled Mass at 30 Cycles (g/m^2)	Change in Scaling Amount from 30 Minutes (%)	Scaled Mass at 60 Cycles (g/m2)	Change in Scaling Amount from 30 Minutes (%)	Damage Occuring in First 15 Cycles (%)
27%	30 Minutes	100.6	-----	142.1	-----	56%
	4 Hours	48.0	-52%	77.0	-46%	45%

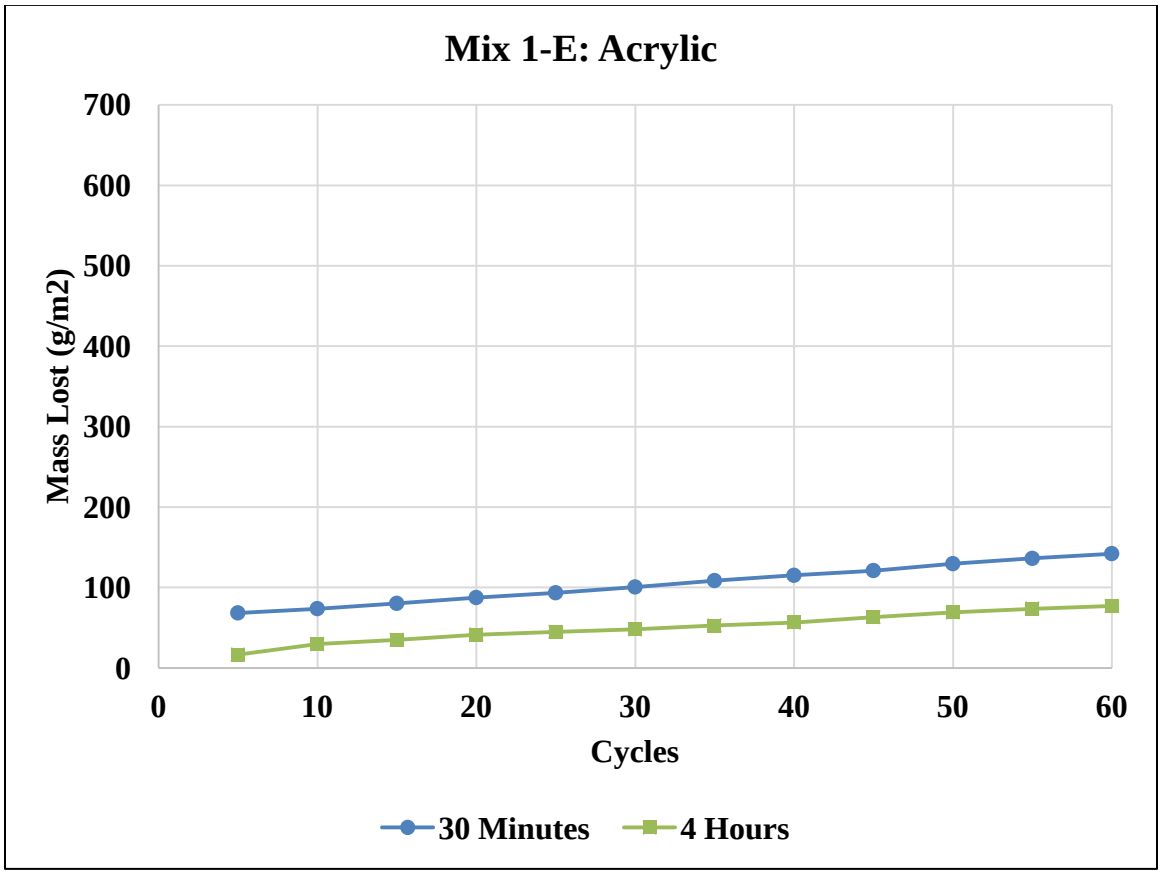

Figure 4-5: Mix 1-E Cumulative Scaling

4.2.2 Effect of Application Time on Mix Type 2: Crushed Limestone and 30% Replacement Slag

Mix Type 2 contained a crushed limestone coarse aggregate and a 30% replacement by weight of Portland Cement with Grade 100 Ground Granulated Blast Furnace Slag. All charts in this section used a scale up to 1400 g/m^2.

4.2.2.1 Wet Room Cured

The scaling data in Table 4-8 indicates that the Wet Room specimens for Mix Type 2 exhibited nearly 180 g/m^2 of average scaling damage after 60 cycles, with nearly half the damage occurring within the first 15 cycles. The damage accumulation pattern in Figure 4-6 displays a progressive increase in the scaling damage over time for Mix 2-A after the first 15 cycles.

Table 4-8: Mix 2-A Scaling Data

Mix 2-A Wet Room Cured			
Relative Humidity	Scaled Mass at 30 Cycles (g/m^2)	Scaled Mass at 60 Cycles (g/m2)	Damage Occuring in First 15 Cycles (%)
24%	121.0	180.9	49%

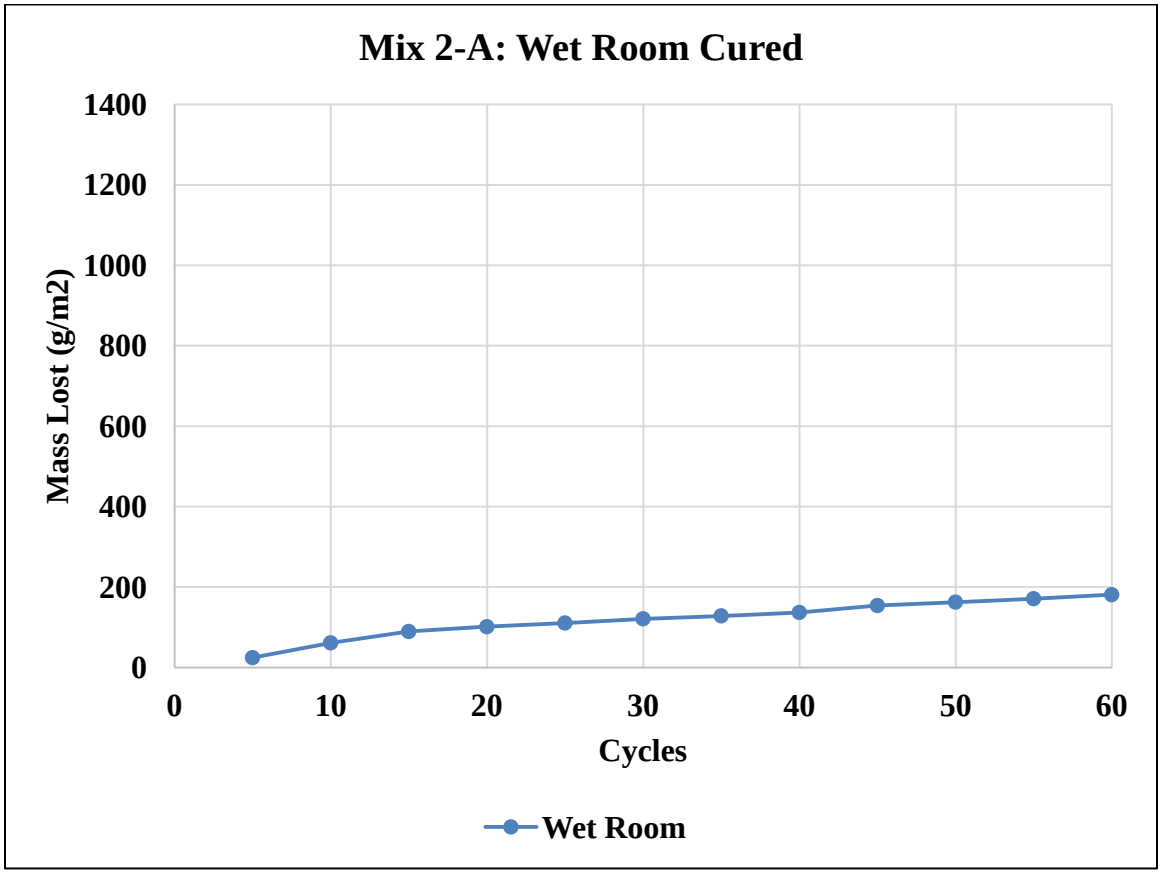

Figure 4-6: Mix 2-A Cumulative Scaling

4.2.2.2 Linseed Oil

In Table 4-9, the total amount of scaling damage exhibited by Mix 2-B's 30 Minute specimens was over 1000 g/m^2; an amount that was significantly reduced in the 2 and 4 Hour specimens. The damage accumulation curves for the 2 and 4 Hour specimens in Figure 4-7 show nearly identical amounts of scaling accumulation over 60 cycles. All three application times resisted early scaling damage, with accelerated accumulation after 15 cycles.

Table 4-9: Mix 2-B Scaling Data

Mix 2-B Linseed Oil						
Relative Humidity	Specimens	Scaled Mass at 30 Cycles (g/m^2)	Change in Scaling Amount from 30 Minutes (%)	Scaled Mass at 60 Cycles (g/m2)	Change in Scaling Amount from 30 Minutes (%)	Damage Occuring in First 15 Cycles (%)
23%	30 Minutes	440.7	-----	1032.1	-----	12%
	2 Hours	128.9	-71%	587.4	-43%	4%
	4 Hours	104.6	-76%	586.8	-43%	4%

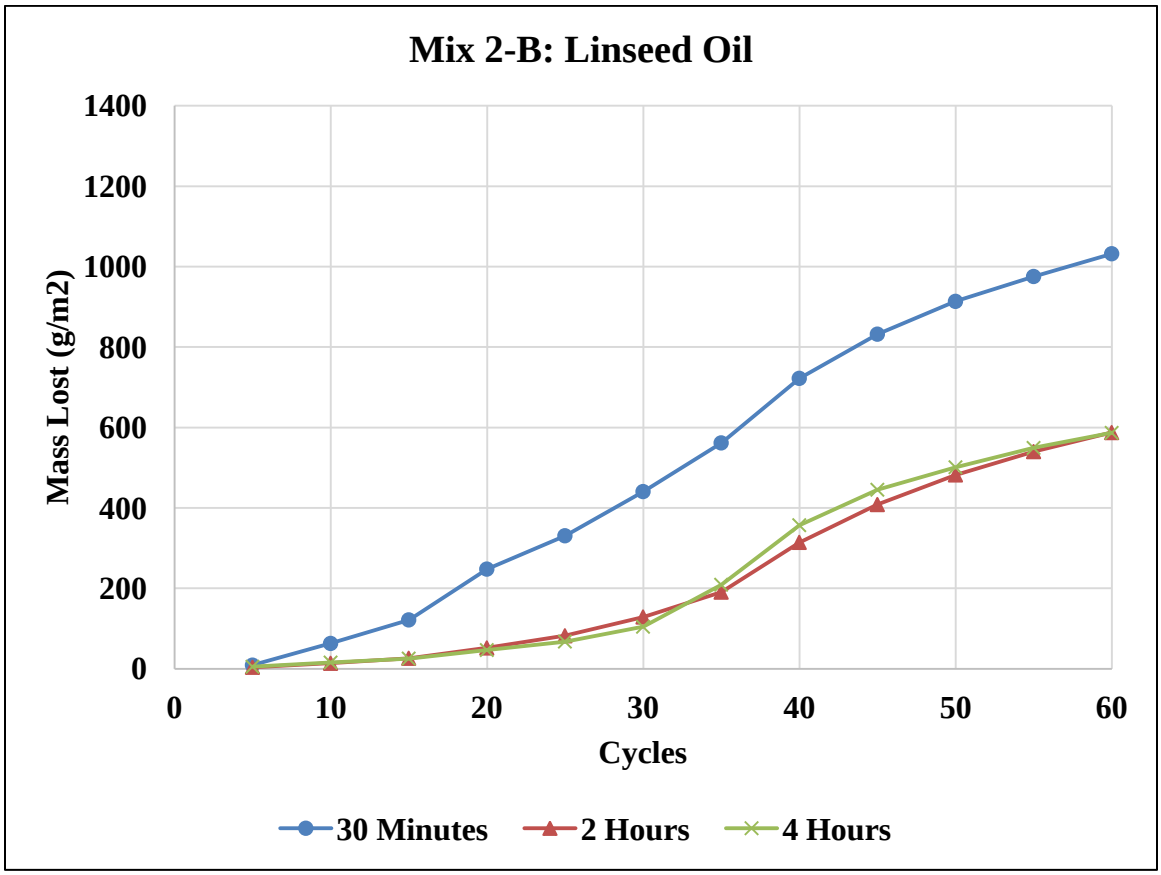

Figure 4-7: Mix 2-B Cumulative Scaling

4.2.2.3 Wax

The scaling accumulation curves for Mix 2-C specimens in Figure 4-8 show nearly identical amounts of scaling damage throughout the first 20 cycles for the 30 Minute and 2 Hour specimens, followed by accelerated damage accumulation in the 2 Hour specimens for the final 40 cycles. The 4

Hour specimens exhibited much less initial scaling than the 30 Minute and 2 Hour specimens. However, both the 30 Minute and 4 Hour specimens appeared to have the same damage accumulation rates throughout the 60 cycles, offset by the initial scaling amounts. In Table 4-10, the 2 Hour specimens accumulated 50% more total scaling than the 30 Minute specimens, while the 4 Hour specimens suffered slightly more than half the amount of scaling of the 30 Minute specimens. Possible explanations for the higher scaling amounts in the 2 Hour specimens are discussed Sections 4.4.1 and 4.4.2.

Table 4-10: Mix 2-C Scaling Data

Mix 2-C Wax						
Relative Humidity	Specimens	Scaled Mass at 30 Cycles (g/m^2)	Change in Scaling Amount from 30 Minutes (%)	Scaled Mass at 60 Cycles (g/m2)	Change in Scaling Amount from 30 Minutes (%)	Damage Occuring in First 15 Cycles (%)
31%	30 Minutes	363.1	-----	546.0	-----	62%
	2 Hours	416.4	15%	818.3	50%	45%
	4 Hours	178.3	-51%	305.2	-44%	52%

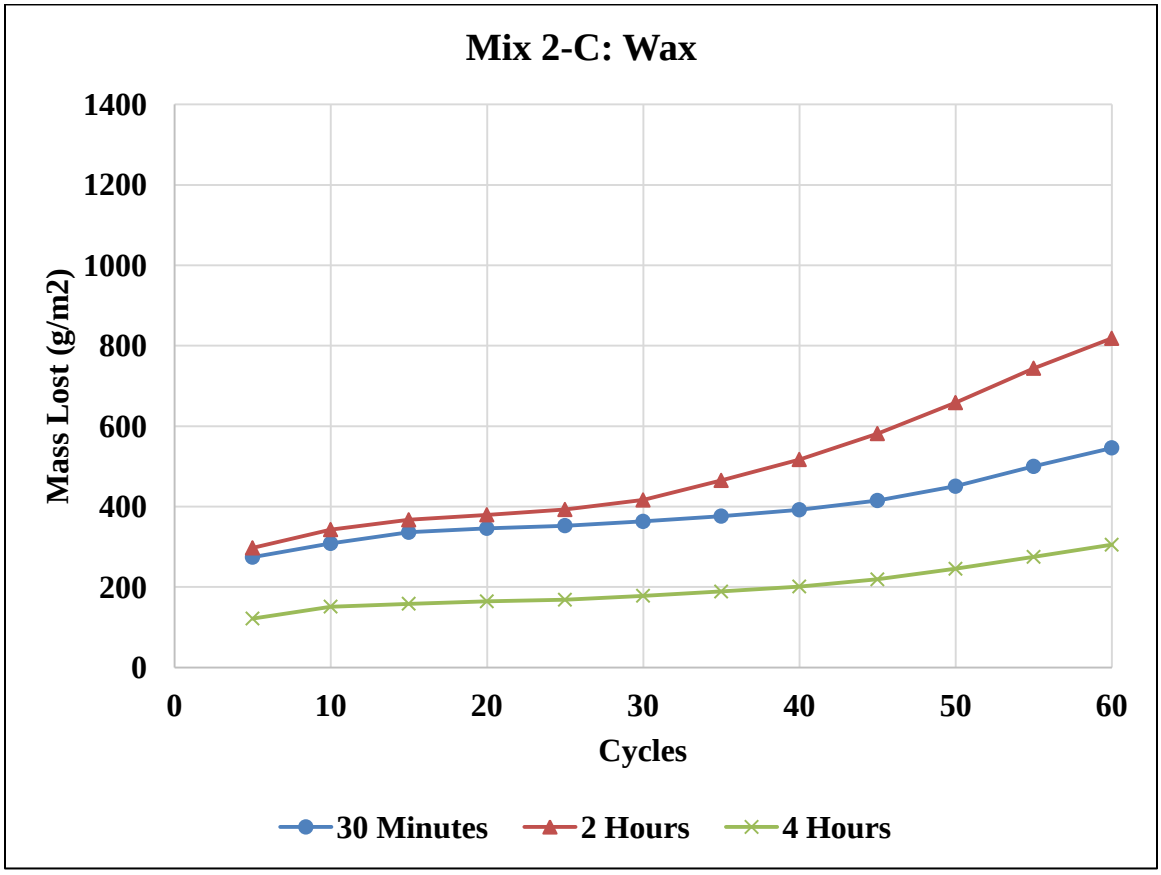

Figure 4-8: Mix 2-C Cumulative Scaling

4.2.2.4 PAMS

As noted in Table 4-11, all three specimen sets for Mix 2-D suffered nearly 80% of their total scaling damage within the first 15 cycles. Each set scaled more than 850 g/m^2, with the 2 Hour specimens scaling over 1200 g/m^2, a 43% increase in damage over the 30 Minute specimens. The damage patterns in Figure 4-9 show that the 30 Minute and 4 Hour specimens scale at nearly the same rate and amounts for the entire test. Possible explanations for the scaling behavior of this slag-containing mix type are discussed Section 4.4.1.

Table 4-11: Mix 2-D Scaling Data

Mix 2-D PAMS						
Relative Humidity	Specimens	Scaled Mass at 30 Cycles (g/m^2)	Change in Scaling Amount from 30 Minutes (%)	Scaled Mass at 60 Cycles (g/m2)	Change in Scaling Amount from 30 Minutes (%)	Damage Occuring in First 15 Cycles (%)
31%	30 Minutes	740.0	-----	867.0	-----	79%
	2 Hours	1063.0	44%	1238.0	43%	82%
	4 Hours	790.0	7%	851.2	-2%	88%

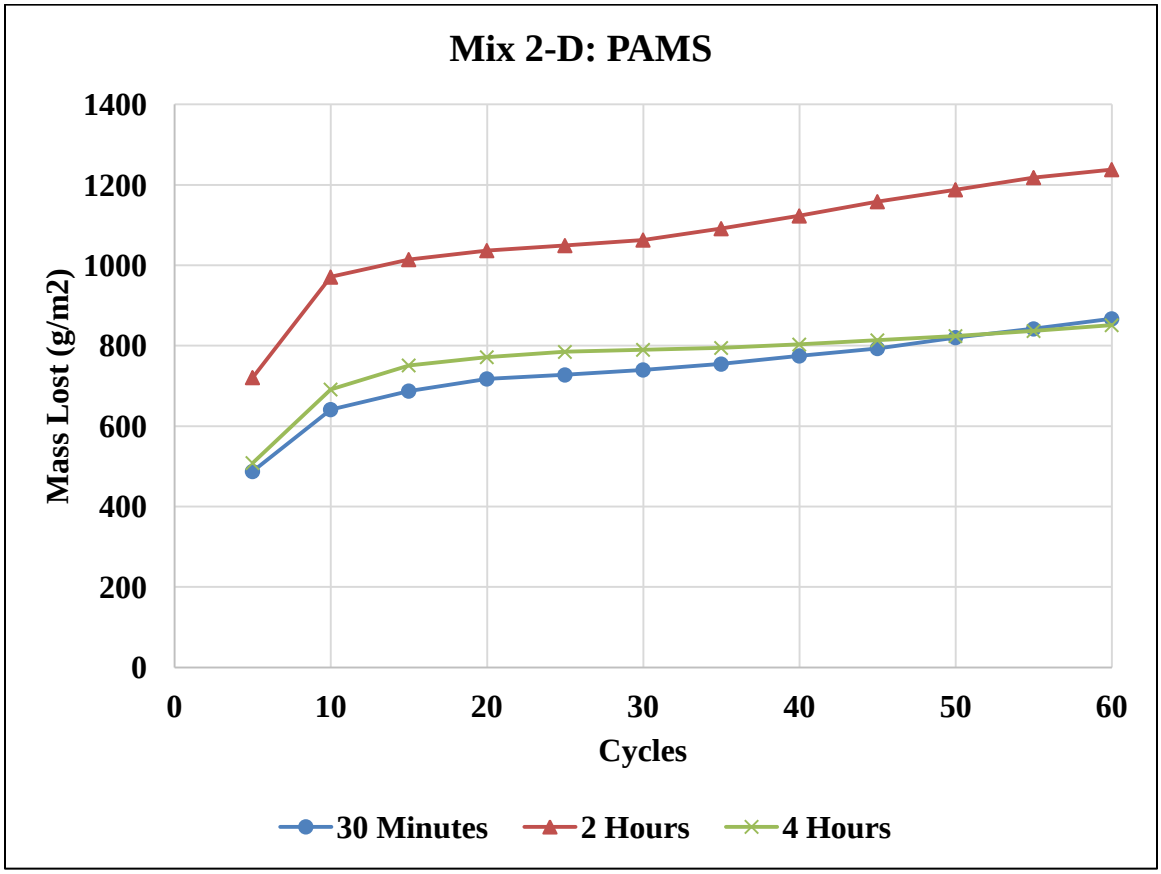

Figure 4-9: Mix 2-D Cumulative Scaling

4.2.2.5 Acrylic

The Mix 2-E scaling data in Table 4-12 shows a nearly 26% decrease in scaling damage suffered in the 4 Hour specimens versus the 30 Minute specimens. Both sets of specimens suffered

most of their total damage within the first 15 cycles. Figure 4-10 shows that the 30 Minute and 4 Hour specimens scaled at approximately the same rates after the first 15 cycles.

Table 4-12: Mix 2-E Scaling Data

Mix 2-E Acrylic						
Relative Humidity	Specimens	Scaled Mass at 30 Cycles (g/m^2)	Change in Scaling Amount from 30 Minutes (%)	Scaled Mass at 60 Cycles (g/m2)	Change in Scaling Amount from 30 Minutes (%)	Damage Occuring in First 15 Cycles (%)
24%	30 Minutes	528.9	-----	617.0	-----	73%
	4 Hours	352.6	-33%	454.5	-26%	63%

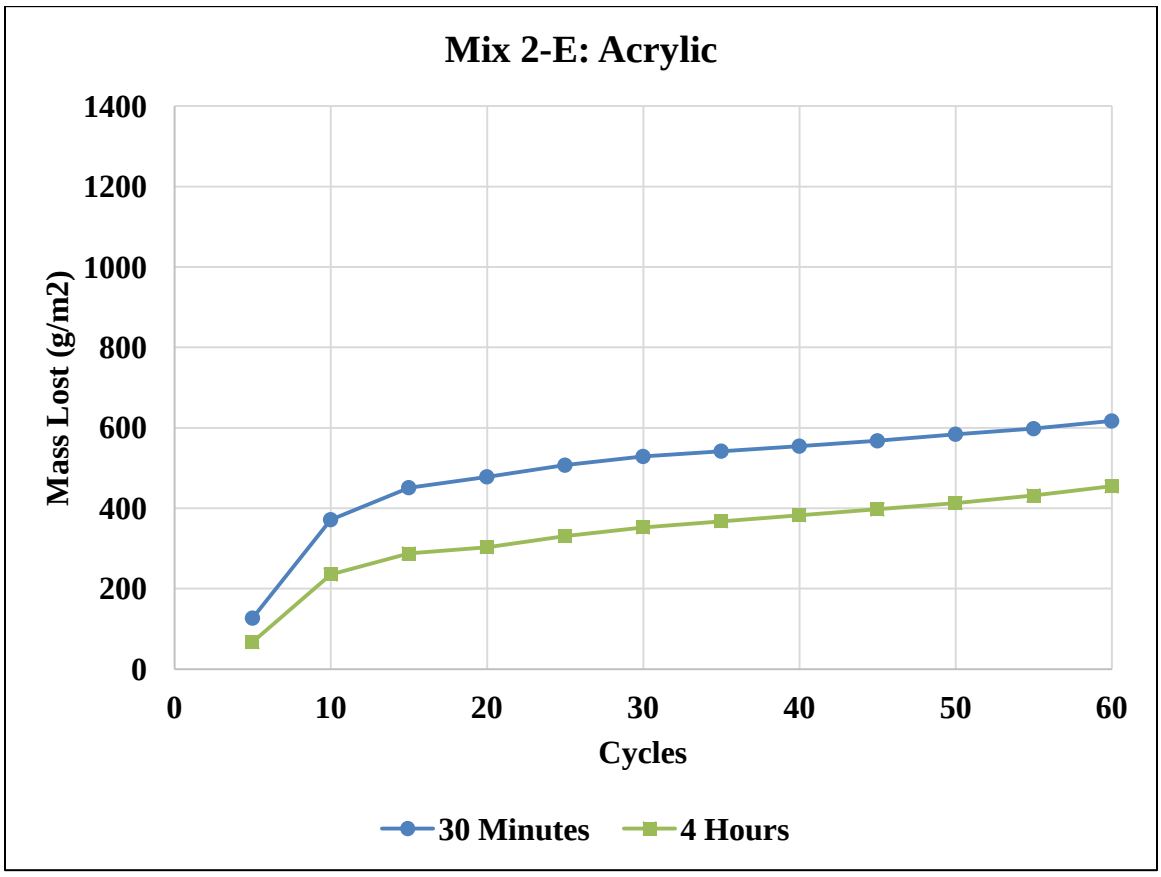

Figure 4-10: Mix 2-E Cumulative Scaling

4.2.3 Effect of Application Time on Mix Type 3: Crushed Limestone and 30% Replacement Fly Ash

Mix Type 3 contained the crushed limestone and a 30% replacement by weight of Portland Cement with Class C Fly Ash. Only two application times were evaluated for this set: 30 Minutes and 4 Hours. As shown in Table 4-1, Mix Type 3 batches possessed slumps higher than the crushed limestone batches that contained just OPC and Slag Cement. All charts in this section used a constant mass loss scale up to 1600 g/m^2.

4.2.3.1 Wet Room Cured

Table 4-13 shows that the Wet Room specimens for Mix Type 3 most of their total scaling damage occurring within the first 15 cycles. This is also shown in Figure 4-11, where very little scaling accumulation occurred after the initial 15 cycles.

Table 4-13: Mix 3-A Scaling Data

Mix 3-A Wet Room Cured			
Relative Humidity	Scaled Mass at 30 Cycles (g/m^2)	Scaled Mass at 60 Cycles (g/m2)	Damage Occuring in First 15 Cycles (%)
32%	81.6	94.7	69%

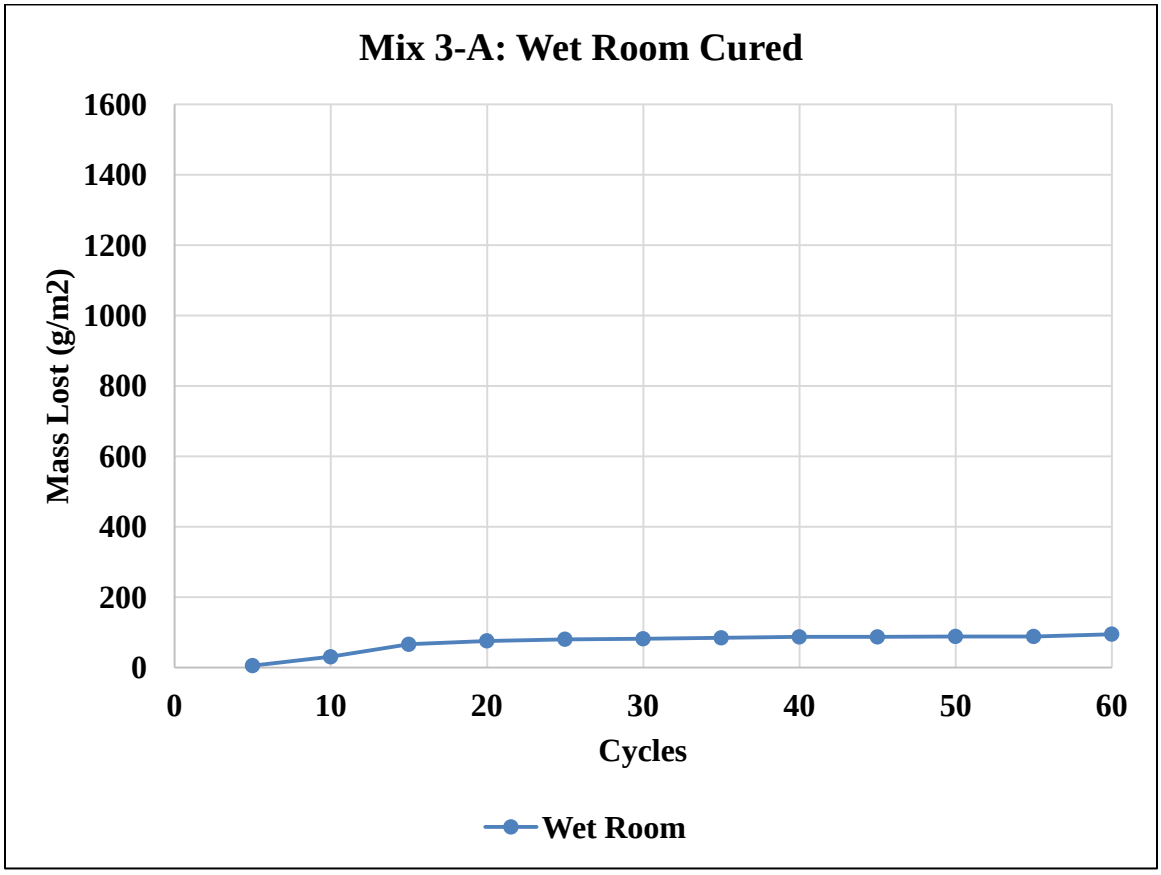

Figure 4-11: Mix 3-A Cumulative Scaling

4.2.3.2 Linseed Oil

In Figure 4-12 for Mix 3-B, a very high amount of scaling in the 30 Minute specimens within the first 15 cycles contrasted with the low amount of scaling accumulation in the 4 Hour specimens during that same time. Both sets of specimens scaled at approximately the same rates during the following 45 cycles. The total scaling damage in the 30 Minute specimens was reduced by over half by extending the application time to 4 Hours, as shown in Table 4-14.

Table 4-14: Mix 3-B Scaling Data

Mix 3-B Linseed Oil						
Relative Humidity	Specimens	Scaled Mass at 30 Cycles (g/m^2)	Change in Scaling Amount from 30 Minutes (%)	Scaled Mass at 60 Cycles (g/m2)	Change in Scaling Amount from 30 Minutes (%)	Damage Occuring in First 15 Cycles (%)
29%	30 Minutes	1151.2	-----	1479.4	-----	68%
	4 Hours	268.4	-77%	642.7	-57%	7%

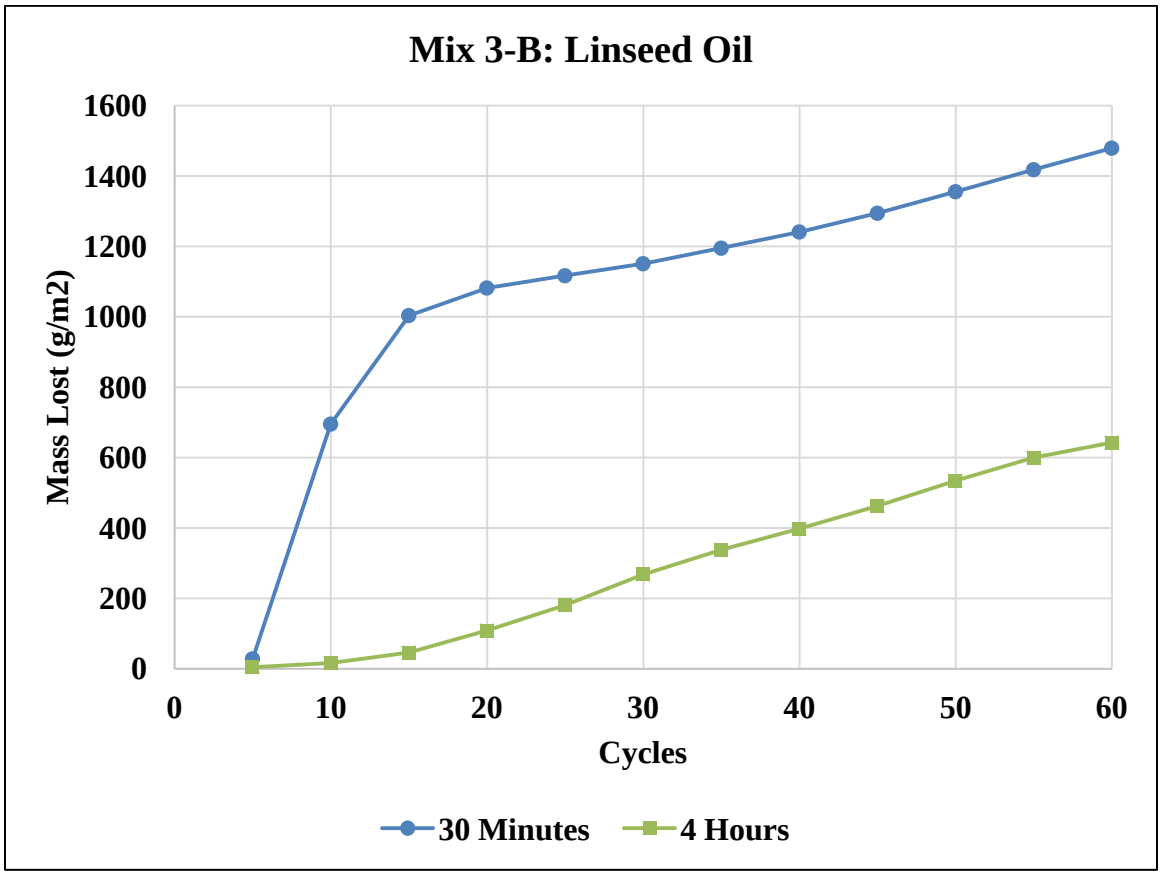

Figure 4-12: Mix 3-B Cumulative Scaling

4.2.3.3 Wax

Mix 3-C scaling data in Table 4-15 shows that the total amount of scaling the 30 Minute specimens was reduced by over half by increasing the application time to 4 Hours. The scaling accumulation curves for both sets of specimens in Figure 4-13 were nearly identical in magnitude for the first 20 cycles. While both set of specimens exhibited increased rates of scaling damage occur

during the final 40 cycles, the 30 Minute specimens suffered higher rates of damage accumulation than the 4 Hour specimens. Extending the application time to 4 hours limited this acceleration of scaling accumulation in the Mix Type 3 Wax coated specimens.

Table 4-15: Mix 3-C Scaling Data

Mix 3-C Wax						
Relative Humidity	Specimens	Scaled Mass at 30 Cycles (g/m^2)	Change in Scaling Amount from 30 Minutes (%)	Scaled Mass at 60 Cycles (g/m2)	Change in Scaling Amount from 30 Minutes (%)	Damage Occuring in First 15 Cycles (%)
32%	30 Minutes	225.6	-----	847.9	-----	16%
	4 Hours	157.9	-30%	394.0	-54%	33%

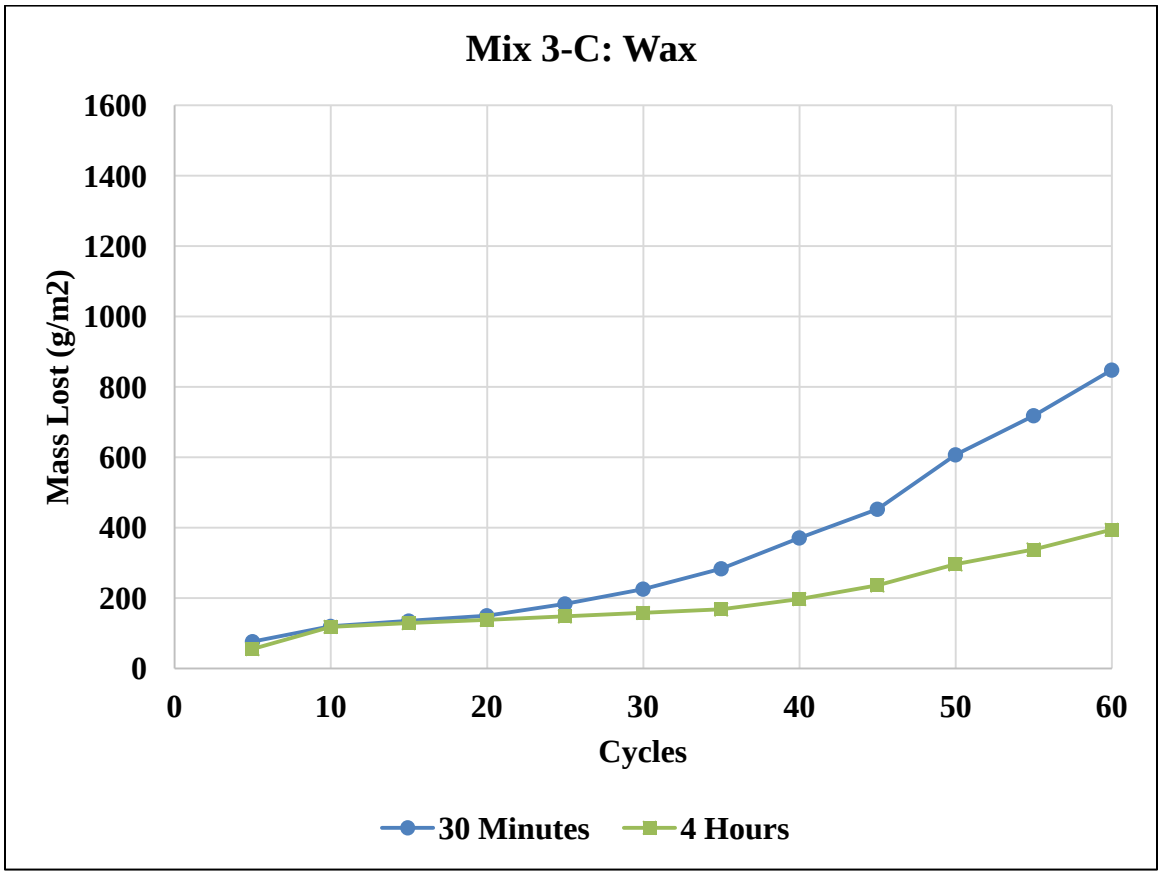

Figure 4-13: Mix 3-C Cumulative Scaling

4.2.3.4 PAMS

Scaling data for Mix 3-D in Table 4-16 shows that the PAMS-coated specimens exhibited levels of scaling resistance within both 30 Minutes and 4 Hours specimen sets averaging total amounts of damage less than 310 g/m^2. The scaling accumulation curves for both application time specimen sets in Figure 4-14 were roughly identical in magnitude for the first 40 cycles, with the 30 Minute specimens suffering slightly higher rates of scaling than the 4 Hour specimens during the final 20 cycles.

Table 4-16: Mix 3-D Scaling Data

Mix 3-D PAMS						
Relative Humidity	Specimens	Scaled Mass at 30 Cycles (g/m^2)	Change in Scaling Amount from 30 Minutes (%)	Scaled Mass at 60 Cycles (g/m2)	Change in Scaling Amount from 30 Minutes (%)	Damage Occuring in First 15 Cycles (%)
27%	30 Minutes	120.4	-----	309.2	-----	26%
	4 Hours	113.8	-5%	211.2	-32%	45%

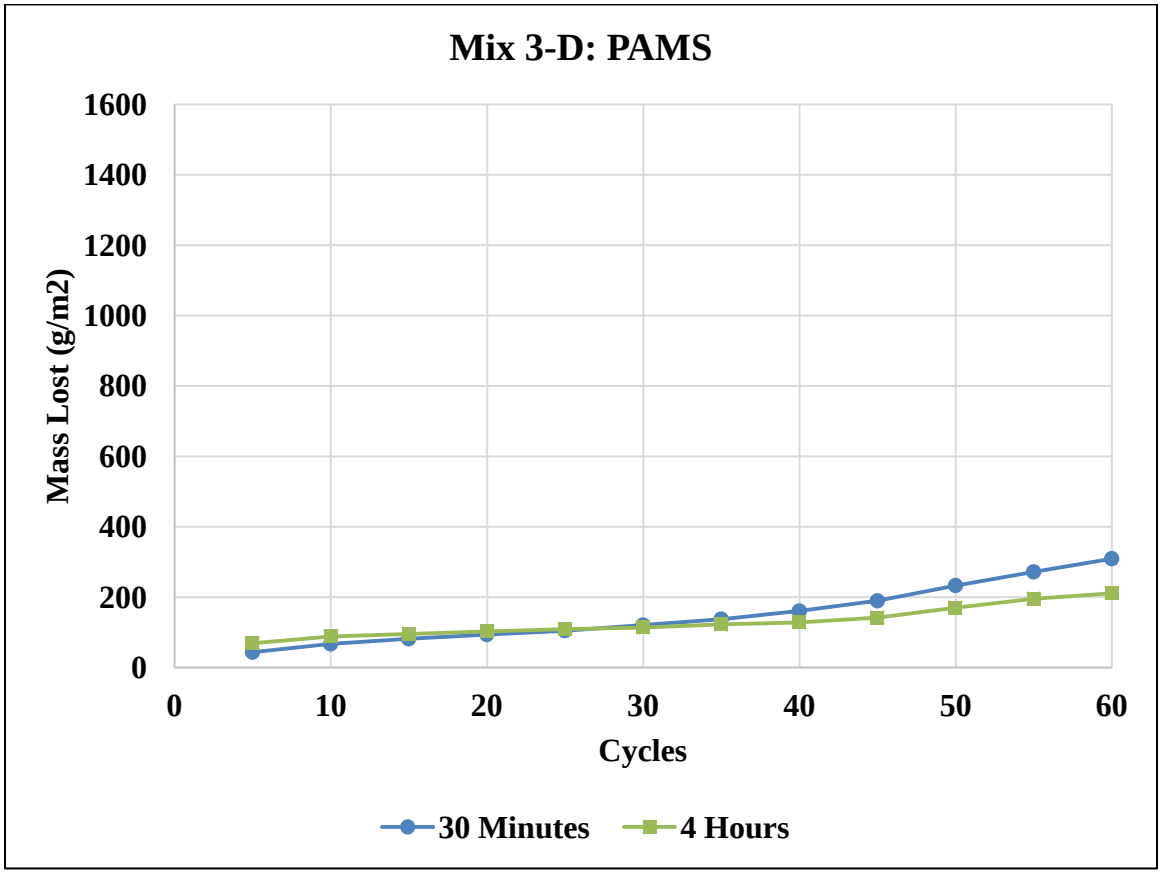

Figure 4-14: Mix 3-D Cumulative Scaling

4.2.3.5 Acrylic

The scaling damage accumulation curves for Mix 3-E acrylic coated specimens in Figure 4-15 indicate that the 30 Minute specimens exhibited significant surface loss between 5 and 10 cycles, while the 4 Hour specimens did not. This is important, as during the final 50 cycles the damage accumulation rates for both the 30 Minute and 4 Hours specimens were both very low. As shown in Table 4-17, extending the application time to 4 Hours resulted in a decrease in total scaling damage of over 80%, or approximately 600 g/m^2.

Table 4-17: Mix 3-E Scaling Data

Mix 3-E Acrylic						
Relative Humidity	Specimens	Scaled Mass at 30 Cycles (g/m^2)	Change in Scaling Amount from 30 Minutes (%)	Scaled Mass at 60 Cycles (g/m2)	Change in Scaling Amount from 30 Minutes (%)	Damage Occuring in First 15 Cycles (%)
36%	30 Minutes	671.0	-----	734.1	-----	83%
	4 Hours	109.9	-84%	130.9	-82%	71%

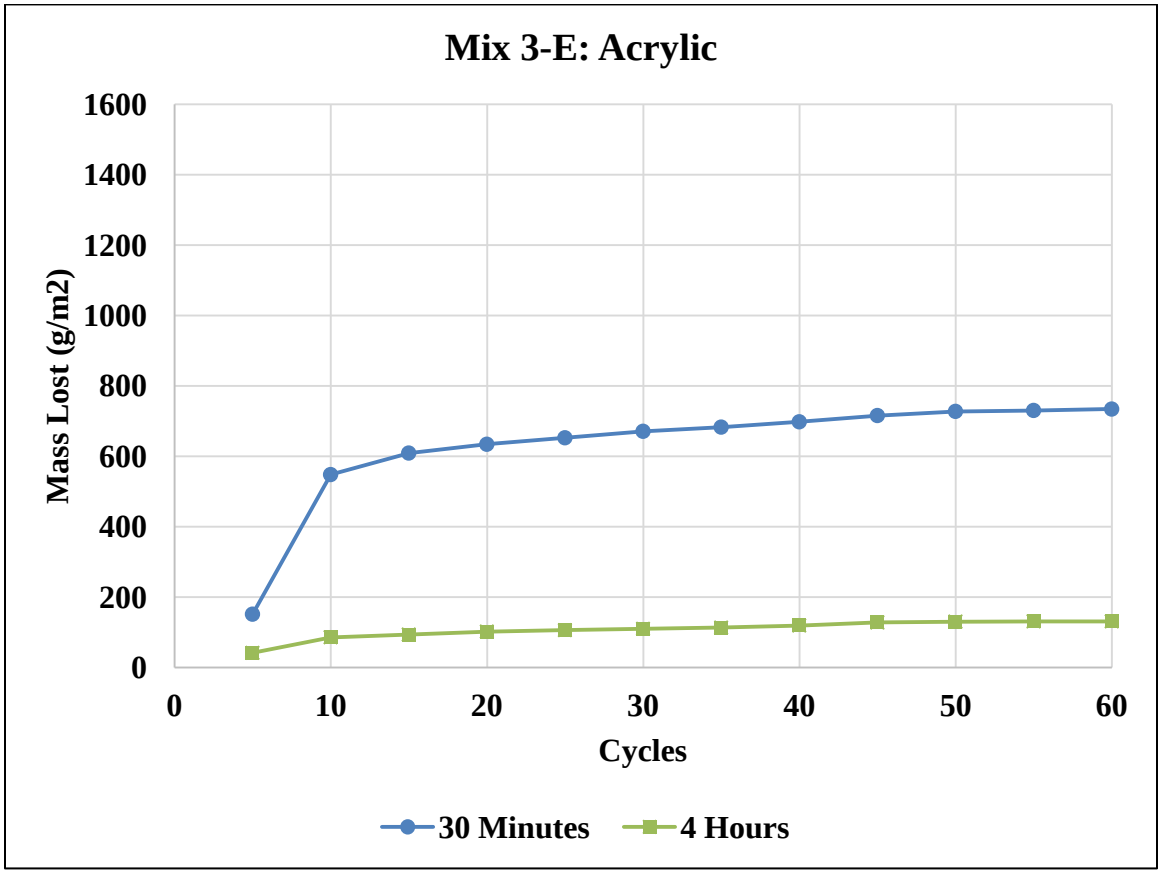

Figure 4-15: Mix 3-E Cumulative Scaling

4.2.4 Effect of Application Time on Mix Type 4: Glacial Gravel and Ordinary Portland Cement

Mix Type 4 consisted of the Glacial Gravel coarse aggregate source along with OPC. Due to workability concerns, batches 4-B, 4-C, and 4-D required an increase in the water/cement ratio to 0.41 from 0.4 to ensure workability requirements were met. In addition to a higher (w/c) ratio, most

of these mixes were mixed in environments with lower relative humidity, possessed a higher air content amount, and lower compressive strength than the other gravel-containing mixes, Mix Types 5 and 6 as summarized in Table 4-1. All charts in this section used a mass loss scale up to 700 g/m^2.

4.2.4.1 Wet Room Cured

Table 4-18 shows that the Wet Room specimens for Mix Type 4 exhibited less than 60 g/m^2 of average total scaling, with only 26% of this damage occurring in the first 15 cycles. This is also reflected in Figure 4-16, where the accumulation of scaled material was relatively constant throughout the duration of the exposure to deicing chemicals.

Table 4-18: Mix 4-A Scaling Data

Mix 4-A Wet Room Cured			
Relative Humidity	Scaled Mass at 30 Cycles (g/m^2)	Scaled Mass at 60 Cycles (g/m2)	Damage Occuring in First 15 Cycles (%)
35%	37.5	57.2	26%

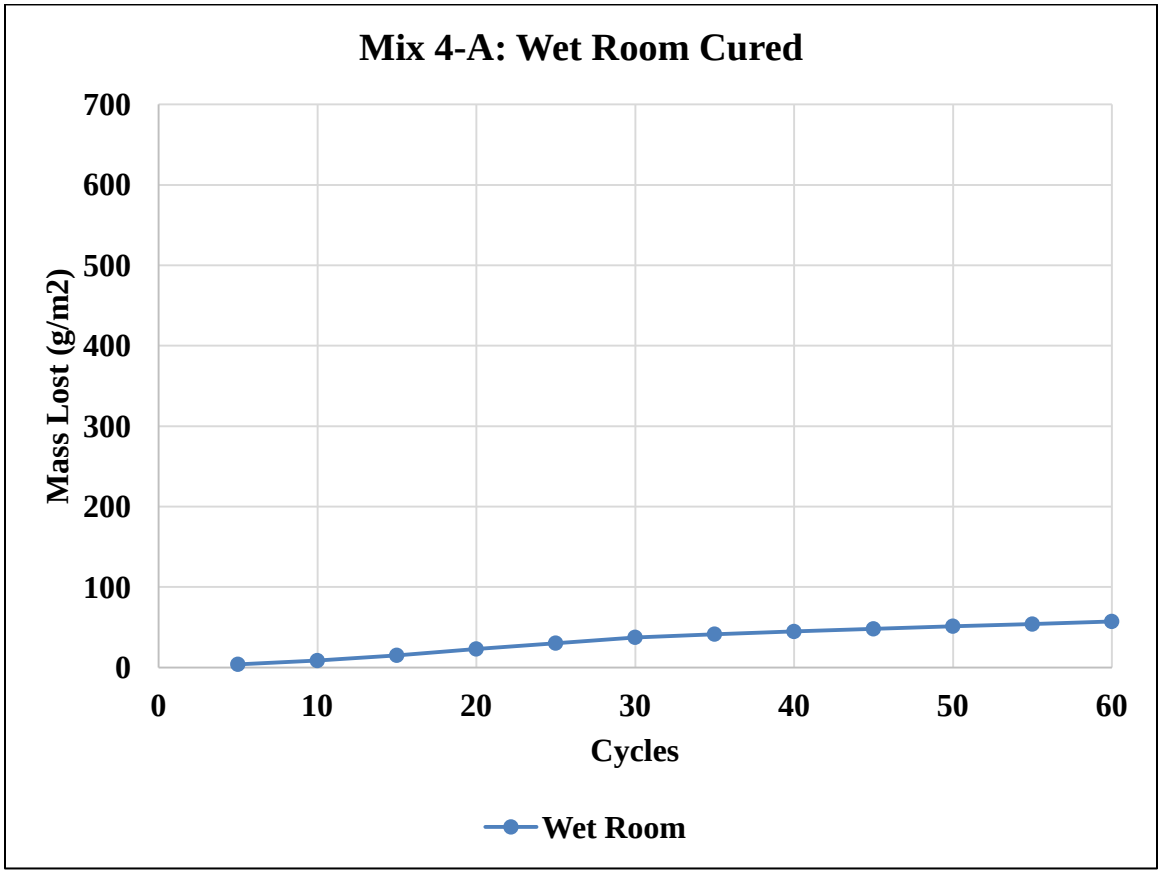

Figure 4-16: Mix 4-A Cumulative Scaling

4.2.4.2 Linseed Oil

Figure 4-17 shows that the Mix 4-B 30 Minute specimens lost over half their total damage within the first 30 cycles, while the 2 Hour and 4 Hour specimens exhibited very little scaling damage during that time. After 30 cycles, all three specimen sets appeared to scale at similar rates. Table 4-18 shows that increasing the application time to 2 Hours reduced the scaling damage in half as compared to the 30 Minute specimens; while an application time of 4 Hours decreased the scaling damage by nearly two thirds.

Table 4-19: Mix 4-B Scaling Data

Mix 4-B Linseed Oil						
Relative Humidity	Specimens	Scaled Mass at 30 Cycles (g/m^2)	Change in Scaling Amount from 30 Minutes (%)	Scaled Mass at 60 Cycles (g/m2)	Change in Scaling Amount from 30 Minutes (%)	Damage Occuring in First 15 Cycles (%)
27%	30 Minutes	381.5	-----	609.1	-----	13%
	2 Hours	69.7	-82%	300.6	-51%	4%
	4 Hours	23.7	-94%	217.1	-64%	2%

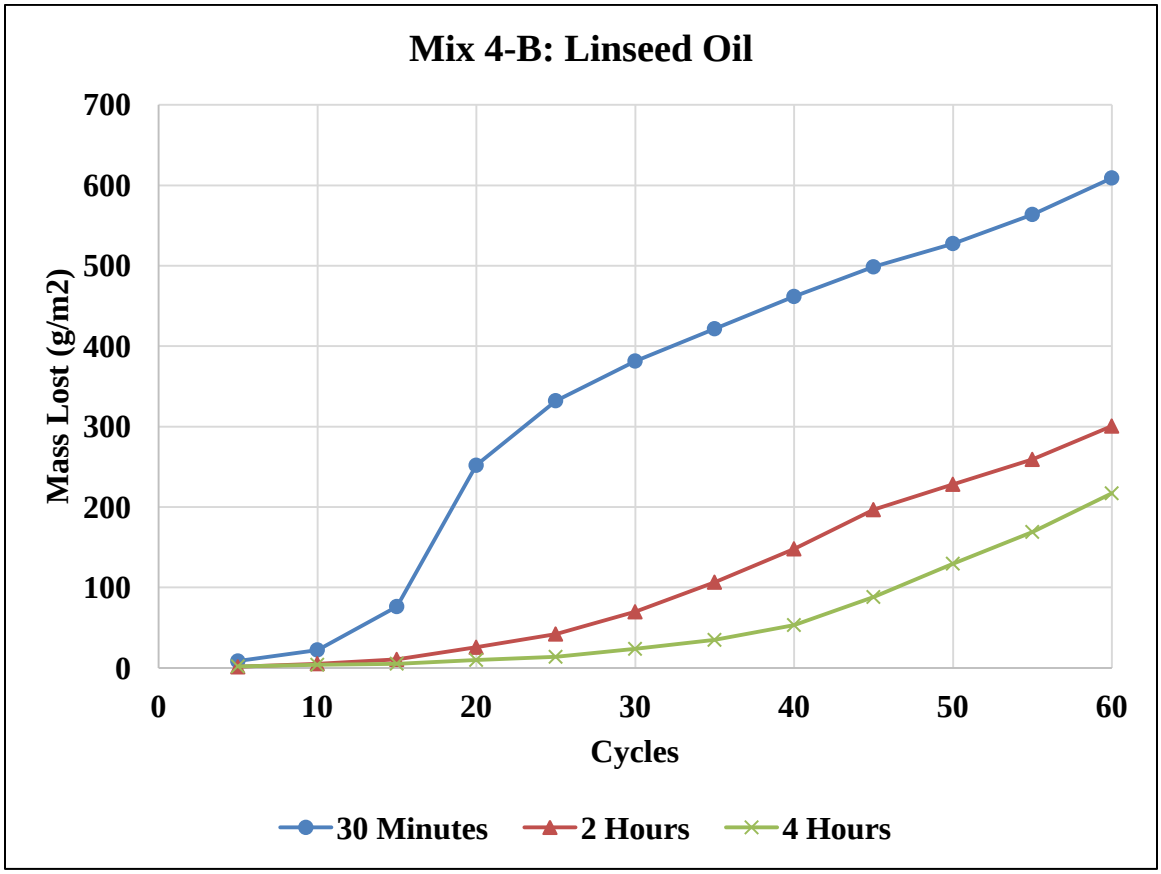

Figure 4-17: Mix 4-B Cumulative Scaling

4.2.4.3 Wax

Scaling data for Mix 4-C in Table 4-20 shows that the while the 4 Hour specimens scaled less than the 30 Minute specimens, the 2 Hour specimens exhibited an increase in scaling damage of 78% over the 30 Minute specimens. The damage accumulation curves in Figure 4-18 show that while all

specimens from all three application times scaled at roughly the same rate from 10-60 cycles, the 2 Hour specimens exhibited higher amounts of scaling within the first 10 cycles than the specimens from the other two application times. Possible reasons as to why the 2 Hour specimens lost more mass than the other application time specimens are discussed in Section 4.4.2.

Table 4-20: Mix 4-C Scaling Data

Mix 4-C Wax						
Relative Humidity	Specimens	Scaled Mass at 30 Cycles (g/m^2)	Change in Scaling Amount from 30 Minutes (%)	Scaled Mass at 60 Cycles (g/m2)	Change in Scaling Amount from 30 Minutes (%)	Damage Occuring in First 15 Cycles (%)
25%	30 Minutes	139.5	-----	178.9	-----	66%
	2 Hours	260.5	87%	317.7	78%	73%
	4 Hours	91.4	-34%	147.3	-18%	38%

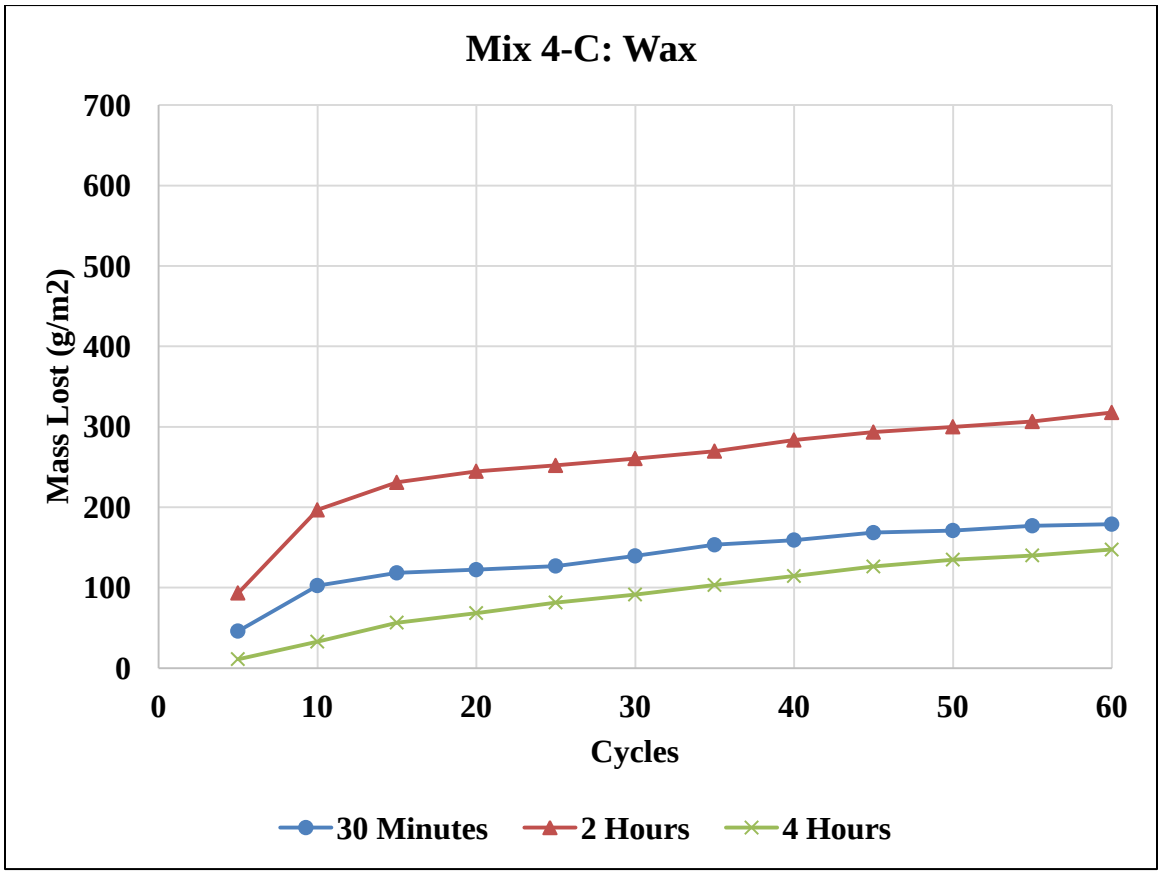

Figure 4-18: Mix 4-C Cumulative Scaling

4.2.4.4 PAMS

In the scaling data for Mix 4-D in Table 4-21, the percentage of total damage occurring within the first 15 cycles decreased with an increase in the application time. This is also shown in Figure 4-19, where the scaling damage accumulation curves show that the total amount of scaling damage was heavily dependent on the amount of scaling that occurred within the first 10 cycles. It should be noted that while the 4 Hour specimens exhibited nearly 29% less scaling damage than the 30 Minute specimens after 60 cycles, the 2 Hour specimens only exhibited a reduction in scaling of about 1%.

Table 4-21: Mix 4-D Scaling Data

Mix 4-D PAMS						
Relative Humidity	Specimens	Scaled Mass at 30 Cycles (g/m^2)	Change in Scaling Amount from 30 Minutes (%)	Scaled Mass at 60 Cycles (g/m2)	Change in Scaling Amount from 30 Minutes (%)	Damage Occuring in First 15 Cycles (%)
28%	30 Minutes	531.5	-----	599.9	-----	77%
	2 Hours	444.0	-16%	591.4	-1%	59%
	4 Hours	246.7	-54%	426.9	-29%	36%

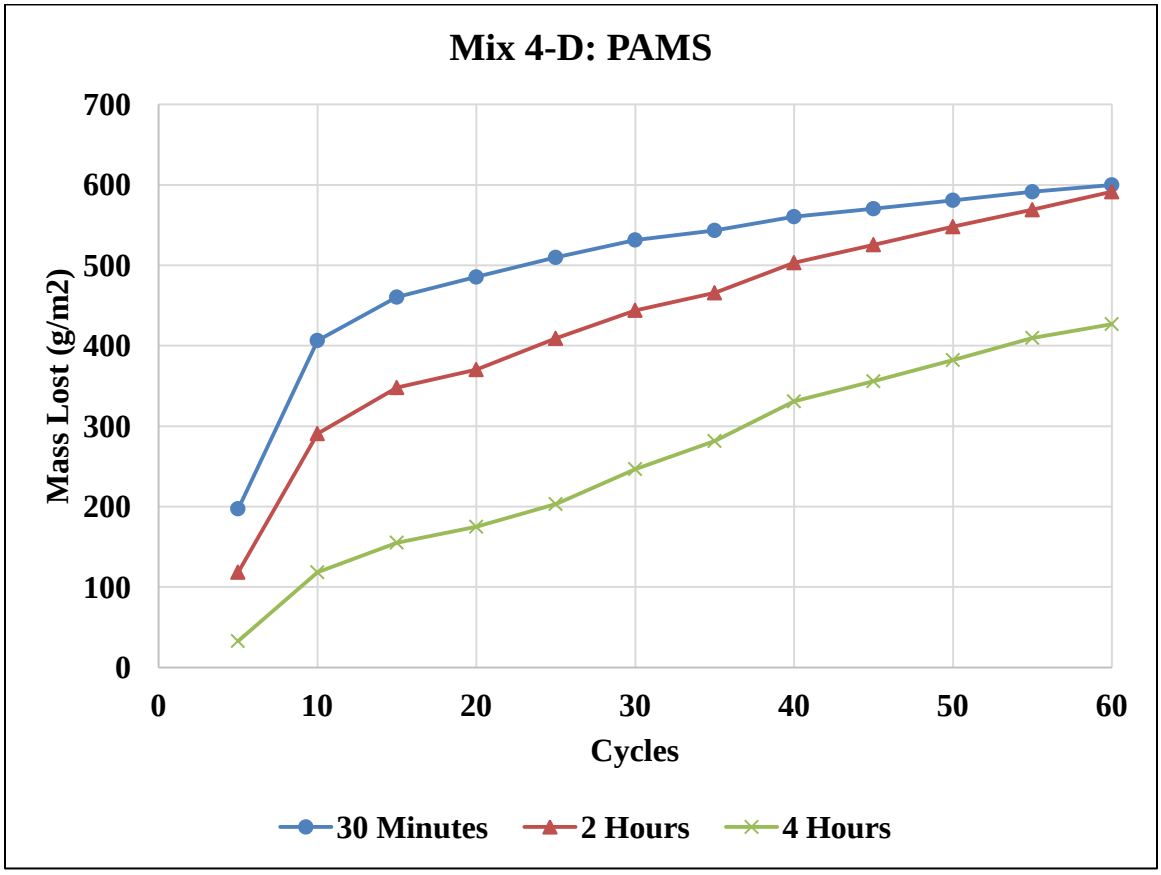

Figure 4-19: Mix 4-D Cumulative Scaling

4.2.4.5 Acrylic

For the Acrylic-coated Mix 4-E specimens within Table 4-22, applying the acrylic at 4 Hours reduced the amount of scaling by over 300 g/m^2 compared to the 30 Minute specimens. In Figure 4-20, the 30 Minute specimens both lost more surface mass initially, and had higher rates of scaling throughout the remainder of the test than the 4 Hour specimens. Both specimen sets suffered nearly half their total damage within the first 15 cycles.

Table 4-22: Mix 4-E Scaling Data

Mix 4-E Acrylic						
Relative Humidity	Specimens	Scaled Mass at 30 Cycles (g/m^2)	Change in Scaling Amount from 30 Minutes (%)	Scaled Mass at 60 Cycles (g/m2)	Change in Scaling Amount from 30 Minutes (%)	Damage Occuring in First 15 Cycles (%)
76%	30 Minutes	277.6	-----	386.1	-----	58%
	4 Hours	35.5	-87%	48.0	-88%	48%

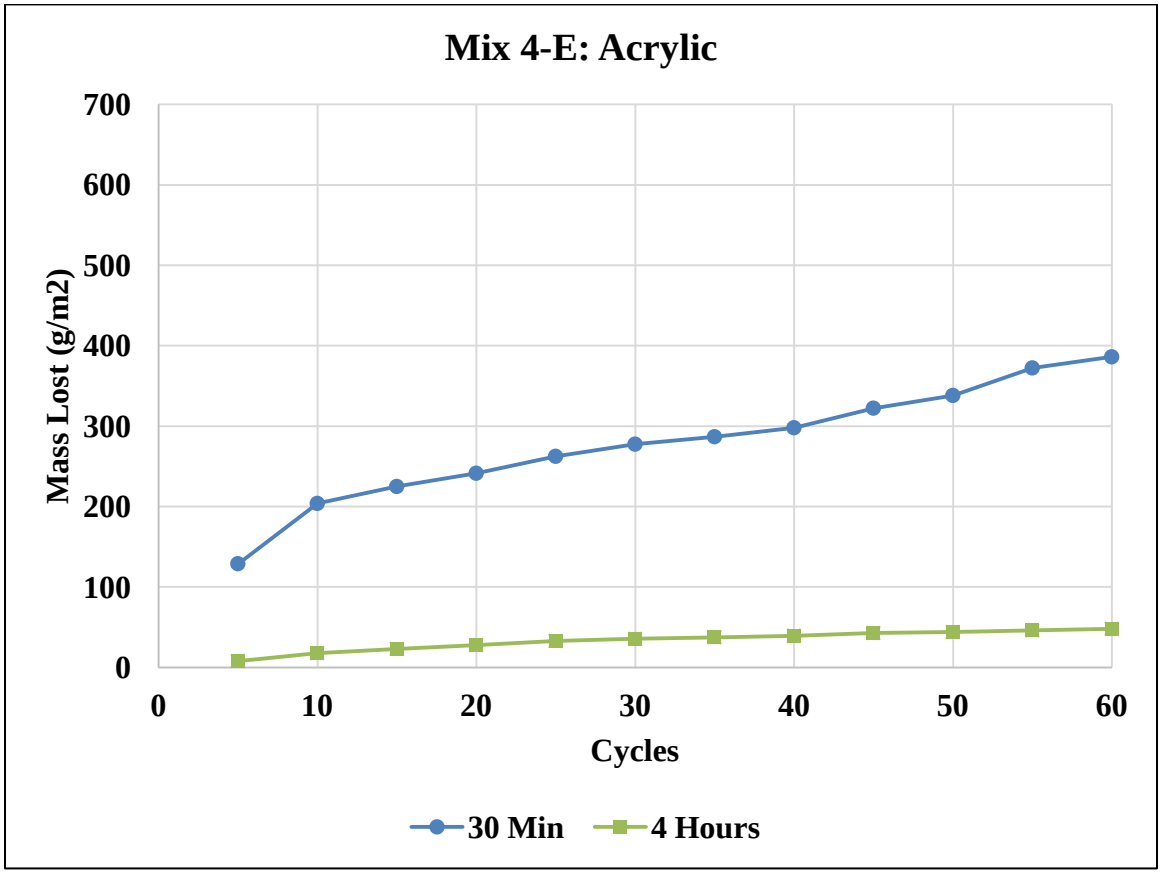

Figure 4-20: Mix 4-E Cumulative Scaling

4.2.5 Effect of Application Time on Mix Type 5: Glacial Gravel and 30% Replacement Slag

Mix Type 5 contained the glacial gravel in addition to a 30% replacement of OPC with Grade 100 Slag Cement. These mixes typically coincided with lower air content values than Mixes 1-4, and the Wet Room, Wax, and Acrylic specimens were poured in environments where the relative

humidity exceeded 60%, as noted in Appendix B. All charts in this section use a mass loss scale of up to 1600 g/m^2.

4.2.5.1 Wet Room Cured

The scaling damage data in Table 4-23 indicates the average total mass loss amount for Mix 5-A Wet Room specimens was over 200 g/m^2, with nearly a third of the damage accumulating in the first 15 cycles. As shown in Figure 4-21, the progressive scaling accumulation was relatively constant over the 60 cycles.

Table 4-23: Mix 5-A Scaling Data

Mix 5-A Wet Room Cured			
Relative Humidity	Scaled Mass at 30 Cycles (g/m^2)	Scaled Mass at 60 Cycles (g/m2)	Damage Occuring in First 15 Cycles (%)
64%	90.1	202.6	29%

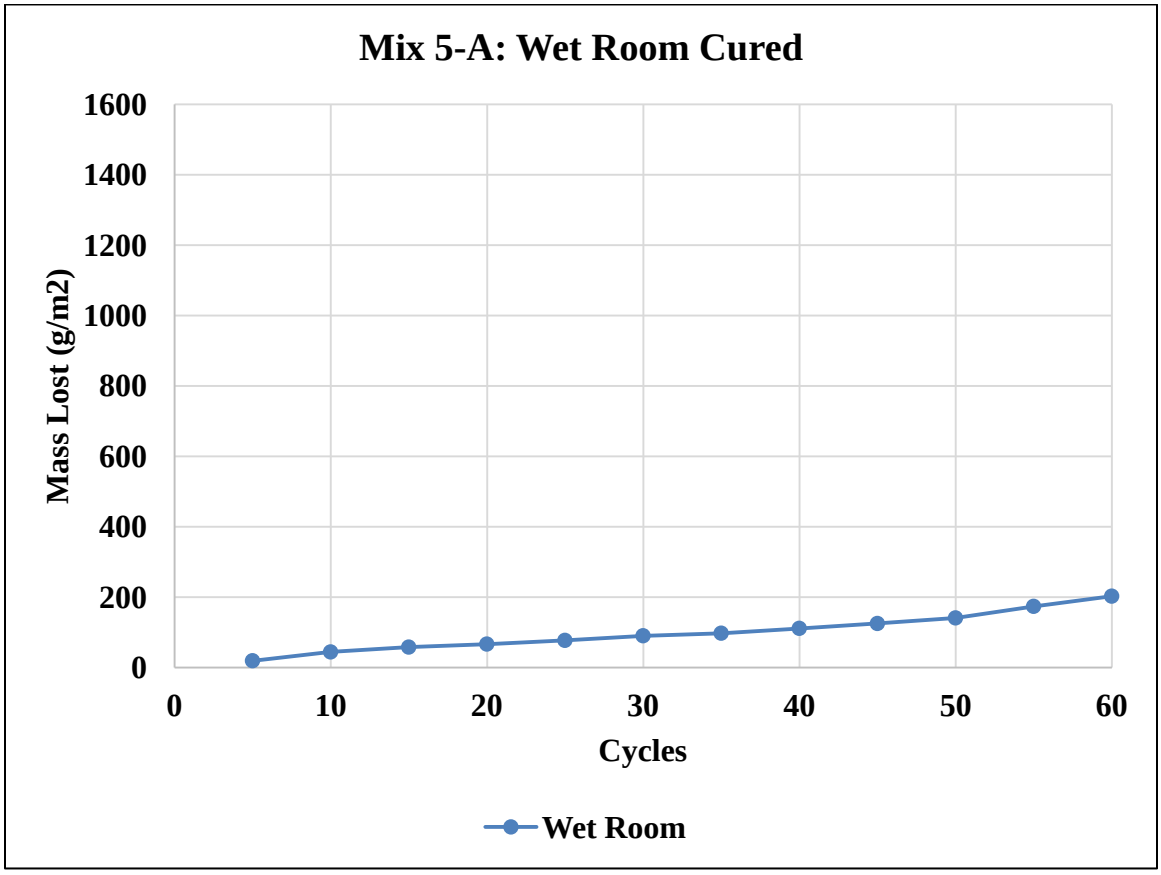

Figure 4-21: Mix 5-A Cumulative Scaling

4.2.5.2 Linseed Oil

In the scaling data for Mix 5-B in Table 4-24, the 30 Minute specimens exhibited an average of 1295 g/m^2 of total damage. By applying the Linseed Oil either at 2 or 4 Hours, total damage was reduced by nearly two-thirds to nearly 480 g/m^2. However, no additional significant scaling resistance was exhibited by increasing the application time from 2 Hours to 4 Hours. The scaling damage accumulation curves in Figure 4-22 show that the 30 Minute specimens lost surface mass much faster than the other two specimen sets, losing over 1000 g/m^2 after 30 cycles.

Table 4-24: Mix 5-B Scaling Data

Mix 5-B Linseed Oil						
Relative Humidity	Specimens	Scaled Mass at 30 Cycles (g/m^2)	Change in Scaling Amount from 30 Minutes (%)	Scaled Mass at 60 Cycles (g/m2)	Change in Scaling Amount from 30 Minutes (%)	Damage Occuring in First 15 Cycles (%)
33%	30 Minutes	1001.8	-----	1295.2	-----	38%
	2 Hours	276.9	-72%	480.2	-63%	33%
	4 Hours	168.4	-83%	478.9	-63%	5%

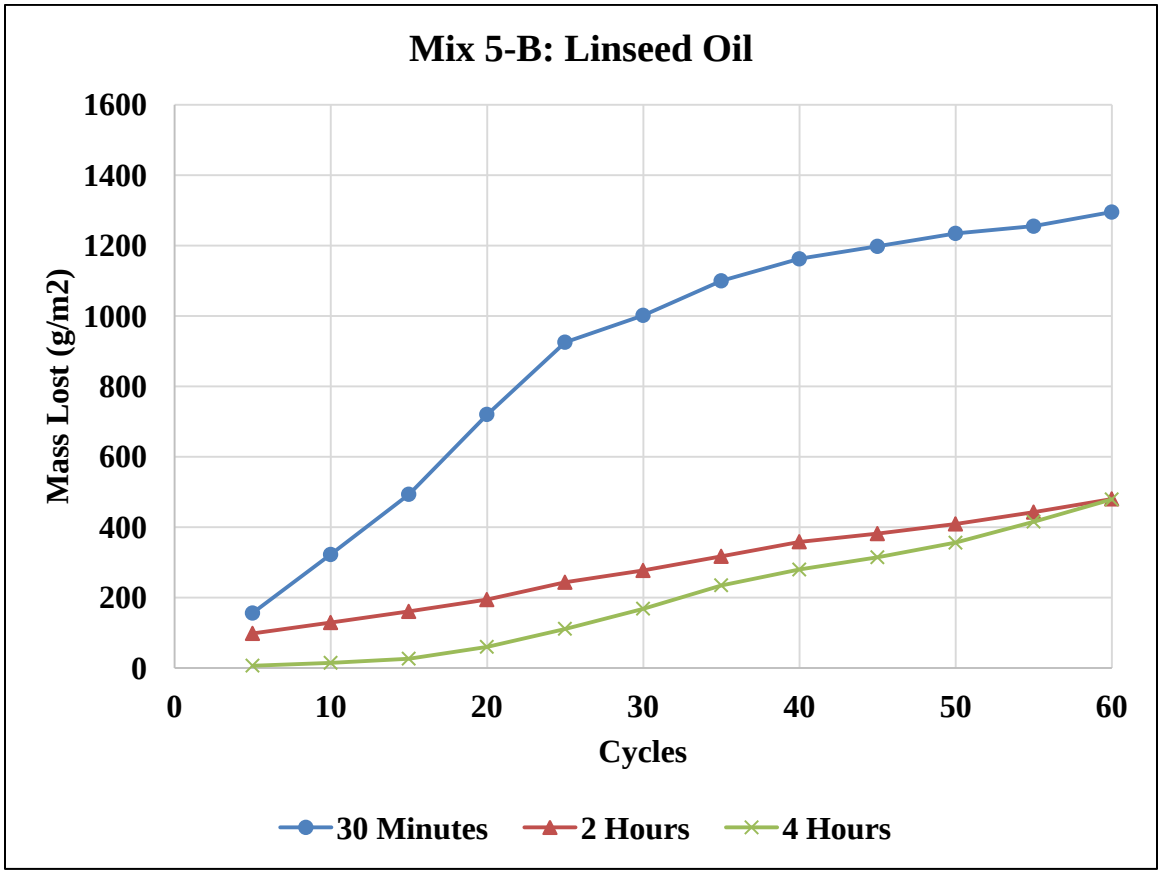

Figure 4-22: Mix 5-B Cumulative Scaling

4.2.5.3 Wax

The scaling results from Mix 5-C's specimens in both Table 4-25 and Figure 4-23 show that all specimen sets from Mix 5-C suffered nearly 70% of their total damage within the first 15 cycles. Additionally, all three specimen sets exhibited scaling damage on average in excess of 1000 g/m^2.

The 30 Minute specimens scaled the least throughout the test, while the 2 Hour specimens scaled the most of the three sets. It is important to note that these specimens have three potential explanations for the magnitude of scaling suffered and the perceived independence of scaling resistance from application time: the inclusion of slag, the use of Wax curing compound and a high relative humidity at time of specimen manufacture. A discussion on the potential effects of these three sources on the poor scaling performance are discussed in Sections 4.4.1, 4.4.2, and 4.4.3, respectively.

Table 4-25: Mix 5-C Scaling Data

Mix 5-C Wax						
Relative Humidity	Specimens	Scaled Mass at 30 Cycles (g/m^2)	Change in Scaling Amount from 30 Minutes (%)	Scaled Mass at 60 Cycles (g/m2)	Change in Scaling Amount from 30 Minutes (%)	Damage Occuring in First 15 Cycles (%)
68%	30 Minutes	881.5	-----	1082.1	-----	75%
	2 Hours	1078.8	22%	1427.4	32%	69%
	4 Hours	1003.8	14%	1331.4	23%	69%

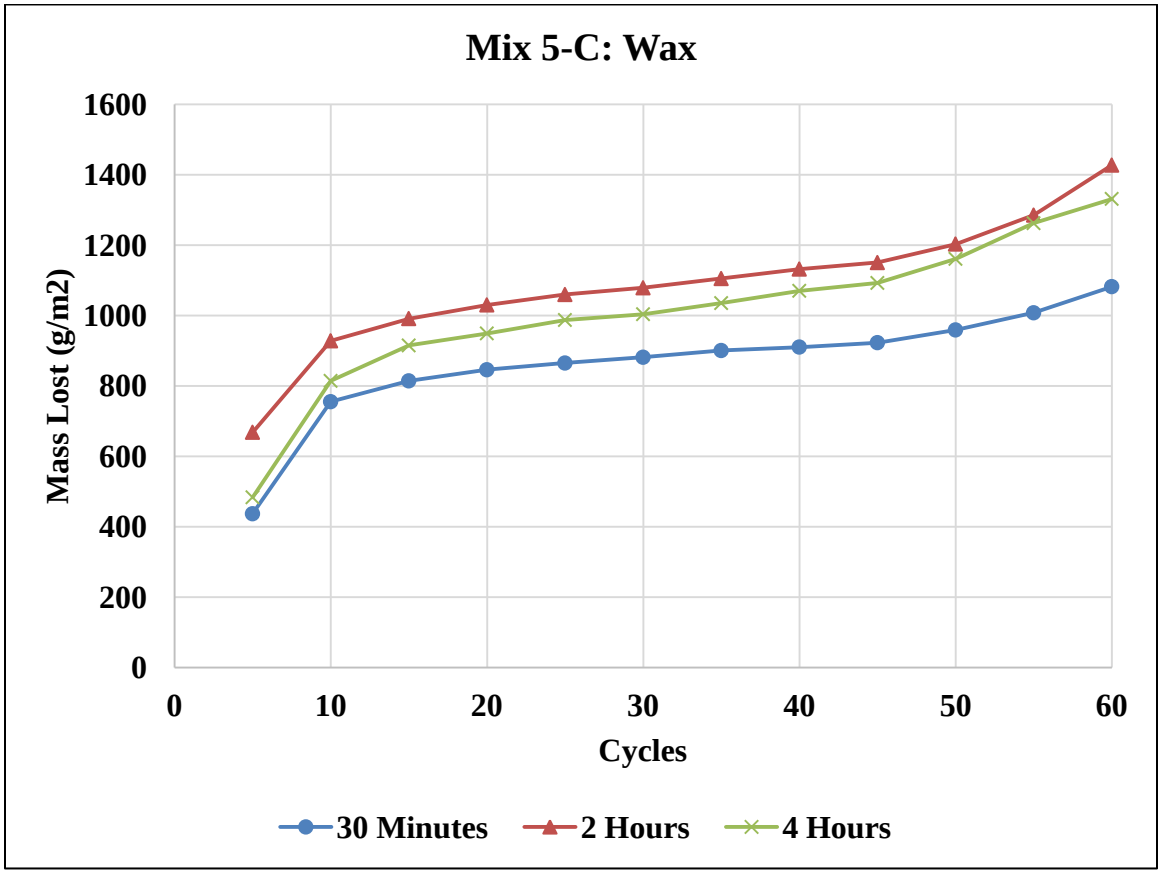

Figure 4-23: Mix 5-C Cumulative Scaling

4.2.5.4 PAMS

In Figure 4-24, all three application time scaling accumulation curves for Mix 5-D scaled nearly identically after 5 cycles and possessed approximately the same rates of mass loss accumulation after 15 cycles. However, Table 4-26 illustrates that the 2 and 4 Hour specimen sets exhibited 64% and 21% more total scaling damage than the 30 Minute specimens, respectively. This is primarily due to the rapid degradation of the concrete surface of both the 2 and 4 Hour specimen sets between 5 and 10 cycles. Possible explanations for why these scaling patterns occurred are discussed Section 4.4.1.

Table 4-26: Mix 5-D Scaling Data

Mix 5-D PAMS						
Relative Humidity	Specimens	Scaled Mass at 30 Cycles (g/m^2)	Change in Scaling Amount from 30 Minutes (%)	Scaled Mass at 60 Cycles (g/m2)	Change in Scaling Amount from 30 Minutes (%)	Damage Occuring in First 15 Cycles (%)
26%	30 Minutes	578.9	-----	655.8	-----	77%
	2 Hours	959.1	66%	1074.8	64%	82%
	4 Hours	691.3	19%	791.3	21%	82%

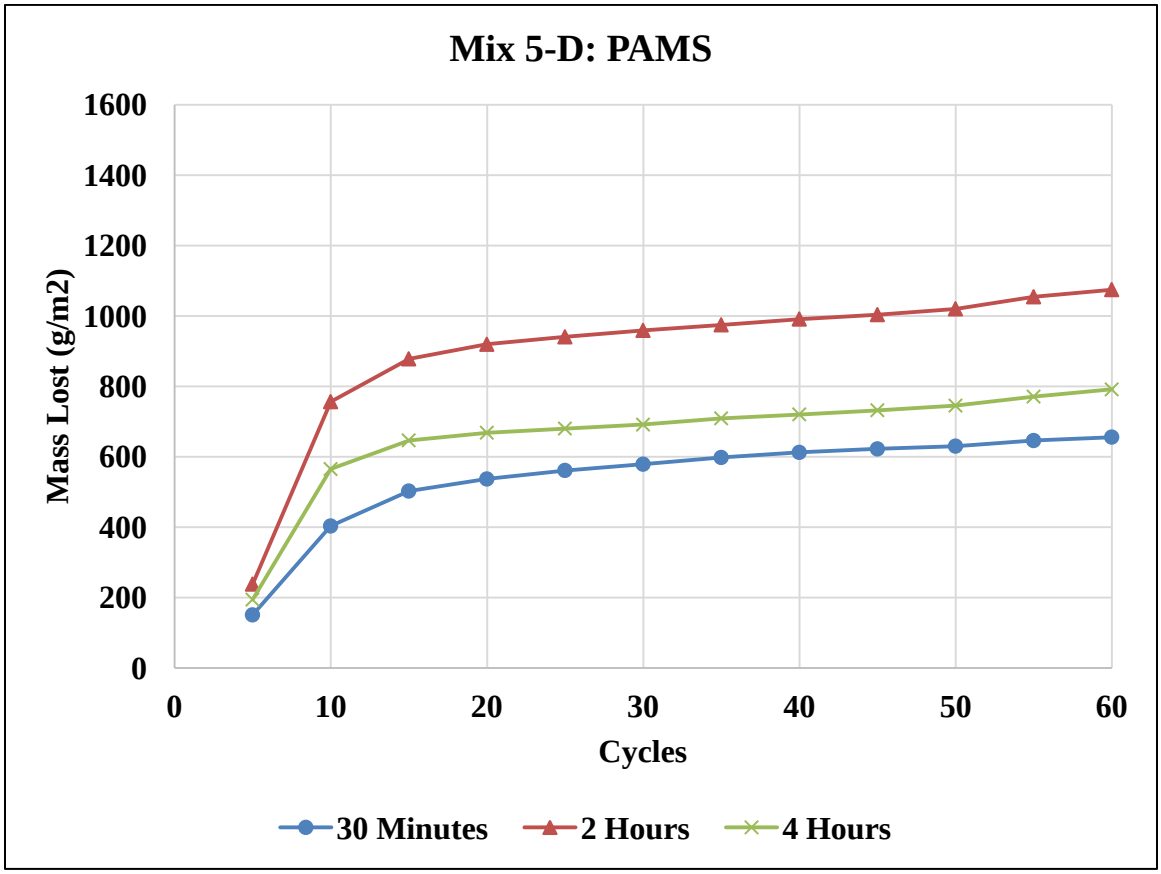

Figure 4-24: Mix 5-D Cumulative Scaling

4.2.5.5 Acrylic

In the scaling data for Mix 5-E listed in Table 4-27, the total mass loss from the 30 Minute application time was reduced by 45% or nearly 360 g/m^2 when the application time was extended to 4 Hours. While both sets of specimens suffered the majority of their total damage early within the first

15 cycles, Figure 4-25 shows that the 30 Minute damage accumulation curve was slightly more severe over the entire 60 cycles than the 4 Hour specimens.

Table 4-27: Mix 5-E Scaling Data

Mix 5-E Acrylic						
Relative Humidity	Specimens	Scaled Mass at 30 Cycles (g/m^2)	Change in Scaling Amount from 30 Minutes (%)	Scaled Mass at 60 Cycles (g/m2)	Change in Scaling Amount from 30 Minutes (%)	Damage Occuring in First 15 Cycles (%)
75%	30 Minutes	536.1	-----	808.4	-----	58%
	4 Hours	380.9	-29%	444.0	-45%	73%

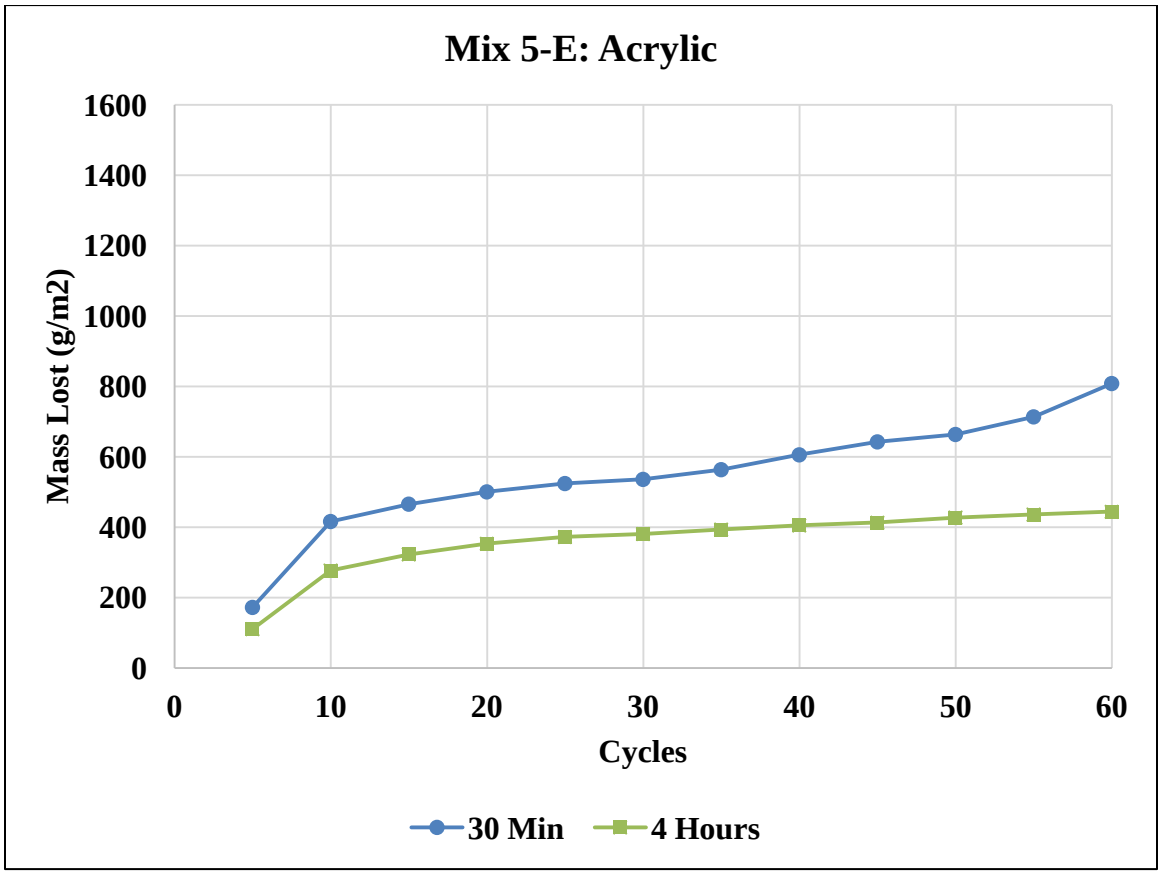

Figure 4-25: Mix 5-E Cumulative Scaling

4.2.6 Effect of Application Time on Mix Type 6: Glacial Gravel and 30% Replacement Fly Ash

Mix Type 6 contained Glacial Gravel with a 30% by weight replacement of cement with Class C Fly Ash. The scaling performance of two application times for each compound were evaluated for this mix type: 30 Minutes and 4 Hours. As noted in Table 4-1, these concrete batches were characterized by high slumps and the Wet Room, Wax, and Acrylic batches were manufactured during periods of high laboratory relative humidity. All charts in this section have a mass loss scale up to 2000 g/m^2.

4.2.6.1 Wet Room

As noted in Table 4-28, the Wet Room cured specimens for Mix Type 6 scaled an average amount of 312.5 g/m^2. It should be noted that the relative humidity at the time of manufacture was high at 83%. The scaling accumulation trend in Figure 4-26 exhibited approximately stable rates of progressive damage accrual.

Table 4-28: Mix 6-A Scaling Data

Mix 6-A Wet Room Cured			
Relative Humidity	Scaled Mass at 30 Cycles (g/m^2)	Scaled Mass at 60 Cycles (g/m2)	Damage Occuring in First 15 Cycles (%)
83%	125.6	312.5	21%

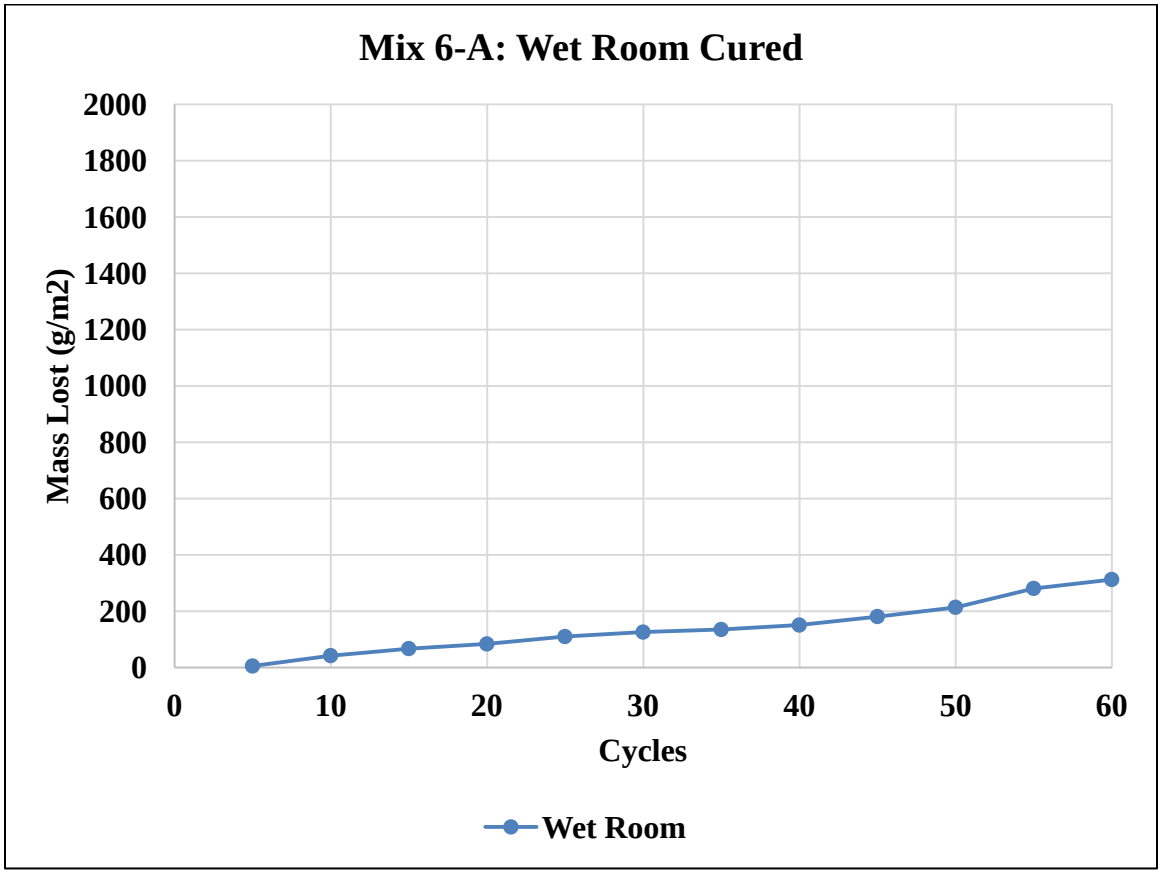

Figure 4-26: Mix 6-A Cumulative Scaling

4.2.6.2 Linseed Oil

In Table 4-29, the Mix 6-B 30 Minute specimens on average exhibited scaling in excess of 1400 g/m^2, while extending the application time to 4 Hours reduced the scaling damage by approximately 50% to an average of approximately 726 g/m^2. Figure 4-27 shows that the 30 Minute specimens suffered significant mass loss immediately, with very high rates of loss throughout the test. In contrast, the 4 Hour specimens exhibited low scaling damage during the first 20 cycles, followed by progressive mass loss at rates nearly equal to the 30 Minute specimens during the final 40 cycles.

Table 4-29: Mix 6-B Scaling Data

Mix 6-B Linseed Oil						
Relative Humidity	Specimens	Scaled Mass at 30 Cycles (g/m^2)	Change in Scaling Amount from 30 Minutes (%)	Scaled Mass at 60 Cycles (g/m2)	Change in Scaling Amount from 30 Minutes (%)	Damage Occuring in First 15 Cycles (%)
31%	30 Minutes	854.5	-----	1461.6	-----	36%
	4 Hours	176.3	-79%	726.2	-50%	3%

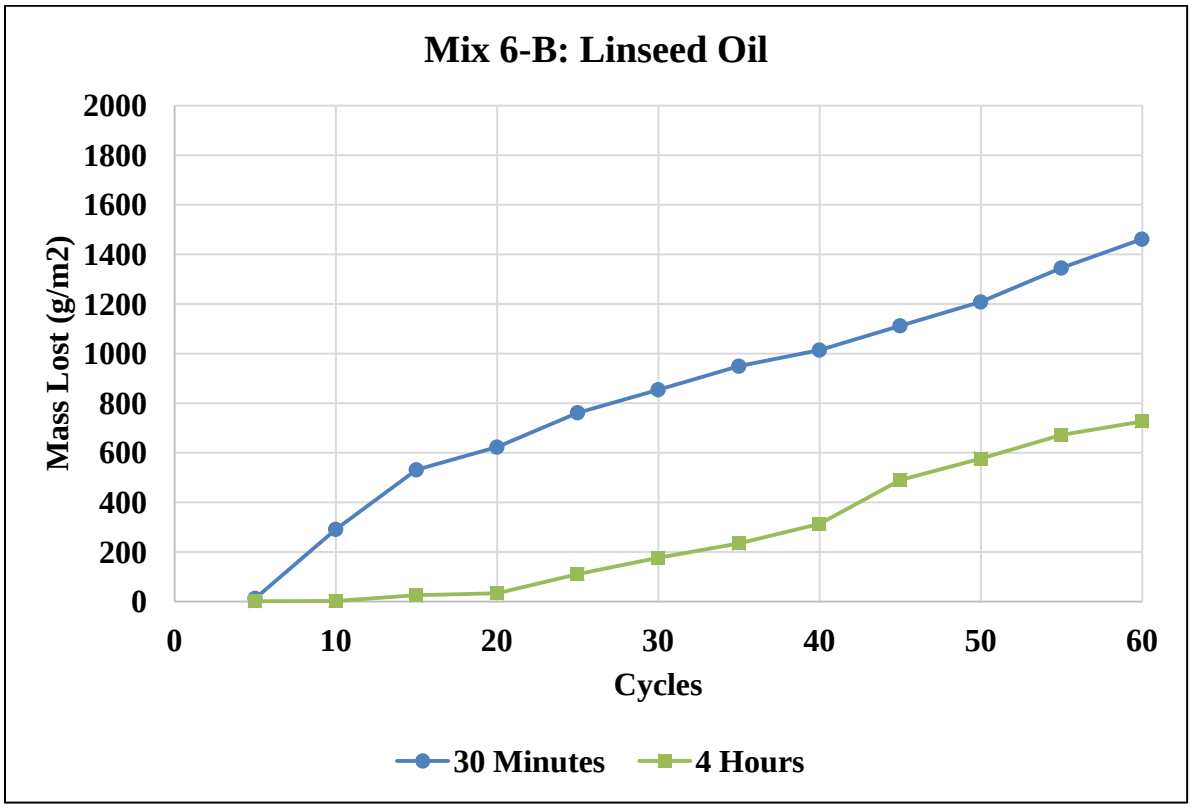

Figure 4-27: Mix 6-B Cumulative Scaling

4.2.6.3 Wax

As shown in Table 4-30, the total scaling amounts of both the 30 Minute and 4 Hour Mix 6-C specimens were nearly identical, with the 4 Hour specimens suffering slightly more damage than the 30 Minute specimens. Throughout the test, the 4 Hour specimens scaled more than the 30 Minute specimens, as shown by Figure 4-28. Both sets of specimens exhibited average total scaling damage levels exceeding 780 g/m^2. The specimens from this batch of concrete were manufactured and coated

when the laboratory air had an elevated relative humidity level of 65%. The potential effects of the Wax curing compound and the elevated laboratory relative humidity on the scaling patterns are discussed in Sections 4.4.2 and 4.4.3, respectively.

Table 4-30: Mix 6-C Scaling Data

Mix 6-C Wax						
Relative Humidity	Specimens	Scaled Mass at 30 Cycles (g/m^2)	Change in Scaling Amount from 30 Minutes (%)	Scaled Mass at 60 Cycles (g/m2)	Change in Scaling Amount from 30 Minutes (%)	Damage Occuring in First 15 Cycles (%)
65%	30 Minutes	380.2	-----	783.4	-----	37%
	4 Hours	506.5	33%	801.2	2%	44%

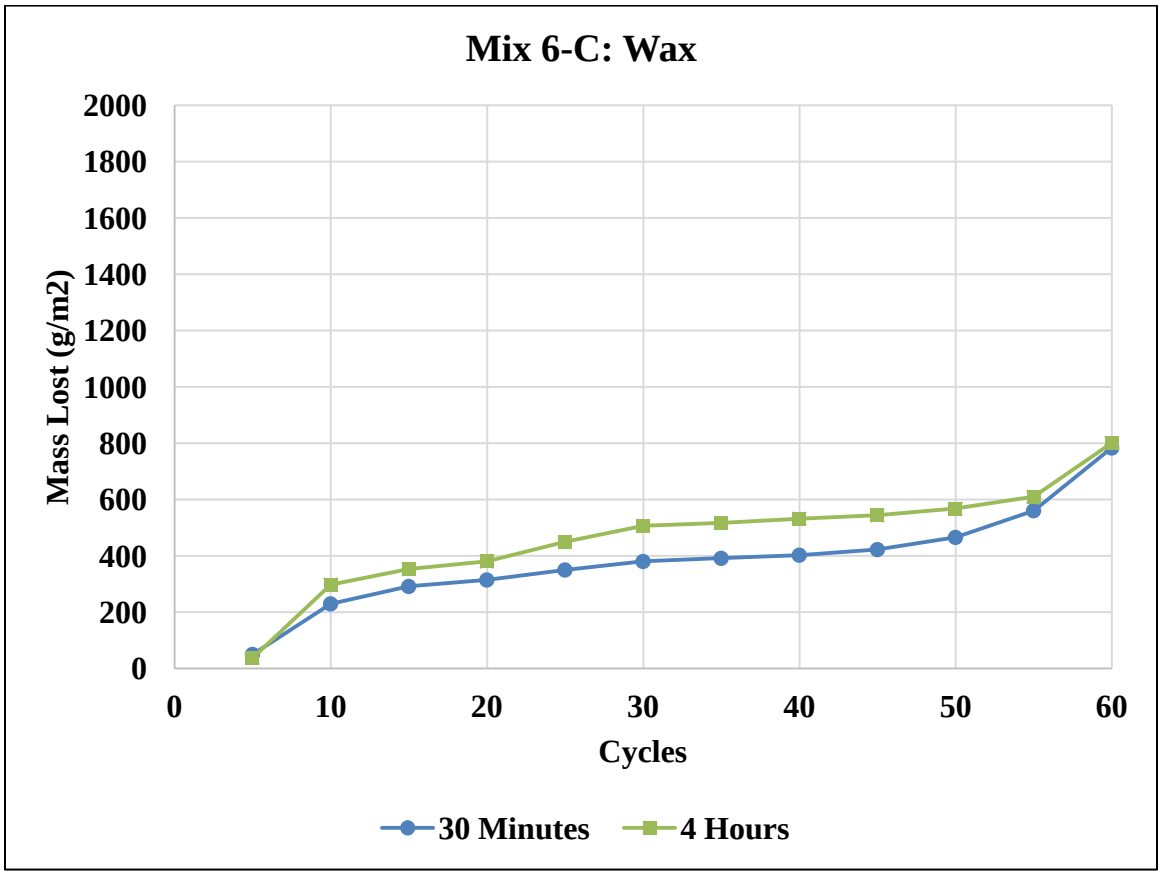

Figure 4-28: Mix 6-C Cumulative Scaling

4.2.6.4 PAMS

Both the 30 Minute and 4 Hour specimens for Mix 6-D exhibited total scaling damage levels under 260 g/m^2, as shown in Table 4-31. The 4 Hour specimen set suffered slightly less total damage than the 30 Minute specimens. The scaling damage accumulation curves in Figure 4-29 show very little difference in scaling damage between the two specimen sets over the 60 cycles. Possible explanations for why the scaling amounts for the two application times were so similar are discussed in Section 4.4.4.

Table 4-31: Mix 6-D Scaling Data

Mix 6-D PAMS						
Relative Humidity	Specimens	Scaled Mass at 30 Cycles (g/m^2)	Change in Scaling Amount from 30 Minutes (%)	Scaled Mass at 60 Cycles (g/m2)	Change in Scaling Amount from 30 Minutes (%)	Damage Occuring in First 15 Cycles (%)
30%	30 Minutes	164.5	-----	257.2	-----	37%
	4 Hours	229.6	40%	251.3	-2%	64%

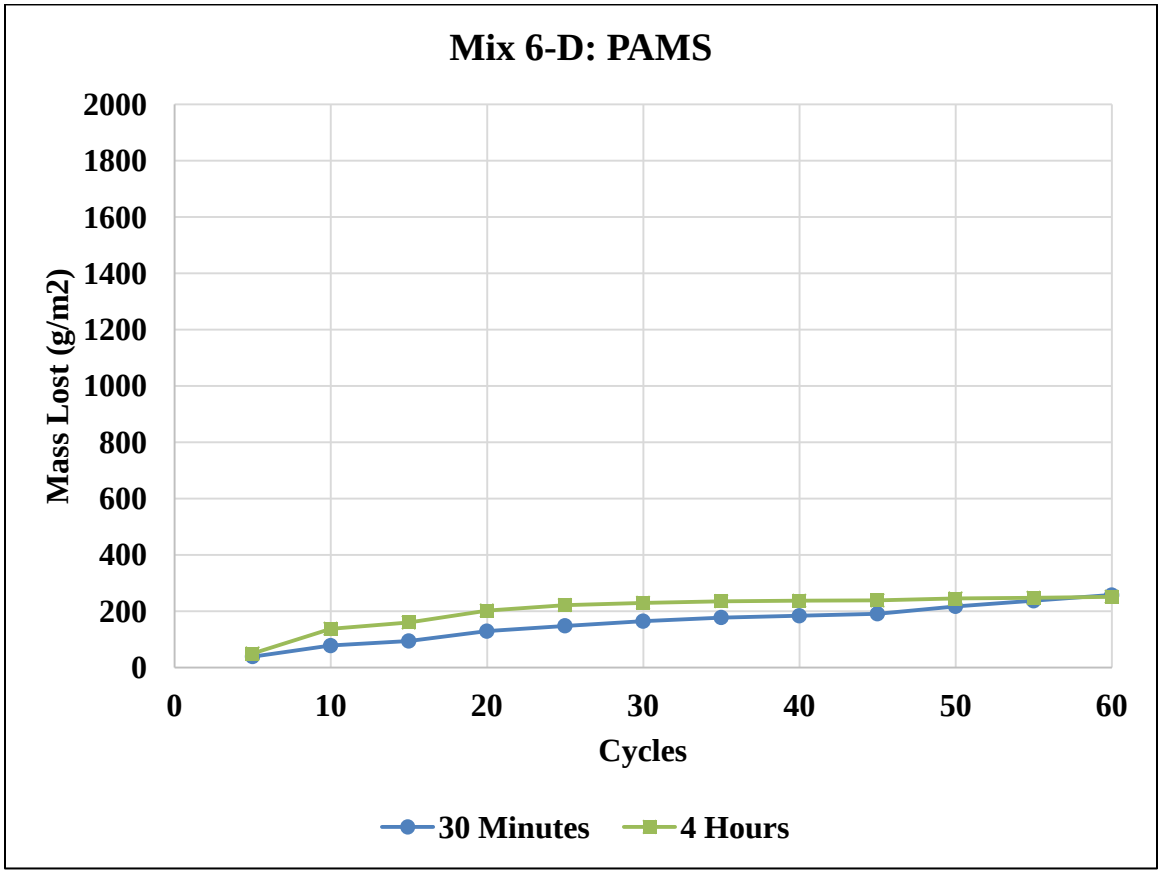

Figure 4-29: Mix 6-D Cumulative Scaling

4.2.6.5 Acrylic

As shown in Table 4-32, the Mix 6-E 30 Minute specimens exhibited amounts of scaling damage at an average in excess of 1900 g/m^2, while the 4 Hour specimens exhibited an average mass loss of slightly more than 210 g/m^2; an overall reduction in damage of 89%. The scaling damage accumulation curve for the 30 Minute specimens in Figure 4-30 demonstrates that an average of over 1000 g/m^2 of surface mass was lost within the first 10 cycles. The relative humidity in the laboratory during the time of specimen manufacture was very high at 83%. The potential effect that this high relative humidity may have had on the very poor scaling resistance of the 30 Minute specimens is discussed in Section 4.4.3.

Table 4-32: Mix 6-E Scaling Data

Mix 6-E Acrylic						
Relative Humidity	Specimens	Scaled Mass at 30 Cycles (g/m^2)	Change in Scaling Amount from 30 Minutes (%)	Scaled Mass at 60 Cycles (g/m2)	Change in Scaling Amount from 30 Minutes (%)	Damage Occuring in First 15 Cycles (%)
83%	30 Minutes	1582.0	-----	1933.9	-----	64%
	4 Hours	173.0	-89%	213.8	-89%	44%

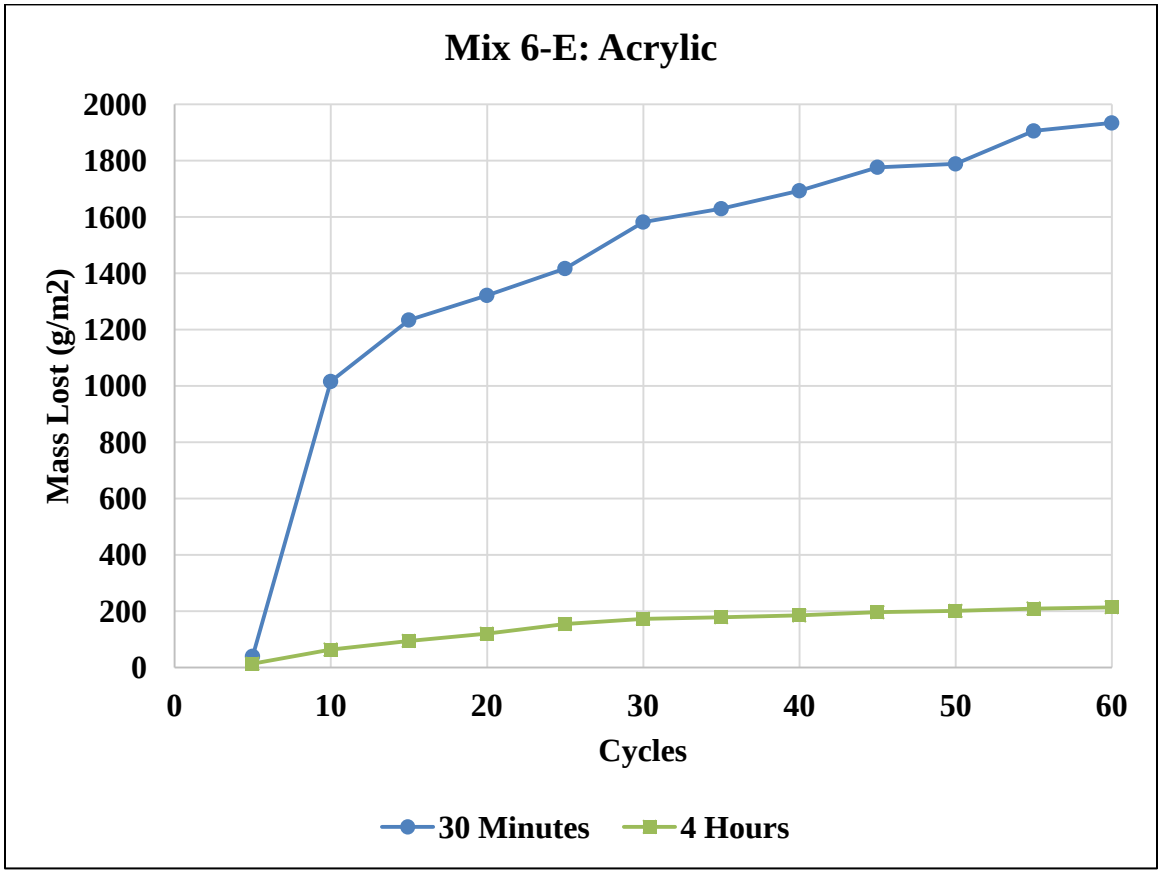

Figure 4-30: Mix 6-E Cumulative Scaling

4.3 Statistical Analysis of ASTM C672 Results

The specimen testing matrix located in Appendix A was assembled with four factors: aggregate type, cementitious material, curing compound type, and application time. Application time

was the primary factor. The analysis within this section was performed using the scaling data from the full factorial population of 198 ASTM C672 specimens to observe scaling damage trends from each factor and to establish statistical significance for comparisons between application times.

Three types of statistical tests were used to analyze the data: Student's t-test for significant difference, one-factor Analysis of Variance (ANOVA), and two-factor ANOVA. For the purpose of analysis within Section 4.3.1, the samples sizes taken from the initial population size of 198 were assumed to be normally distributed. Although the full distribution of scaling data from all 198 specimens may not have strictly followed the Normal Distribution, the Central Limit Theorem allows for the assumption of normality if the sample sizes taken from the total population number 30 data points or larger (Nelson, 2003).

For the ANOVA tests within Sections 4.3.2 and 4.3.3, the samples sizes for each test were less than 30, so normality could not assumed immediately by the Central Limit Theorem. However, normality can be assumed for the purpose of the ANOVA test if the residuals of the samples means are approximately normal (Nelson, 2003). A derivation that confirms that this was true for the scaling data set used in this study is located in Appendix E. The Student's t-tests performed in Section 4.3.4 assumed unpaired samples with unequal variances being tested to identify significant differences between the sample means. The sample sizes for each test were three, corresponding to the three replicates of each mix type-curing compound-application time subset. While it is certainly ideal to have larger sample sizes, the Student's t-test has been determined to be robust enough to analyze samples sizes as small as two (de Winter, 2013).

It is important to note that the specimen testing matrix in Appendix A did not include 2 Hour specimens for all batches containing fly ash or batches coated with Acrylic. In order to perform ANOVA testing, the data sets must be balanced. Therefore, it was not possible run ANOVA tests on data sets with missing replicates of entire factors without introducing potentially inaccurate

inferences. Where fly ash or acrylic were included in the ANOVA analysis, all other 2 Hour specimens from the other treatment types were not included to prevent unbalanced data sets. Wet Room specimens were also not included in analysis where curing compound or application time were factors.

4.3.1 Analysis by Concrete Composition

The first two factors, aggregate type and cementitious material were analyzed for significance with respect to scaling resistance in this section. This included two levels of aggregate type: limestone and glacial gravel; along with three levels of cementitious material: OPC, 30% slag replacement and 30% fly ash replacement.

4.3.1.1 Impact of Coarse Aggregate on Concrete Scaling

A one-factor ANOVA test was performed on the total population of scaling data to compare differences between the two aggregates used within this study. A confidence level of 95% was used to assess the statistical difference between the means of the two aggregates. Of the 198 specimens evaluated in this study, 99 contained the crushed limestone and 99 contained the glacial gravel. As shown in Table 4-33, this analysis returned that the difference in overall mean of scaling data between the two aggregates were statistically significant. Statistically significant differences imply that the two means can be compared directly. Gravel-containing specimens typically scaled more than Limestone-containing specimens within this project.

Table 4-33: One-Factor ANOVA Analysis of Scaling Data between Aggregates

Aggregate	Sample Sizes	Scaling Mean (g/m^2)	Statistical Significance
Limestone	99	481.6	YES
Gravel	99	627.1	

4.3.1.2 Impact of Cementitious Material

A single-factor ANOVA analysis was performed on the specimen scaling data to understand the impact on scaling resistance from alterations in the cementitious content of the concretes. As shown in Table 4-34 the ANOVA results showed statistical significance of difference between the means of the scaling data between the three cementitious materials. Two-tailed, unequal variance Student's t-test were performed comparing the three conditions without 2 Hour specimens. The threshold level was altered in accordance with Bonferroni Correction for multiple t-tests within the same sample groups (Abdi, 2007). Statistical significance was identified between the means of OPC and slag and OPC and fly ash, but not between slag and fly ash for specimen sets not containing the 2 Hour specimen sets. An additional t-test between the OPC and slag scaling data containing their 2 Hour specimen data also found significance between the two cementitious materials, as shown in Table 4-35. Slag and fly ash-containing specimens typically scaled more than OPC-only specimens.

Table 4-34: ANOVA and t-test results of scaling data between Cementitious Materials

Single -Factor ANOVA for Cementitious Materials				t-Test	
Cementitious Material	**Sample Sizes**	**Mean (g/m^2)**	**Statistical Significance**	**t-test Comparison**	**Statistical Significance**
OPC	54	248.9	YES	OPC vs Slag	YES
Slag	54	696.1		OPC vs FA	YES
FlyAsh	54	643.6		Slag vs FA	NO

Table 4-35: Alternate t-test results for OPC/Slag with 2 Hour scaling data included

t-test Comparison	Sample Sizes	Scaling Mean (g/m^2)	Statistical Significance
OPC	72	285.2	YES
Slag	72	756.5	

4.3.2 Analysis by Mix Type

Two-factor ANOVA analysis to compare the scaling damage means was performed on each mix type twice: once for all three application times with Linseed/Wax/PAMS and again on only the 30 Minute and 4 Hour specimens for all four curing compounds, including Acrylic. The purpose of this was to determine for every mix type whether the curing compound, the application time, or an interaction between the curing compound and application time impacted the amount of scaling damage on that particular mix type at a statistically significant level. An interaction is where the impact of changing the level one factor such as application time on the scaling resistance of concrete is dependent upon the level of the other factor; in this case being the curing compound selection. The results are summarized in Table 4-36, where a 'YES' indicates whether the level of that factor or the interaction between the two factors has a significant effect on the amount of scaling damage at a 95% confidence level. A 'NO' in the table indicates that changing the level of a factor or the interaction between the two factors does not significantly alter the scaling damage amount.

Statistically significant interaction effects were observed between the curing compound and application time in every test except for Mix Type 1 and 2 when only the 30 Minute and 4 Hour specimens were tested. This lack of interaction is overshadowed by the fact that the ANOVA tests at all three application times for Linseed, Wax, and PAMS for Mix Type 1 and 2 did observe significant interaction. The presence of interaction effects prevented overall conclusions about whether the choice of curing compound or the choice of application time was more important for determining the scaling resistance of a given mix type.

Table 4-36: Two-Factor ANOVA Results Comparing Application Time and Curing Compound Choice on Scaling Amounts on Selected Mix Types

Mix Type	Linseed/Wax/PAMS between Three Application Times				All Curing Compounds between 30 Minutes and 4 Hours			
	Curing Compound	Application Time	Interaction	Sample Size	Curing Compound	Application Time	Interaction	Sample Size
1	YES	YES	YES	27	YES	NO	NO	24
2	YES	YES	YES	27	YES	YES	NO	24
3					YES	YES	YES	24
4	YES	YES	YES	27	YES	YES	YES	24
5	YES	NO	YES	27	YES	NO	YES	24
6					YES	YES	YES	24

4.3.3 Analysis by Curing Compound-Trend of Application Times

Due to the interaction effects, the influence or lack of an influence of application time on the scaling resistance of concrete was analyzed by grouping the scaling data by curing compound. A one-factor ANOVA analysis was performed on the scaling data for each curing compound individually, with the data segregated into three different levels by application time. Unlike two-factor ANOVA analysis, balanced data sets are not required. This allowed the fly ash data sets to be included. The results from this are shown in Table 4-37.

Statistically significant differences between the means of the applications times were found in the Linseed Oil specimens and the Acrylic specimens, but not the Wax or PAMS specimens. Therefore, a direct comparison of the scaling damage means between the application times for the Linseed Oil and the Acrylic specimens across all mix types can be made at a 95% confidence level. For both Linseed Oil and Acrylic, the amount of scaling damage decreased with an increase in application time. For the Wax and PAMS formulations, the lack of statistically significant differences indicated that direct comparisons between the mean scaling amounts of the application times across all mixes could not be made initially. Therefore, identifying significant differences on a mix-by-mix

basis would be necessary to identify the impact of application time on scaling resistance for Wax and PAMS.

Table 4-37: ANOVA Analysis of Application Time on Scaling Damage for Each Curing Compound

Curing Compound	Sample Size	Application Time	Mean Scaling Amount (g/m^2)	Statistically Significant Differences
Linseed Oil	18	30 Minutes	1059.5	YES
	12	2 Hours	564.7	
	18	4 Hours	499.4	
Wax	18	30 Minutes	623.4	NO
	12	2 Hours	796.3	
	18	4 Hours	539.8	
PAMS	18	30 Minutes	457.2	NO
	12	2 Hours	747.9	
	18	4 Hours	444.2	
Acrylic	18	30 Minutes	770.3	YES
	18	4 Hours	228.0	

4.3.4 Analysis of Application Time on Scaling Damage for Each Mix Type-Curing Compound Combination

Student's t-tests were performed to determine if meaningful comparisons between application times could be made for each mix-type curing compound combination within this study. These tests were grouped by Mix Type. A sample size of three replicate specimens was used for each application time within each mix type-curing compound combination. The tests for significance between the means of the scaling data within this analysis assumed the means were the same as a null hypothesis, were two-tailed, and at a confidence level of 95%. If significance between the means was identified, indicated by a 'YES' within the tables, then a meaningful comparison of the scaling damage means could be made to assess if application time increased or decreased the scaling damage. If no

significance difference was found, a comparison between the two application times could not be made confidently.

4.3.4.1 Mix Type 1: t-tests for Significance Differences within Scaling Damage Means of Application Time

The comparisons of scaling damage results for all application times of all curing compounds on Mix Type 1 are summarized in Table 4-38. For Linseed Oil and PAMS, no statistically significant differences of scaling damage were observed between application times. For Wax, statistically significant differences were observed when comparing the 30 Minute or 4 Hour specimens to the 2 Hours specimens. Significant differences were observed between the 30 Minute and 4 Hour Acrylic specimens.

Table 4-38: t-Tests for Significance Differences between Application times for Mix Type 1 Specimens

Curing Compound	Application Time	Mean Scaling Amount (g/m^2)	Comparison	Statistically Different Means
Linseed Oil	30 Minutes	479.5	30 Min v. 2 Hr	NO
	2 Hours	446.0	30 Min v. 4 Hr	NO
	4 Hours	344.0	2 Hr v. 4 Hr	NO
Wax	30 Minutes	301.9	30 Min v. 2 Hr	YES
	2 Hours	621.6	30 Min v. 4 Hr	NO
	4 Hours	259.8	2 Hr v. 4 Hr	YES
PAMS	30 Minutes	53.9	30 Min v. 2 Hr	NO
	2 Hours	87.5	30 Min v. 4 Hr	NO
	4 Hours	133.5	2 Hr v. 4 Hr	NO
Acrylic	30 Minutes	142.1	30 Min v. 4 Hr	YES
	4 Hours	77.0		

4.3.4.2 Mix Type 2: t-tests for Significance Differences within Scaling Damage Means of Application time

The comparisons of scaling damage results for all application times of all curing compounds on Mix Type 2 are summarized in Table 4-39. For Acrylic and PAMS, no statistically significant differences were observed between application times. Linseed Oil 30 Minute specimens were significantly different than the 2 and 4 Hour specimens, but no significant differences were found between the 2 and 4 Hour specimen sets. For Wax, statistically significant differences were observed when comparing the 30 Minute to the 2 Hours specimens, but statistically significant differences were discovered between the 30 Minute and 2 Hour specimens when independently compared to the 4 Hour specimens.

Table 4-39: t-Tests for Significance Differences between Application times for Mix Type 2 Specimens

Curing Compound	Application Time	Mean Scaling Amount (g/m^2)	Comparison	Statistically Different Means
Linseed Oil	30 Minutes	1032.1	30 Min v. 2 Hr	YES
	2 Hours	587.4	30 Min v. 4 Hr	YES
	4 Hours	586.8	2 Hr v. 4 Hr	NO
Wax	30 Minutes	546.0	30 Min v. 2 Hr	NO
	2 Hours	818.3	30 Min v. 4 Hr	YES
	4 Hours	305.2	2 Hr v. 4 Hr	YES
PAMS	30 Minutes	867.0	30 Min v. 2 Hr	NO
	2 Hours	1238.0	30 Min v. 4 Hr	NO
	4 Hours	851.2	2 Hr v. 4 Hr	NO
Acrylic	30 Minutes	617.0	30 Min v. 4 Hr	NO
	4 Hours	454.5		

4.3.4.3 Mix Type 3: t-tests for Significance Differences within Scaling Damage Means of Application time

The comparisons of scaling damage results for all application times of all curing compounds on Mix Type 3 are summarized in Table 4-40. Statistically significant differences between means of the application times were observed within the Linseed Oil, Wax, and Acrylic specimen sets, but not within the PAMS specimen sets.

Table 4-40: t-Tests for Significance Differences between Application times for Mix Type 3 Specimens

Curing Compound	Application Time	Mean Scaling Amount (g/m^2)	Comparison	Statistically Different Means
Linseed Oil	30 Minutes 4 Hours	1479.4 642.7	30 Min v. 4 Hr	YES
Wax	30 Minutes 4 Hours	847.9 394.0	30 Min v. 4 Hr	YES
PAMS	30 Minutes 4 Hours	309.2 211.2	30 Min v. 4 Hr	NO
Acrylic	30 Minutes 4 Hours	734.1 130.9	30 Min v. 4 Hr	YES

4.3.4.4 Mix Type 4: t-tests for Significance Differences within Scaling Damage Means of Application time

The comparisons of scaling damage results for all application times of all curing compounds on Mix Type 4 are summarized in Table 4-41. Statistically significant differences in the scaling means were observed between all three application times for Linseed Oil. No statistically significant differences were observed between any application time for the Wax, PAMS, and Acrylic specimen sets. It is important to note that using the two-way t-test examines statistically significant differences in the means as being either larger or smaller than one another. As a result, Type II statistical error (Nelson, 2003), where no significant difference is detected when it might actually exist can occur in

cases where one mean is distinctly larger or smaller than the other, such as the case with Acrylic. The standard deviations for the Acrylic 30 Minute and 4 Hour specimen sets were 175.4 and 8.9 g/m^2, respectively. Using these along with the means, it is evident that these means are distinctly different despite the lack of statistical significance. This implies that Type II error occurred within this test.

Table 4-41: t-Tests for Significance Differences between Application times for Mix Type 4 Specimens

Curing Compound	Application Time	Mean Scaling Amount (g/m^2)	Comparison	Statistically Different Means
Linseed Oil	30 Minutes	609.1	30 Min v. 2 Hr	YES
	2 Hours	300.6	30 Min v. 4 Hr	YES
	4 Hours	217.1	2 Hr v. 4 Hr	YES
Wax	30 Minutes	178.9	30 Min v. 2 Hr	NO
	2 Hours	317.7	30 Min v. 4 Hr	NO
	4 Hours	147.3	2 Hr v. 4 Hr	NO
PAMS	30 Minutes	599.9	30 Min v. 2 Hr	NO
	2 Hours	591.4	30 Min v. 4 Hr	NO
	4 Hours	426.9	2 Hr v. 4 Hr	NO
Acrylic	30 Minutes	386.1	30 Min v. 4 Hr	NO
	4 Hours	48.0		

4.3.4.5 Mix Type 5: t-tests for Significance Differences within Scaling Damage Means of Application time

The comparisons of scaling damage results for all application times of all curing compounds on Mix Type 5 are summarized in Table 4-42. No statistically significant differences were observed between application times for Linseed Oil, Wax, or PAMS. Acrylic was the only curing compound within Mix Type 5 where scaling damage between application time sets were statistically significant. It is important to note that Type II error appeared to occur within the Linseed Oil set, similar to the Acrylic specimens from Mix Type 4. The standard deviations for the 30 Minute, 2 Hour and 4 Hour sets for Linseed Oil are 394.1, 132.8, and 166.9 g/m^2 respectively. The standard deviation for the 30 Minute set was large enough to prevent significance differences from being established within a two-

way t-test at a 95% confidence level. Despite this, the distinct difference in scaling amounts between the 2 and 4 Hour sets versus the 30 Minute sets indicate that Type II error may have occurred.

Table 4-42: t-Tests for Significance Differences between Application times for Mix Type 5 Specimens

Curing Compound	Application Time	Mean Scaling Amount (g/m^2)	Comparison	Statistically Different Means
Linseed Oil	30 Minutes	1295.2	30 Min v. 2 Hr	NO
	2 Hours	480.2	30 Min v. 4 Hr	NO
	4 Hours	478.9	2 Hr v. 4 Hr	NO
Wax	30 Minutes	1082.1	30 Min v. 2 Hr	NO
	2 Hours	1427.4	30 Min v. 4 Hr	NO
	4 Hours	1331.4	2 Hr v. 4 Hr	NO
PAMS	30 Minutes	655.8	30 Min v. 2 Hr	NO
	2 Hours	1074.8	30 Min v. 4 Hr	NO
	4 Hours	791.3	2 Hr v. 4 Hr	NO
Acrylic	30 Minutes	808.4	30 Min v. 4 Hr	YES
	4 Hours	444.0		

4.3.4.6 Mix Type 6: t-tests for Significance Differences within Scaling Damage Means of Application time

The comparisons of scaling damage results for all application times of all curing compounds on Mix Type 6 are summarized in Table 4-43. Statistically significant differences were observed between the application times for the Linseed Oil and Acrylic specimen sets, but not in the Wax or PAMS specimen sets.

Table 4-43: t-Tests for Significance Differences between Application times for Mix Type 6 Specimens

Curing Compound	Application Time	Mean Scaling Amount (g/m^2)	Comparison	Statistically Different Means
Linseed Oil	30 Minutes 4 Hours	1461.6 726.2	30 Min v. 4 Hr	YES
Wax	30 Minutes 4 Hours	783.4 801.2	30 Min v. 4 Hr	NO
PAMS	30 Minutes 4 Hours	257.2 251.3	30 Min v. 4 Hr	NO
Acrylic	30 Minutes 4 Hours	1933.9 213.8	30 Min v. 4 Hr	YES

4.3.5 Analysis of Wet Room Specimen Data

Wet Room cured specimens from each mix type were tested to represent a theoretically ideal curing condition. Based upon a review of existing literature, it was thought that specimens cured in this manner would exhibit a baseline level of minimum scaling damage in which to compare the performance of the curing compounds relative to. To make these comparisons, the average scaling amounts from every curing compound-application time specimen set were normalized to the Wet Room scaling damage amounts for each mix type. The result of this normalization were damage factors by which a curing compound-application time specimen set scaled at relative to the Wet Room specimen set. The average and range of these damage factors across mix types for each curing compound-application time are presented in Table 4-44.

Table 4-44: Scaling Damage Factors of Curing Compounds Relative to Wet Room Specimens

Curing Compound	Application Time	Range of Factors		Average
		Min	Max	
Linseed Oil	30 Minutes	4.7	28.0	11.8
	2 Hours	2.4	26.1	9.2
	4 Hours	2.3	20.1	6.4
Wax	30 Minutes	2.5	17.7	6.8
	2 Hours	4.5	36.3	13.4
	4 Hours	1.7	15.2	5.5
PAMS	30 Minutes	0.8	10.5	4.3
	2 Hours	5.1	10.3	6.9
	4 Hours	0.8	7.8	4.5
Acrylic	30 Minutes	3.4	8.3	6.1
	4 Hours	0.7	4.5	2.0

In all specimen sets except PAMS 30 Minutes, PAMS 4 Hours, and Acrylic 4 Hours, the curing compounds at a minimum exhibited increased scaling relative to the Wet Room specimens. At a maximum, select specimen sets from Linseed Oil and Wax at all application times and PAMS at 30 Minutes and 4 Hours displayed scaling damage amounts that were at least an order of magnitude higher than the Wet Room specimens. Averaged across all mix types, the curing compound specimens exhibited scaling damage that exceeded the Wet Room specimens from a factor of 2.0 within the Acrylic 4 Hour specimens to a factor of 13.4 within the Wax 2 Hour specimens.

4.4 Discussion of Outlying Data

A review the data in Section 4.2 revealed that from the 30 non-Wet Room subsets, approximately 21 of them had scaling patterns that followed the hypothesis that scaling resistance increased with an increase in the application time based upon magnitude alone. These included all of the Linseed Oil and Acrylic coated specimen sets. The remaining nine subsets that did not immediately fit the prediction all exhibited levels of scaling in the 2 Hour or 4 Hour specimen sets that exceeded the 30 Minutes scaling amounts. All were either coated with the Wax or the PAMS compounds, with four of them being applied to concretes containing slag. At least one of the following four factors were present in these nine outlier batches:

1. The effect of the inclusion of slag cement
2. The use of the Wax-based curing compound,
3. The impact of pouring concrete specimens and applying curing compounds at a high ambient relative humidity
4. The impact of high deviation in scaling losses between samples from the 1-D and 6-D mixes.

This section discusses the potential impact that these factors may have had on the scaling patterns of the nine outlier batches. For reference, Table 4-45 summarizes each affected mix and factors that may explain their outlying scaling patterns.

Table 4-45: Mixes with Outlying Scaling Data

Affected Mixes	Potential Explanations			
	Impact of Slag	Wax Curing Compound	High Relative Humidity	1-D/6-D
1-C		X		
1-D				X
2-C	X	X		
2-D	X			
4-C		X		
5-C	X	X	X	
5-D	X			
6-C		X	X	
6-D				X

4.4.1 The Impact of Slag Cement

Affected mixes: 2-C, 2-D, 5-C, 5-D

Previous research at the University of Wisconsin-Madison and at other institutions has shown that concretes made with partial replacement of OPC with Slag Cement typically feature lower freeze-thaw scaling resistance than concretes made with plain OPC. Carbonation of hydration products within the cement paste at the concrete surface has been identified as a primary cause of this reduction in scaling resistance in slag-containing concretes. Including slag as a replacement for cement reduces the amount of calcium hydroxide (CH) during the hydration reactions shown in equations (1) and (2) from Section 2.2.This slows the growth of the hydration products in the paste, resulting in a fresh surface that bleeds for longer and increasing the time to set. Ambient carbon dioxide in the air surrounding the concrete will infiltrate the paste, and react preferentially with CH to form calcium carbonate, a product that densifies the surface over time. In slag-containing concretes that do not supply enough CH, the carbon dioxide will react with the CSH gel by combining with the calcium in the gel, to form calcium carbonate. This results in a decalcified CSH microstructure of the

paste, reducing the volume and increasing the porosity of the surface; ultimately reducing the scaling resistance of the surface layer. (Battaglia et al. 2010)

Within Battaglia's findings, it was identified that while carbonation is a primary mechanism by which slag-containing concretes experience extensive scaling, carbonation does not control scaling loss when a Wax or PAMS-type curing compound is used. Research by Wainwright and Ait-Aider confirmed that slag cement as a replacement for OPC had the dual effect of increasing the both the rate and amount of bleeding (1995), most likely as a result of the delayed growth of hydration products (Battaglia et al. 2010). The application of a curing compound immediately reduces the moisture loss of unbound water at a concrete surface (Wang et al. 1994). However, the disassociation of a curing compound membrane may occur due to the carrier emulsion possibly having a lower density than that of the bleed water it envelopes. The precise densities of the compound emulsions used in this study could not be ascertained due to their proprietary nature.

Therefore, it is hypothesized that the because the inclusion of slag increases the amount of bleeding, more unevaporated bleed water is standing on the surface than other non-slag concrete mixes when the Wax and PAMS curing compound are applied at two hours. As these compounds are applied, they mix with or float on the surface of the bleed water, preventing the membrane from fully forming to ensure proper curing and limits dicer ingress. Additionally, because moisture loss is immediately limited upon application, applying at two hours increases the (w/c) ratio of the top layer by sealing the bleed water in. This increase of the (w/c) ratio of the mortar layer along with any corresponding microstructural changes due to incomplete membrane formation could produce a less durable surface layer, resulting in higher rates of scaling within the 2 Hour specimens. By applying these curing compounds at 30 Minutes, the membrane may solidify prior to being disassociated by additional bleed water unlike the 2 Hour specimens, despite trapping further bleed water that would create a surface layer with a theoretically higher (w/c) ratio. Applying them at 4 Hours could prevent

excess water from being trapped within the surface layer. The effects of carbonation over time do increase the scaling susceptibility of a slag-containing concrete, regardless of curing compound application time. However, more research is needed to identify if significant carbonation occurs in the fresh concrete prior to curing compound application that would ultimately increase scaling susceptibility.

4.4.2 The Impact of Wax-Based Curing Compound

Affected Mixes: 1-C, 2-C, 3-C, 4-C, 5-C, 6-C

The Wax, PAMS, and Linseed Oil curing compounds used on this study were emulsions consisting of a solid portion suspended in a water carrier. Upon placement, the water carrier evaporates and deposits the solid portion, which forms the membrane. PAMS and Linseed Oil were ASTM C309 defined Type II Class B curing compounds, specifying the solids portion as organic resins with typically high molecular weights. The Wax curing compound however was defined as a Type II Class A curing compound, which doesn't specify any particular structure for the solids portion. The manufacturer specification defined the solids portion to be a wax of petroleum origin, most likely a form of paraffin wax. It was characterized by appearing to have a lower viscosity and density than the other emulsion-based curing compounds. This is most likely due to the manufacturer specifying the solids portion between 15 to 25% of the emulsion, as compared with 40 to 50% for the Linseed Oil and approximately 52.5% for the PAMS. Because all three compounds had identical spray rates; this meant that the Wax deposited less of the solid, or active component of the membrane by weight than the other two emulsions.

By visual inspection, the Wax coating appeared thinner and less dense than the other emulsions. This was especially prevalent when sprayed upon the 30 Minute and 2 Hour specimens; where the coating appeared to float on the surface of the bleed water layer and very thin but

noticeable cracks developed where bleed water appeared to disassociate the pigmentation. During ASTM C672 testing, the Wax layer stripped off in thousands of small flakes within the first 10-15 cycles for all specimens; indicative of a poorly bonded coating to the surface of the concrete. While the high amounts of scaling within the 2 Hour specimens relative to the other two application times remain beyond explanation based upon the observations of this study, the composition of the Wax emulsion may provide insight into further investigations.

4.4.3 The Impact of High Relative Humidity at the Time of Curing Compound Application

Affected Mixes: 5-C, 6-C

Relative humidity is the measure of the level of water vapor within a sample of air expressed as a percentage of the maximum amount that air could possibly hold at that temperature. The capacity of the air to hold water vapor is dependent upon the temperature, so directly comparing relative humidities is only feasible when temperatures are nearly equivalent. In this study, all specimens were cast in a controlled laboratory setting where temperatures ranged between 70-74^{o}Fahrenheit at the time of casting; so the comparisons of the relative humidities are nearly direct comparisons to the amount of water vapor within the air. When air temperature is held constant with no turbulence, the rate of evaporation decreases with an increase in the relative humidity.(Uno, 1998)

Mixes 4-E, 5-A, 5-C, 5-E, 6-A, 6-C, and 6-E were poured in times of elevated ambient relative humidities, as defined by being 60% or above measured by the laboratory hygrometer. All other mixes were poured at relative humidities between 21% and 36%. Two of these mixes, 5-C and 6-C exhibited scaling amounts after 60 cycles within their 2 and 4 Hour application time specimens that exceeded the scaling in their 30 Minute specimens. Both of these mixes used Wax curing

compound as well; with 5-C possessing slag. Mix 5-C did experience the highest amount of scaling across all three application times of all mixes save for the 30 Minute specimens from Mix 6-E, which may imply that the detrimental effects previously discussed in Sections 4.4.1 and 4.4.2 stacked, leading to reduced scaling resistance. The other mixes poured at high relative humidities did not have additional 2 Hour specimens to analyze. It is hypothesized that due to reduced evaporation rates as a result of high relative humidities, bleed water remained on the surface of these concretes when the Wax was applied at 2 and 4 Hours for mixes 5-C and 6-C. The presence of bleed water on the surface at these application times may have induced areas of disassociated membrane, leaving the surface more susceptible to improper curing and deicer ingress. Small, yet noticeable pinholes and cracks in the solid membrane were detected by eye in these specimens after demolding to support this. This potentially had the effect of reducing the Wax's ability to provide an adequate membrane, and by extension, reduced the scaling resistance of the concrete.

The very high laboratory relative humidity of 83% when Mix 6-E specimens were manufactured and coated may have reduced the evaporation of bleed water significantly, resulting in the entrapment of large amounts of bleed water when the Acrylic was applied at 30 Minutes. This entrapment of bleed water may have severely reduced the scaling resistance of these specimens, which resulted in the very high scaling damage exhibited in Figure 4-30.

4.4.4 Mix 1-D and Mix 6-D

Affected mixes: 1-D, 6-D

Both Mix 1-D and 6-D possessed scaling accumulation curves that were worthy of further analysis. Mix 1-D as shown in Figure 4-4, exhibited very low scaling and very similar scaling accumulation curves across all three application times. The behavior that warranted further review

was that the 30 Minute specimens scaled the least and the 4 Hour specimens scaled the most. Alternatively, Mix 6-D as shown in Figure 4-29, did exhibit more total scaling in the 30 Minute specimens than the 4 Hour specimens, but only after the 4 Hour specimens had sustained a higher level of scaling for the first 55 cycles.

Figure 4-31 and Figure 4-32 show the standard deviation of the samples of scaled mass collected from each application time subset of specimens for mixes 1-D and 6-D, respectively. Unlike most of the other graphs in this study, these are not cumulative charts. Sharp peaks in the standard deviation indicate that one of the specimens in the subset scaled much more than the other. For Mix 1-D, this shows that the overall scaling amount for the 4 Hour specimens were driven by the premature failure of just one specimen that occurred at the 10 cycle mark. This was followed by less variable scaling behavior for the remainder of the test. Because Mix 1-D exhibited such low scaling across all three application times, the scaling results were very susceptible to variability of one specimen.

For Mix 6-D, the high standard deviation shown by the three peaks at 5, 10, and 20 cycles for the 4 Hour specimens, in addition to the 3 peaks at 5, 50, and 55 cycles for the 30 Minute specimens, indicate times where a single specimen experienced failure. This demonstrates that even with rigorous experimental controls, the complexity of concrete composition, the curing process, and sample preparation can result in unintended variability within the scaling patterns, resulting in averages among sets that are influenced greatly by large deviations within one specimen.

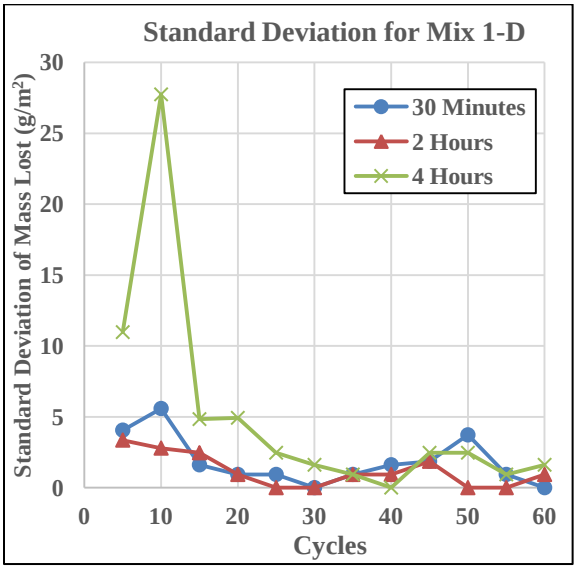

Figure 4-31: Standard Deviaton of Mass Lost per Cycle for 1-D

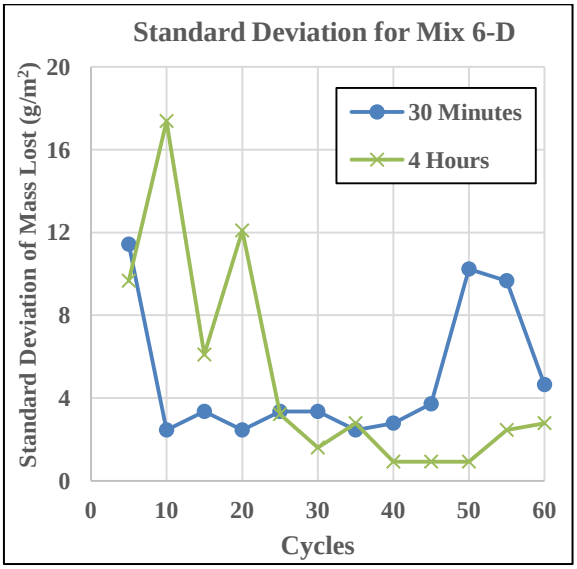

Figure 4-32: Standard Deviation of Mass Lost per Cycle for 6-D

4.5 ARCHERS Results and Discussion

The design of the ARCHERS logic was continually revised through the project to improve system response. However, it was discovered that despite attempts to recalibrate, the hygrometers whose measurements were used to drive the fan did not consistently generate the same readings when subjected to the same air conditions. When exposed to the same laboratory air, the chamber hygrometer typically read relative humidity values 0-8% higher than the outlet hygrometer. Due to time constraints, exploration of other hygrometers that might provide more consistent measurements was not pursued. Despite this, the ARCHERS was still run on concrete mixes used within this study both as a proof of concept of the technology and to gather any data that might be of some relevance.

4.5.1 ARCHERS Performance and Data Analysis

Ideal performance from the ARCHERS was predicated upon notifying an operator about the operation of the fan duty cycle graphically. Bleeding as it was thought to occur would dictate the

response of the fan speed in three distinct operational phases as shown with approximate times in Figure 4-33:

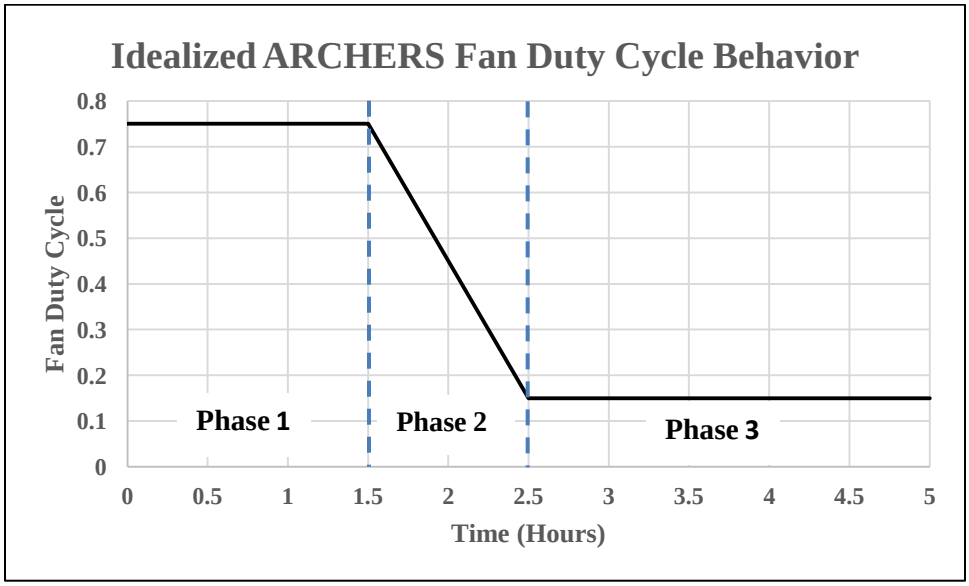

Figure 4-33: Ideal Fan Duty Cycle Performance for ARCHERS During Concrete Bleeding

Phase 1. Bleeding (0 to around 1.5 hours): Bleed water migrates to surface of concrete, and water is present on the surface. Evaporated water is continually measured by the outlet hygrometer, which sustains the FDC at or near its upper operational limit.

Phase 2. Evaporation (1.5 to 2.5 Hours): Concrete bleeding terminates. The remaining standing water evaporates, bringing the relative humidity measurements at the outlet down to inlet levels gradually. FDC responds accordingly, gradually reducing speed towards the lower limit.

Phase 3. Curing (2.5 Hours and beyond): The relative humidity levels at the inlet and outlet equalize in the absence of bleed water. FDC flat lines at the lower operational limit, which notifies the operator that bleeding has ceased and application of curing compounds can begin.

This idealized performance of the fan duty cycle from the ARCHERS was not achieved in the vast majority of concrete testing situations during development and application. Table 4-46 shows the average ARCHERS FDC at the times used for curing compound application. The range of values for the FDC was between 0 and 1. The ARCHERS updated the FDC every 5 seconds, so the FDC value for each test was generated by averaging the FDC over a 15 minute interval around the application time. The numbers reported in Table 4-46 are the averages of these FDC values over the number of tests within the same mix type.

Table 4-46: Average ARCHERS FDC Values at Curing Compound Application times

Average ARCHERS Fan Duty Cycle at Application Times				Number of Tests
Mix Type	30 Min	2 Hr	4 Hr	
1	0.40	0.15	0.15	3
2	0.24	0.15	0.15	2
3	0.18	0.15	0.15	2
4	0.48	0.45	0.19	4
5	0.54	0.51	0.51	5
6	0.15	0.15	0.15	4

While the FDC does decrease from 30 Minute to 4 Hours for most of the Mix Type tests, the magnitude and trend of the FDC was not repeatable across all mix types. The use of relative humidity to drive the FDC was highly temperature dependent and did not result in a direct comparison of the amount of water vapor in the air between the two measurement points. However, analysis of the relative humidity and temperature data from ARCHERS on several mixes did show promising results for the future operational capacity of the device.

Empirical relationships between temperature, relative humidity, and vapor pressure exist that allow for a determination of the partial pressure water vapor if volumes and absolute pressure are assumed constant. This can be used to measure the amount of water vapor in a section of air by using the August-Roche-Magnus approximation to relate saturation vapor pressure and temperature, and

convert to a partial pressure of water vapor through the definition of relative humidity (Perry & Green, 2008).

By converting the chamber and outlet relative humidity values into vapor pressures, the change in the water profile evaporating from the concrete surface over time could be quantified more directly than using the relative humidities. Table 4-47 shows the difference in the vapor pressures between the outlet and chamber hygrometers from ARCHERS, calculated in the same way as the FDC values from Table 4-46.

Table 4-47: Average Difference in Vapor Pressure between Outlet and Chamber Hygrometers from ARCHERS Results, per Mix Type at Application times

Average Calculated Difference in Vapor Pressure at Application Times (hPa)				Number of Tests
Mix Type	30 Min	2 Hr	4 Hr	
1	2.41	0.44	0.13	3
2	0.63	0.50	-0.33	2
3	0.57	0.32	-0.03	2
4	1.80	1.04	0.67	4
5	3.62	2.49	1.30	5
6	2.67	2.10	1.04	4

The results in Table 4-47 show that the differences in vapor pressure between the hygrometers was larger at the start of the test and that the difference decreases over time as the bleed water evaporates. This method offers the advantage of directly detecting the changing amount of water in the air as an indicator for the presence of bleed water on the concrete surface over time, rather than the indirect way of using the FDC. Zero or negative values of this difference indicate that no additional water has evaporated, implying that bleeding has finished and that the curing compound application can begin. Ultimately, this shows that although the ARCHERS operation based on the FDC was insufficient, by measuring the vapor pressure difference, the presence of bleed water could be evaluated. Therefore, this identifies the potential that the ARCHERS has for operational use with further modifications and updates.

4.5.2 Analysis of ARCHERS Results

ARCHERS data from two separate concrete batches was analyzed using the relative humidity-vapor pressure relationships to further demonstrate the operational potential of the ARCHERS. The shape of the FDC response curves from these batches were both poor relative to the idealized behavior, and very different from one another. In addition, the results from ARCHERS operation on Mix 5-C in Section 4.5.2.2 were chosen due to the high ambient laboratory relative humidity. ARCHERS recorded the relative humidity and temperature, and adjusted the FDC every five seconds. Due to the sporadic nature of sampling data at such a high rate, this analysis averages the data over 10 minute increments to reveal the greater trends that occurred. The purpose of analyzing these trends was to evaluate the operational capacity of the ARCHERS.

4.5.2.1 Mix 4-B

Mix 4-B was chosen for further analysis due to the shape of the FDC curve and the scaling patterns that decreased with an increase in application time. The ambient relative humidity at the time of concrete specimen manufacture for Mix 4-B was approximately 27%. This corresponded to an ambient vapor pressure of 7.2 hPa. Figure 4-34 is a plot of the Fan Duty Cycle over time for Mix 4-B, with readings registered every 5 seconds. The initial 2.5 hours of the test behaved as predicted, but the following 3.5 hours did not. The sharp peaks and valleys of the FDC curve indicate that the factors that controlled system response were poorly tuned and overly sensitive to the input readings, resulting in an FDC curve with erratic ringing performance. Instituting a longer running average than 5 seconds or more optimal PID gains would improve this performance. Figure 4-35 displays the partial pressure of water vapor in the ARB and at the outlet of the contactor relative to the ambient conditions. Perturbations of the vapor pressure within the ARB were observed in the outlet vapor pressure, indicating that the ARB's contribution to the FDC was not insignificant, and better instrument design would attempt to limit this. Figure 4-36 shows the difference in vapor pressures

between the outlet and the ARB. This provides the best estimate for the behavior of the bleed water on the surface of the concrete over time. It is evident that over time that the vapor pressure of the outlet air is increased for the first hour of the test, as a direct result of the concrete bleed water. Over time, a nearly linear decrease in the outlet vapor pressure approaches that of the chamber, an indicator that the bleeding process has ceased. Despite performance from the FDC graph that would indicate that bleeding may not have ceased due to the FDC oscillations, the vapor pressure data reveals a more accurate picture of the behavior immediately above the concrete surface.

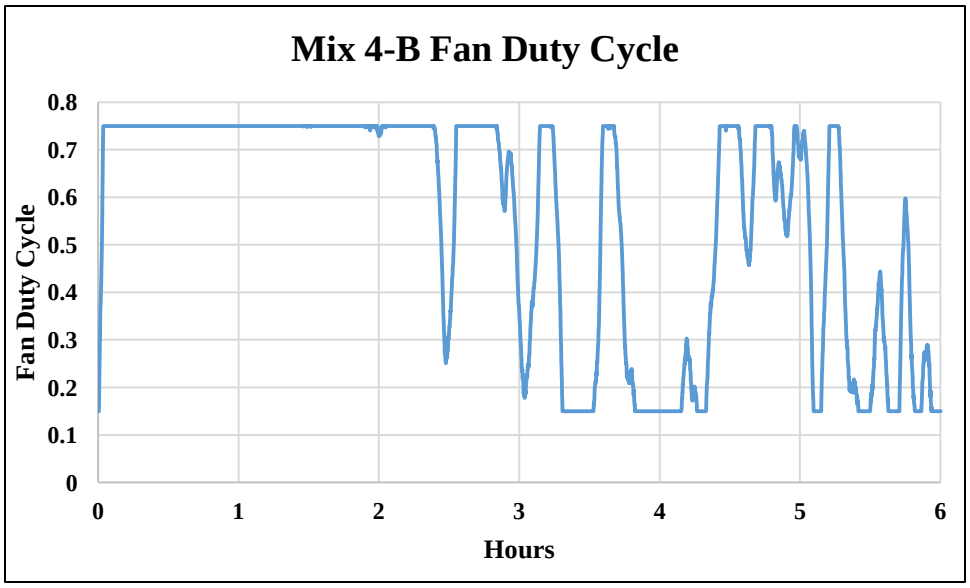

Figure 4-34: Fan Duty Cycle of ARCHERS Operation on Mix 4-B

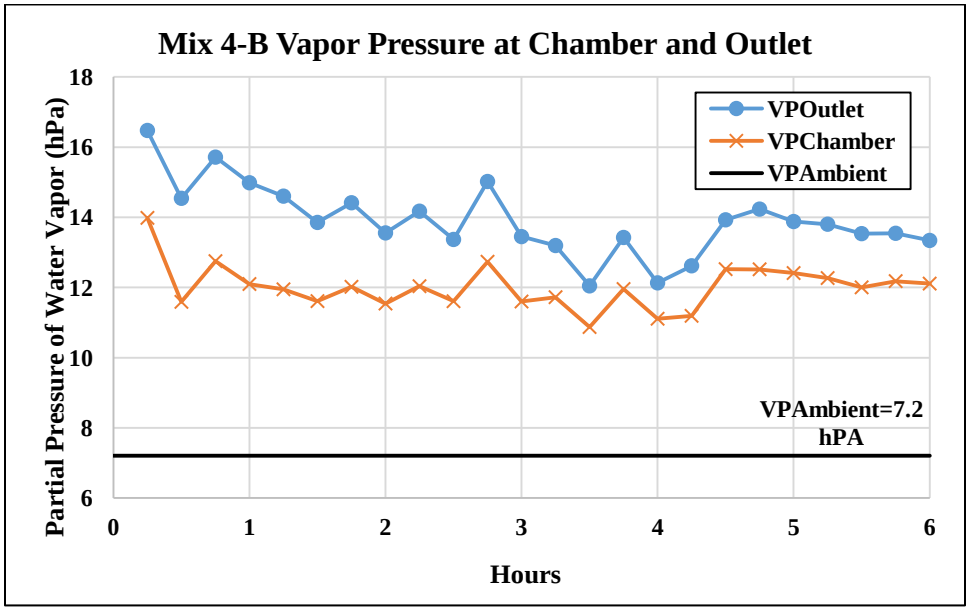

Figure 4-35: Vapor Pressure Measurements from ARCHERS on Mix 4-B

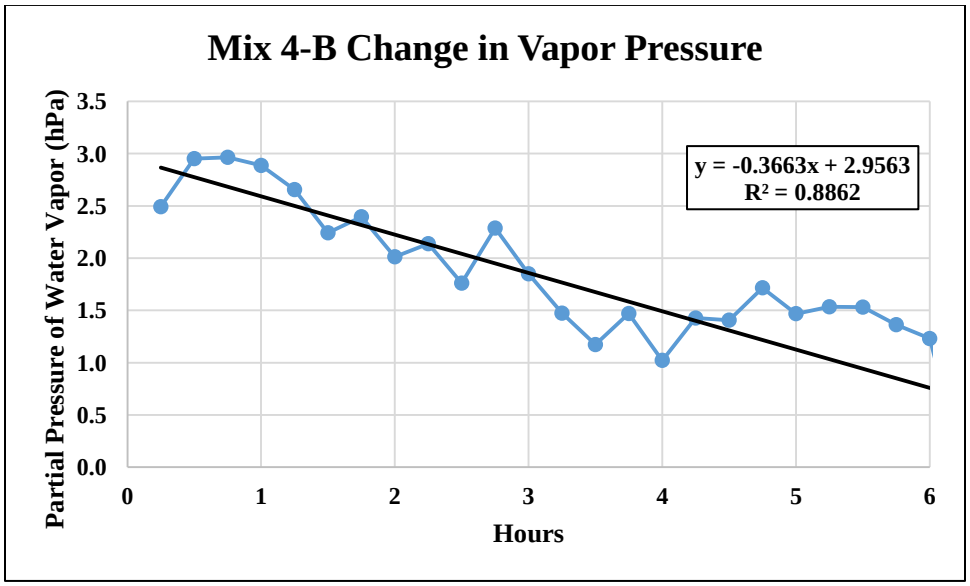

Figure 4-36: Vapor Pressure Reading Difference for Mix 4-B

4.5.2.2 Mix 5-C: High Relative Humidity Condition

ARCHERS' performance was heavily impacted by the ambient conditions during concrete placement. When ARCHERS was used on the mixes that were poured on days with high relative humidity, the FDC curve that was generated was similar to that in Figure 4-37, which indicated that bleeding had ended early due to low perceived differences in relative humidity. Mix 5-C was poured when the relative humidity in the testing laboratory was detected at 68%, as compared to Mix 4-B which was at 27% for approximately the same temperature. Figure 4-34 shows that the ambient vapor pressure at the time Mix 4-B was poured indicates a relatively low 7.2 hPa; an amount that neither the chamber nor the outlet appeared to be approaching. The opposite is true in Figure 4-38 where the ambient vapor pressure is much higher at 18.1 hPa; a level that both the chamber and the outlet appeared to approach.

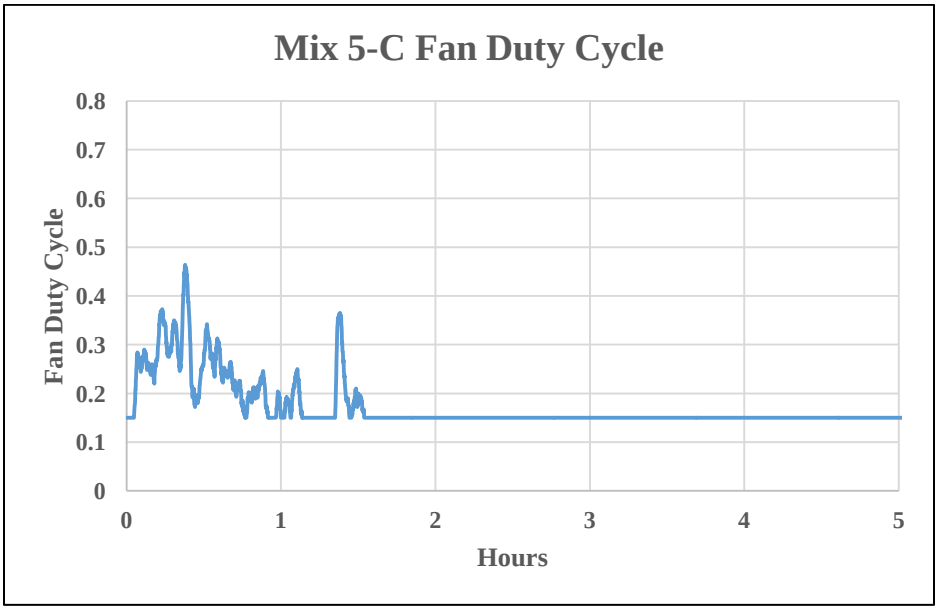

Figure 4-37: Fan Duty Cycle of ARCHERS Operation on Mix 5-C

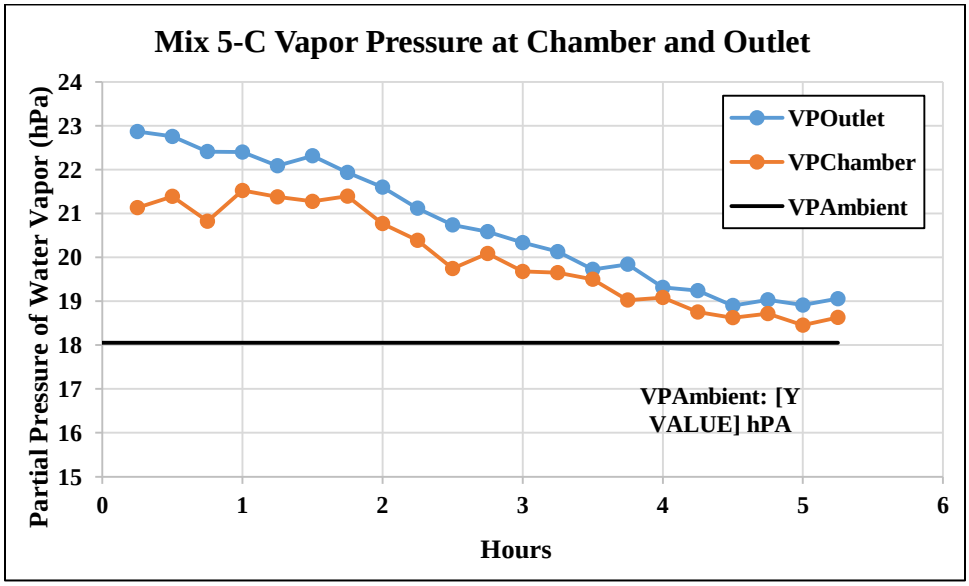

Figure 4-38: Vapor Pressure Measurements from ARCHERS on Mix 5-C

It is understood that as the amount of water vapor in a section of air increases with temperature remaining constant, evaporation rates decrease. Mix 5-C displayed heavy scaling damage across all three application times, in excess of 1000 g/m^2. While the levels of vapor pressure at the outlet versus the ambient vapor pressure do not confirm directly the presence of bleed water due to the high relative humidity of the laboratory, the results from the ARCHERS do confirm that ambient vapor pressures for this mix, and other mixes with similar ambient relative humidities, were much higher than most other mixes. This indeed may have resulted in high levels of scaling at the 2 and 4 Hour application times as a result of lower evaporation rates of bleed water.

Over time, the difference in vapor pressure between the chamber and outlet did appear to decrease. However, the ARCHERS' FDC output did not respond to this because the measured relative humidity difference was not high enough to warrant a higher fan speed. Therefore, future designs of the ARCHERS may experience better FDC response by measuring differences in vapor

pressure, a true estimate of the amount of water vapor in the air, than the indirect temperature-dependent relative humidity.

4.5.3 Recommendations for ARCHERS Improvement

It is evident that the current design of the ARCHERS is not ready for field use to indicate the presence. However, the device does demonstrate a level of potential for evaluating the psychrometric environment immediately above a concrete surface that would warrant future investment towards operational improvement. The following list of recommendations identifies several strategies to build upon the current design of the ARCHERS that could result in improved operational capability:

- Process variable and performance indicator selection: The error between the measured relative humidity difference at the outlet and chamber versus the relative humidity difference set point was the process variable used within the PID logic to control the fan speed duty cycle, which was used to indicate performance during testing. As shown, evaluating the difference in vapor pressure as the process variable and the performance indicator would provide a better assessment of the bleed water presence on the concrete surface.
- Changes to instrument calibration, sampling rate, system tuning, data smoothing, and other modifications would improve the performance of the ARCHERS.
- Additional components: The water vapor content at the outlet was partially dependent on the water vapor content within the chamber and the ambient conditions. Adding a condenser prior to treating the air in the ARB could reduce the amount of water vapor in the air to a uniform level prior to contact with the concrete surface, leading to a better assessment of the evaporative behavior of the bleed water. A longer air path for the contactor may provide a

better assessment of the overall concrete surface by accounting for areas with differential levels of bleeding.

Chapter 5 Conclusions and Recommendations

5.1 Summary of Research and Major Findings

The primary goal of this research was to evaluate the impact that the application time of membrane-forming curing compounds has on the freeze-thaw scaling damage resistance of concrete made with materials used in Wisconsin highway paving. Three application times were examined, chosen to correspond to three distinct phases of the bleeding process: at 30 Minutes to ensure the concrete was still bleeding, at 4 Hours to ensure that the bleeding had ended and that bleed water was no longer present, and 2 Hours as an intermediate time where the progress of bleeding was undetermined. Five curing conditions were evaluated: three emulsion-based curing compounds, one sealing compound, and one untreated wet room control. Two sources of coarse aggregate were used; one crushed limestone from Southeast Wisconsin and a glacial gravel from Northwestern Wisconsin. One fine aggregate source was used. Three cementitious materials were used: one ordinary Type I Portland Cement (OPC), one Grade 100 Ground Granulated Blast Furnace Slag, and one Class C Fly Ash. A total of six concrete mix types were used. The results of interest were the cumulative scaling damage amounts of each mix type-curing compound-application time combination. The effect of application time on the scaling resistance of concrete was evaluated using statistical analysis of these results.

A secondary goal of this research was to design and evaluate the operational potential of a thermohygrometer apparatus, the ARCHERS, for the purpose of monitoring the presence of bleed water upon a concrete's surface over time. The purpose of this device was to be able to reliably determine when the concrete bleeding process had terminated. The results of interest were the trends within the output fan duty cycle, the temperature and relative humidity trends over the time length of each test.

The results revealed that while application time did influence the amount of scaling damage suffered by the MFCC-coated concretes from this study, the magnitude of damage at the different application times was dependent upon the curing compound chosen. For nearly every mix type-curing compound combination, the 4 Hour specimens suffered the least amount of damage of the different application times. However, the magnitude of scaling damage suffered at an application time of 2 Hours compared to the other application times appeared to be dependent upon the curing compound type rather than a sequential time-dependent order. Results by curing compound are as follows:

The Wet Room specimens were made to represent the ideal curing condition, where high scaling resistance was expected. As predicted, the untreated Wet Room cured specimens scaled the least out of all the curing conditions. It was clear that the curing compounds were unable to replicate the level of surface durability achieved by the Wet Room cured specimens. Scaling of specimens treated with curing compounds was nearly 2 to 36 times greater than those specimens subject to Wet Room curing. The scaling patterns of the Wet Room specimen sets also were indicative of the scaling trends between both the aggregate types and the cementitious materials.

Application time had a profound effect on scaling resistance for Linseed Oil-coated concretes. After two hours, all mix types exhibited large reductions in accumulated scaling damage. However, scaling resistance between the application times of 2 and 4 Hours typically did not increase by statistically significant amounts.

Increasing the application time did not appear to have a statistically significant effect on increasing the scaling resistance of specimens coated with Wax. The highest amounts of scaling damage suffered by concretes coated with Wax were observed at 2 Hours, with only marginal differences in scaling damage between the 30 Minute and 4 Hour specimens. Very poor scaling was observed in the two Wax-coated concretes poured at high relative humidities. All specimens coated with Wax lost over 90% of the distinctive white pigmentation prior to the 30 cycle mark; oftentimes

within the first 10 cycles. This is a concern if reflective pigmentation throughout the entire lifetime of the pavement is desired.

Application time did not appear to have a statistically significant effect on increasing the scaling resistance of concrete coated with PAMS. Differences between the scaling damage between application times for PAMS specimens were not statistically significant in any instance. While PAMS typically scaled less than other formulations on concrete with OPC or fly ash, high scaling amounts across all three application times of slag concretes coated with PAMS indicate a possible incompatibility between slag and PAMS.

Concrete coated with the Acrylic sealing compound displayed excellent reductions in amount of scaling damage with an increase in the application time. When applied at 4 Hours, Acrylic offered excellent scaling resistance compared to other formulations.

Trends within the results revealed that the scaling resistance of concrete is dependent upon the materials that compose it, especially if supplementary cementitious materials such as slag or fly ash are included in the mix design. The mixes containing glacial gravel typically exhibited higher amounts of scaling damage than the mixes containing crushed limestone; most likely due to a difference in the frost resistance between heterogeneous geology of the gravel versus the more homogeneous limestone. Slag and fly ash containing mixes typically suffered a higher total amount of scaling than OPC concrete. The slag concrete results from this study were similar to the scaling performance predicted in literature, where poor scaling resistance of slag-containing concrete is most likely due to poor microstructural development within the exposed surface layer.

The results indicated that increased levels of relative humidity at the time of concrete pouring, in the absence of evaporative factors such as direct sunlight or wind, have the potential to extend the time and amount of water that remains on a fresh concrete surface. This can essentially

make the concrete surface at later application times have similar hydraulic properties as those at a 30 Minute application time, which may result in similarly decreased level of scaling resistance even at later application times.

Finally, the immediate results from the ARCHERS system did not accurately nor repeatedly identify the absences of bleed water as a sign of cessation of the bleeding process. It did however provide an excellent proof of concept for the measurement of the psychrometric behavior of the air immediately above the concrete surface as an indicator for the hydraulic behavior on the concrete surface. The operational capability of the device could be improved dramatically by directly measuring changes in vapor pressure along with modest improvements to instrument accuracy, control loop tuning, and craftsmanship improvements.

5.2 Hypothesis Verification

Based upon a review of existing literature, two hypotheses, one primary and one secondary were formulated for the purpose of this study. Each one is restated, followed by comments regarding their acceptance or rejection.

- A Portland cement concrete pavement will suffer more freeze-thaw scaling damage the sooner a curing compound is applied after concrete placement.

Upon analysis of the data from this study, this hypothesis is accepted for the use of the Linseed Oil and the Acrylic formulations. For both compounds, scaling damage was reduced by in specimens when the application time was increased beyond 30 Minutes. The differences in scaling damage at either 2 Hour or 4 Hours as compared to the 30 Minute specimens were considered statistically significant for both Linseed Oil and Acrylic, with the exceptions of Mixes 1-B, 2-E, 4-E, and 5-B. Therefore, it is within reason to accept that increasing the application time for the Linseed

Oil and Acrylic compounds increases the scaling resistance of the concrete coated with these formulations based upon the results from this study.

However, this hypothesis is rejected for use with the Wax and PAMS compounds. The Wax formulation suffered increased scaling damage within their 2 Hour application time specimens when compared to their 30 Minutes specimens; while no statistically significant differences were observed between application times for PAMS. While an initial comparison of scaling damage magnitude between the 30 Minutes and 4 Hours specimens of Wax and PAMS may suggest that damage was reduced by an increase in application time, the statistical analysis showed that the differences between these two application times were only statistically significant for Wax on Mix Types 2 and 3. Due to the lack of statistically significant differences in scaling magnitudes, it is unclear if the scaling damage was reduced by increasing the application time to 4 Hours. Therefore, is within reason to reject this hypothesis that scaling damage is reduced by increasing the application time of either the Wax or PAMS formulations based upon the results of this study.

- An instrument can be developed to reliably detect the presence of bleed water by evaluating changes in relative humidity immediately above the concrete surface over time

This hypothesis is rejected because the ARCHERS did not accurately nor repeatedly identify the presence of bleed water by using changes in relative humidity above the concrete surface over time. However, further analysis revealed that the ARCHERS did provide an excellent proof of concept for the measurement of the psychrometric behavior of the air immediately above the concrete surface, and could eventually be used as an indicator for the hydraulic behavior on the concrete surface. While the potential operational capability of a future device that does not rely on relative humidity is evident, the ARCHERS in its current design did not demonstrate the ability to detect the presence of bleed water. Therefore this hypothesis must be rejected.

5.3 Conclusions and Recommendations

Analysis of the results within this study ultimately indicated that the impact of MFCC application time on freeze-thaw scaling resistance is dependent upon the type of curing compound used. Scaling damage was reduced by increasing the application time for the Linseed Oil and Acrylic formulations. As a result of both the presence of increased scaling at 2 Hours and the lack of statistically significant differences between the 30 Minute and 4 Hours specimens within this study, increasing the application time cannot be reasonably thought to reduce the scaling damage of concretes coated with Wax or PAMS based upon the results from this study. The use of curing compounds did not establish levels of scaling resistance similar to the ideal curing method of Wet Room curing. The ARCHERS in its current form did not satisfy the operational requirements that were desired of it for this study. However, further analysis of the data collected by ARCHERS did reveal that there is operational potential for detecting the presence of bleed water on a concrete surface with further modifications.

Based upon the conclusions of this study, the following recommendations are suggested for future work in this field of study:

- Further concrete scaling evaluation projects should evaluate directly if curing compounds that are applied during the bleeding process trap bleed water within the top layer of the concrete surface, and evaluate the potential impact on scaling resistance directly, as opposed to the indirect method of application time used in this study. Results from petrographic analysis or from a moisture loss test for curing compounds may have the potential to evaluate this. There is currently a standard for evaluating the moisture loss of concretes coated with curing compounds, ASTM C156. However, this testing method

was not used in this study for two reasons: it is a test for mortar samples that do not contain coarse aggregates, and that the procedure instructs that the curing compounds must be applied once the mortar samples have finished bleeding. Further testing should evaluate the potential loss or retention of bleed water in the presence of curing compounds by following the same procedure as ASTM C156, but by applying the curing compounds to actual mix-designed concrete prior to bleeding cessation.

- Concrete scaling was evaluated in this study using the testing procedure for ASTM C672. Within the standard, there is no proper guidance within the 'Precision and Bias' section for how to properly account for variability within the scaling damage results at the single operator level or a multi-laboratory level. It is believed that this is hindering the growth of knowledge regarding concrete scaling by not establishing variability limits that researchers can reliably use to validate their results. In addition, further research should be implemented to relate C672 results to field pavement scaling damage performance.
- Mass loss limits for the amount of acceptable scaling damage within laboratory specimens that are related to field results should be established in order to provide guidance to DOTs and contractors for ensuring quality, scaling resistant concrete.
- Application rates for curing compounds are printed by their manufacturers on their product labels in terms of coverage rate per unit volume of compound, typically in 'sq ft/gallon' increments. Converting those rates into masses for this project was done by using the apparent density of the compound in emulsion form provided by the manufacturers. However, the total sprayed mass of the emulsion does not accurately describe how much of the active component that forms the membrane, the solids fraction, reaches the surface. Only a fraction of the emulsion is this solids portion. For spray rates that were similar, such as the Linseed Oil, PAMS, and Wax compounds used in this study, differing amounts of this active component remained on the surface of the concrete

after the remaining part of the emulsion had evaporated. Therefore, it should be determined whether the spray rate or the actual amount of solids that form the membrane impact the scaling resistance more.

- The potential effects of highly evaporative conditions such as direct solar radiation and high ambient relative humidity at the time of concrete placement and curing compound application on the scaling resistance of the concrete should be explored further.
- The results from this study demonstrate that concrete freeze-thaw scaling susceptibility is not only influenced by one factor such as curing compound application time, but is the result of the interaction of many factors. The analysis from this study showed that choice of curing compound, application time, coarse aggregate, cementitious materials, and environmental conditions such as high ambient relative humidity all displayed impacts on the scaling damage patterns and magnitudes. Future research on freeze-thaw scaling may be better served by experimental design that evaluates previously identified factors as probabilistic influences on concrete scaling rather than deterministic ones.

References

Abdi, H. (2007). The Bonferonni and Šidák corrections for multiple comparisons. *Encyclopedia of Measurement and Statistics*, *3*, 103–107.

Abrams, D. A. (1920). *Design of concrete mixtures*. Chicago: Structural Materials Research Laboratory, Lewis Institute. Retrieved from http://catalog.hathitrust.org/Record/006587153

ACI Comittee 308, A. C. I. (2001). *Guide to curing concrete*. Farmington Hills, Mich.: American Concrete Institute.

Afrani, I., & Rogers, C. (1994). The Effects of Different Cementing Materials and Curing on Concrete Scaling. *Cement, Concrete and Aggregates*, *16*(2), 132. doi:10.1520/CCA10291J

Battaglia, I., Muñoz, J., & Cramer, S. (2010). Proposed Behavioral Model for Deicer Scaling Resistance of Slag Cement Concrete. *Journal of Materials in Civil Engineering*, *22*(4), 361–368. doi:10.1061/(ASCE)MT.1943-5533.0000029

Bentz, D. P. (2008). A review of early-age properties of cement-based materials. *Cement and Concrete Research*, *38*(2), 196–204. doi:10.1016/j.cemconres.2007.09.005

Bouzoubaâ, N., Bilodeau, A., Fournier, B., Hooton, R. D., Gagné, R., & Jolin, M. (2008). Deicing salt scaling resistance of concrete incorporating supplementary cementing materials: laboratory and field test data. *Canadian Journal of Civil Engineering*, *35*(11), 1261–1275. doi:10.1139/L08-067

Boyd, A., & Hooton, R. (2007). Long-Term Scaling Performance of Concretes Containing Supplementary Cementing Materials. *Journal of Materials in Civil Engineering*, *19*(10), 820–825. doi:10.1061/(ASCE)0899-1561(2007)19:10(820)

Choi, S., Yeon, J. H., & Won, M. C. (2012). Improvements of curing operations for Portland cement concrete pavement. *Construction and Building Materials*, *35*(0), 597–604. doi:10.1016/j.conbuildmat.2012.04.065

Çopuroğlu, O., & Schlangen, E. (2008). Modeling of frost salt scaling. *Cement and Concrete Research*, *38*(1), 27–39. doi:10.1016/j.cemconres.2007.09.003

Dale P. Bentz and Paul E. Stutzman. (2006). Curing, Hydration, and Microstructure of Cement Paste. *Materials Journal*, *103*(5). doi:10.14359/18157

De Winter, J. C. F. (2013). Using the Student's t-test with extremely small sample sizes. *Practical Assessment, Research & Evaluation*, *18*(10), 2.

Giergiczny, Z., Glinicki, M. A., Sokołowski, M., & Zielinski, M. (2009). Air void system and frost-salt scaling of concrete containing slag-blended cement. *Construction and Building Materials*, *23*(6), 2451–2456. doi:10.1016/j.conbuildmat.2008.10.001

Jana, D. (2007). Concrete Scaling–A Critical Review. *Proceeding to the 29 Th Coference on Cement Microscopy Quebec City, Canada*, 91–130.

Josserand, L. (2004). A method for concrete bleeding measurement. *Materials and Structures*, *37*(274), 666–670. doi:10.1617/14052

Josserand, L., Coussy, O., & de Larrard, F. (2006). Bleeding of concrete as an ageing consolidation process. *Cement and Concrete Research*, *36*(9), 1603–1608. doi:10.1016/j.cemconres.2004.10.006

Kropp, R., Cramer, S. M., & Anderson, M. (2012). *Laboratory Study of High Performance Curing Compounds for Concrete Pavements–Phase I*. Retrieved from http://trid.trb.org/view.aspx?id=1239131

Mamlouk, M. S. (2006). *Materials for civil and construction engineers* (2nd ed.). Upper Saddle River, N.J: Pearson Prentice Hall.

Nassif, H., Suksawang, N., & Mohammed, M. (2003). Effect of Curing Methods on Early-Age and Drying Shrinkage of High-Performance Concrete. *Transportation Research Record: Journal of the Transportation Research Board*, *1834*(-1), 48–58. doi:10.3141/1834-07

Nelson, P. R. (2003). *Introductory statistics for engineering experimentation*. Amsterdam□; Boston: Academic Press.

Ollivier, J. P., Maso, J. C., & Bourdette, B. (1995). Interfacial transition zone in concrete. *Advanced Cement Based Materials*, *2*(1), 30–38.

Perry, R. H., & Green, D. W. (Eds.). (2008). *Perry's chemical engineers' handbook* (8th ed.). New York: McGraw-Hill.

Radocea, A. (1992). A new method for studying bleeding of cement paste. *Cement and Concrete Research*, *22*(5), 855–868. doi:10.1016/0008-8846(92)90110-H

Snyder, K. A., & Bentz, D. P. (2004). Suspended hydration and loss of freezable water in cement pastes exposed to 90% relative humidity. *Cement and Concrete Research*, *34*(11), 2045–2056. doi:10.1016/j.cemconres.2004.03.007

Song, H.-W., & Kwon, S.-J. (2007). Permeability characteristics of carbonated concrete considering capillary pore structure. *Cement and Concrete Research*, *37*(6), 909–915. doi:10.1016/j.cemconres.2007.03.011

State of Wisconsin Department of Transportation. (2013). Standard Specifications for Highway and Structure Construction. Online: http://roadwaystandards.dot.wi.gov/standards/stndspec/

Sun, Z., & Scherer, G. W. (2010). Effect of air voids on salt scaling and internal freezing. *Cement and Concrete Research*, *40*(2), 260–270. doi:10.1016/j.cemconres.2009.09.027

Taylor, H. F. W. (1997). *Cement chemistry* (2nd ed.). London: T. Telford.

Taylor, P. C., Morrison, W., & Jennings, V. A. (2004). The Effect of Finishing Practices on Performance of Concrete Containing Slag and Fly Ash as Measured by ASTM C 672 Resistance to Deicer Scaling Tests. *Cement, Concrete, and Aggregates*, *26*(2), 155–159.

Topçu, İ. B., & Elgün, V. B. (2004). Influence of concrete properties on bleeding and evaporation. *Cement and Concrete Research*, *34*(2), 275–281. doi:10.1016/j.cemconres.2003.07.004

Uno, P. J. (1998). Plastic shrinkage cracking and evaporation formulae. *ACI Materials Journal*, *95*(4). Retrieved from http://www.concrete.org/Publications/InternationalConcreteAbstractsPortal.aspx?m=details&i=379

Valenza II, J. J., & Scherer, G. W. (2007a). A review of salt scaling: II. Mechanisms. *Cement and Concrete Research*, *37*(7), 1022–1034. doi:10.1016/j.cemconres.2007.03.003

Valenza II, J. J., & Scherer, G. W. (2007b). A review of salt scaling: I. Phenomenology. *Cement and Concrete Research*, *37*(7), 1007–1021. doi:10.1016/j.cemconres.2007.03.005

Valenza, J. J., & Scherer, G. W. (2006). Mechanism for Salt Scaling. *Journal of the American Ceramic Society*, *89*(4), 1161–1179. doi:10.1111/j.1551-2916.2006.00913.x

Vandenbossche, J. M. (1999). A Review of the Curing Compounds and Application Techniques Used by the Minnesota Department of Transportation for Concrete Pavements. Retrieved from http://trid.trb.org/view.aspx?id=697944

Verbeck, G. J., & Klieger, P. (1957). Studies of "Salt" Scaling of Concrete. *Highway Research Board Bulletin*, (150). Retrieved from http://trid.trb.org/view.aspx?id=101892

Wainwright, P. J., & Rey, N. (2000). The influence of ground granulated blastfurnace slag (GGBS) additions and time delay on the bleeding of concrete. *Cement and Concrete Composites*, *22*(4), 253–257. doi:10.1016/S0958-9465(00)00024-X

Wang, J., Dhir, R. K., & Levitt, M. (1994). Membrane curing of concrete: Moisture loss. *Cement and Concrete Research*, *24*(8), 1463–1474. doi:10.1016/0008-8846(94)90160-0

Winslow, D., & Liu, D. (1990). The pore structure of paste in concrete. *Cement and Concrete Research*, *20*(2), 227–235. doi:10.1016/0008-8846(90)90075-9

Wu, Z., Shi, C., Gao, P., Wang, D., & Cao, Z. (2014). Effects of Deicing Salts on the Scaling Resistance of Concrete. *Journal of Materials in Civil Engineering*, 04014160. doi:10.1061/(ASCE)MT.1943-5533.0001106

Ye, D., Shon, C., Mukhopadhyay, A., & Zollinger, D. (2010). New Performance-Based Approach to Ensure Quality Curing during Construction. *Journal of Materials in Civil Engineering*, *22*(7), 687–695. doi:10.1061/(ASCE)MT.1943-5533.0000068

Standards

ASTM C39 (2012). *Standard Test Method for Compressive Strength of Cylindrical Concrete Specimens.*

ASTM C117 (2013). *Standard Test Method for Materials Finer than 75-μm (No. 200) Sieve in Mineral Aggregates by Washing.*

ASTM C127 (2012). *Standard Test Method for Density, Relative Density (Specific Gravity), and Absorption of Coarse Aggregate.*

ASTM C128 (2012). *Standard Test Method for Density, Relative Density (Specific Gravity), and Absorption of Fine Aggregate.*

ASTM C136 (2006). *Standard Test Method for Sieve Analysis of Fine and Coarse Aggregates.*

ASTM C143 (2012). *Standard Test Method for Slump of Hydraulic-Cement Concrete.*

ASTM C156 (2011). *Standard Test Method for Water Loss [from a Mortar Specimen] Through Liquid Membrane-Forming Curing Compounds for Concrete.*

ASTM C192 (2013). *Standard Practice for Making and Curing Concrete Test Specimens in the Laboratory.*

ASTM C231 (2010). *Standard Test Method for Air Content of Freshly Mixed Concrete by the Pressure Method.*

ASTM C232 (2013). *Standard Test Method for Bleeding of Concrete.*

ASTM C309 (2011). *Standard Specification for Liquid Membrane-Forming Compounds for Curing Concrete.*

ASTM C617 (2012). *Standard Practice for Capping Cylindrical Concrete Specimens.*

ASTM C672 (2012). *Standard Test Method for Scaling Resistance of Concrete Surfaces Exposed to Deicing Chemicals.*

ASTM C1315 (2011). *Standard Specification for Liquid Membrane-Forming Compounds Having Special Properties for Curing and Sealing Concrete.*

Appendix A Specimen Matrix

Table A-1: Specimen Manufacture Mix Matrix

Materials			MFCC Application Times and Specimen Group Labels			Number of Samples
Mix/Compound Label	**Components**	**Curing Compound**	**30 Minutes (α)**	**2 Hours (β)**	**4 Hours (ø)**	
1-A	Limestone/OPC	Wet Room	1-A-α	-	-	3
1-B		Linseed	1-B-α	1-B-β	1-B-φ	9
1-C		Wax	1-C-α	1-C-β	1-C-φ	9
1-D		PAMS	1-D-α	1-D-β	1-D-φ	9
1-E		Acrylic	1-E-α	-	1-E-φ	6
2-A	Limestone/Slag	Wet Room	2-A-α	-	-	3
2-B		Linseed	2-B-α	2-B-β	2-B-φ	9
2-C		Wax	2-C-α	2-C-β	2-C-φ	9
2-D		PAMS	2-D-α	2-D-β	2-D-φ	9
2-E		Acrylic	2-E-α	-	2-E-φ	6
3-A	Limestone/Fly Ash	Wet Room	3-A-α	-	-	3
3-B		Linseed	3-B-α	-	3-B-φ	6
3-C		Wax	3-C-α	-	3-C-φ	6
3-D		PAMS	3-D-α	-	3-D-φ	6
3-E		Acrylic	3-E-α	-	3-E-φ	6
4-A	Gravel/OPC	Wet Room	4-A-α	-	-	3
4-B		Linseed	4-B-α	4-B-β	4-B-φ	9
4-C		Wax	4-C-α	4-C-β	4-C-φ	9
4-D		PAMS	4-D-α	4-D-β	4-D-φ	9
4-E		Acrylic	4-E-α	-	4-E-φ	6
5-A	Gravel/Slag	Wet Room	5-A-α	-	-	3
5-B		Linseed	5-B-α	5-B-β	5-B-φ	9
5-C		Wax	5-C-α	5-C-β	5-C-φ	9
5-D		PAMS	5-D-α	5-D-β	5-D-φ	9
5-E		Acrylic	5-E-α	-	5-E-φ	6
6-A	Gravel/Fly Ash	Wet Room	6-A-α	-	-	3
6-B		Linseed	6-B-α	-	6-B-φ	6
6-C		Wax	6-C-α	-	6-C-φ	6
6-D		PAMS	6-D-α	-	6-D-φ	6
6-E		Acrylic	6-E-α	-	6-E-φ	6

Appendix B Fresh Concrete Mix Data

Table B-1: Properties of Fresh Concrete Mixes

Mix ID	w/c Ratio	Batch Size (ft^3)	AEA (mL)	WRA (mL)	Slump (in)	Unit Weight (lb/ft^3)	Air Content (%)	Ambeint Relative Humidity (%)	ASTM C672 Specimens Made	Compresssive Strength (Psi)
1-A	0.40	2.7	9	200	1.25	145.4	6.5%	27%	9	6370
1-B	0.40	2.7	12	160	1.25	145.6	6.4%	21%	9	6583
1-C	0.40	2.7	8	200	1	146.2	6.0%	25%	9	6420
1-D	0.40	2.7	12	160	1.25	144.6	6.9%	21%	9	5427
1-E	Made in Same Batch as 1-A									
2-A	0.40	2.7	14	175	1	147.0	5.4%	24%	9	6487
2-B	0.40	2.7	15	175	1.5	143.8	6.9%	23%	9	6653
2-C	0.40	2.7	14	175	1.75	143.0	7.1%	31%	9	5373
2-D	0.40	2.7	13	175	1.25	146.7	6.1%	31%	9	5927
2-E	Made in Same Batch as 2-A									
3-A	0.40	2.7	7	75	2.5	145.8	6.4%	32%	9	5630
3-B	0.40	2.0	6	50	2	147.7	5.4%	29%	6	6017
3-C	Made in Same Batch as 3-A									
3-D	0.40	2.0	6	60	2.5	144.0	6.7%	27%	6	5333
3-E	0.40	2.0	6	60	3	146.6	6.1%	36%	6	6273
4-A	0.40	2.7	18	140	1.25	144.6	6.1%	35%	3	5287
4-B	0.41	2.7	12	175	2	140.9	5.8%	27%	9	5517
4-C	0.41	2.7	12	200	2.25	142.2	7.5%	25%	9	5353
4-D	0.41	2.7	12	175	1	142.6	6.4%	28%	9	5583
4-E	0.40	2.7	18	140	1.375	144.7	6.2%	76%	9	5000
5-A	0.40	2.7	15	175	1	144.2	6.3%	64%	3	5923
5-B	0.40	2.7	13	175	1	145.0	5.2%	33%	9	6223
5-C	0.40	2.7	15	160	1.25	145.0	6.0%	68%	9	6103
5-D	0.40	2.7	14	200	2	145.0	6.4%	26%	9	6317
5-E	0.40	2.7	13	160	1.5	145.2	5.3%	75%	6	6080
6-A	0.40	2.7	8	80	2.75	144.7	6.4%	83%	9	5603
6-B	0.40	2.0	6	55	2.5	145.4	5.6%	31%	6	6363
6-C	0.40	2.0	8	70	2.25	144.9	5.8%	65%	6	5700
6-D	0.40	2.0	6	65	3	145.4	5.9%	30%	6	5603
6-E	Made in Same Batch as 6-A									

Appendix C ASTM C672 Scaling Mass Loss Data

Table C-1: Scaling Mass Loss Data for Mix Type 1 Specimens

Mix Type 1-Scaling Damage Accumulation per Cycle (g/m^2)													
Compound	**Application Time**	**Label**	**Cycles**										
			5	**10**	**15**	**20**	**25**	**30**	**35**	**40**	**45**	**50**	**55**	**60**
Wet Room	----	1-A	0.0	0.7	2.0	2.0	2.0	2.0	2.0	2.0	2.0	2.6	10.5	17.1
Linseed Oil	30 Minutes	1-B-α	5.9	13.2	19.1	30.3	52.0	149.3	225.0	284.8	363.8	412.4	449.3	479.5
	2 Hours	1-B-β	11.2	18.4	32.9	47.4	87.5	135.5	207.2	282.2	332.2	371.7	408.5	446.0
	4 Hours	1-B-φ	11.2	13.2	14.5	15.1	18.4	30.3	56.6	105.9	173.0	251.9	301.9	344.0
Wax	30 Minutes	1-C-α	26.3	39.5	44.7	48.0	51.3	53.9	55.3	57.2	59.2	112.5	246.0	301.9
	2 Hours	1-C-β	19.7	52.0	58.5	69.7	88.1	105.2	120.4	129.6	145.4	259.2	491.4	621.6
	4 Hours	1-C-φ	3.3	22.4	34.9	44.1	51.3	56.6	60.5	63.8	65.1	88.8	173.7	259.8
PAMS	30 Minutes	1-D-α	17.1	30.9	36.8	41.4	44.1	46.0	47.4	49.3	50.7	53.3	53.9	53.9
	2 Hours	1-D-β	34.2	63.8	74.3	79.6	81.6	83.5	84.9	85.5	86.8	86.8	86.8	87.5
	4 Hours	1-D-φ	36.8	90.8	106.6	115.1	119.7	121.7	123.0	125.0	127.6	130.2	131.6	133.5
Acrylic	30 Minutes	1-E-α	68.4	73.7	80.3	87.5	93.4	100.6	108.5	115.1	121.0	129.6	136.2	142.1
	4 Hours	1-E-φ	16.4	29.6	34.9	41.4	44.7	48.0	52.6	56.6	63.1	69.1	73.7	77.0

Table C-2: Scaling Mass Loss Data for Mix Type 2 Specimens

Mix Type 2-Scaling Damage Accumulation per Cycle (g/m^2)													
Compound	**Application Time**	**Label**	**Cycles**										
			5	**10**	**15**	**20**	**25**	**30**	**35**	**40**	**45**	**50**	**55**	**60**
Wet Room	----	2-A	24.3	61.2	89.5	101.3	110.5	121.0	128.3	136.8	153.9	162.5	171.0	180.9
Linseed Oil	30 Minutes	2-B-α	9.2	63.1	121.7	248.0	330.9	440.7	561.8	722.3	832.1	913.7	975.5	1032.1
	2 Hours	2-B-β	3.9	13.8	26.3	52.0	82.2	128.9	190.8	314.4	408.5	482.2	540.1	587.4
	4 Hours	2-B-φ	5.3	15.8	25.7	46.7	67.8	104.6	209.2	357.2	445.3	501.2	549.3	586.8
Wax	30 Minutes	2-C-α	274.3	308.5	336.1	346.0	352.6	363.1	376.3	392.0	415.1	450.6	499.9	546.0
	2 Hours	2-C-β	297.3	342.7	367.1	379.6	392.7	416.4	465.1	517.0	581.5	658.5	744.0	818.3
	4 Hours	2-C-φ	121.7	151.3	158.5	164.5	168.4	178.3	188.8	201.3	219.0	245.4	275.0	305.2
PAMS	30 Minutes	2-D-α	487.4	641.4	687.4	717.7	727.5	740.0	754.5	774.9	793.3	820.3	842.0	867.0
	2 Hours	2-D-β	720.9	970.9	1014.3	1036.7	1049.2	1063.0	1091.3	1122.9	1158.4	1188.0	1218.2	1238.0
	4 Hours	2-D-φ	508.5	691.3	751.2	771.6	784.8	790.0	794.6	803.2	813.7	824.2	836.7	851.2
Acrylic	30 Minutes	2-E-α	127.0	371.7	451.3	478.2	507.2	528.9	542.0	554.5	567.7	584.1	597.9	617.0
	4 Hours	2-E-φ	67.1	235.5	287.5	303.2	330.9	352.6	367.7	382.8	397.3	413.1	431.5	454.5

Table C-3: Scaling Mass Loss Data for Mix Type 3 Specimens

Mix Type 3-Scaling Damage Accumulation per Cycle (g/m^2)													
Compound	**Application Time**	**Label**	Cycles										
			5	**10**	**15**	**20**	**25**	**30**	**35**	**40**	**45**	**50**	**55**	**60**
Wet Room	----	3-A	5.3	30.3	65.8	75.6	80.3	81.6	84.2	86.8	86.8	88.1	88.1	94.7
Linseed Oil	30 Minutes	3-B-α	28.3	695.3	1003.8	1082.1	1116.9	1151.2	1195.2	1241.3	1294.6	1355.7	1418.2	1479.4
	4 Hours	3-B-φ	4.6	15.8	46.0	108.5	180.9	268.4	338.1	398.0	462.4	534.1	599.9	642.7
Wax	30 Minutes	3-C-α	76.3	119.7	134.8	150.0	183.5	225.6	283.5	371.0	452.6	607.2	718.3	847.9
	4 Hours	3-C-φ	55.3	118.4	128.9	138.1	148.0	157.9	167.7	197.3	236.2	296.0	338.1	394.0
PAMS	30 Minutes	3-D-α	43.4	67.1	81.6	93.4	104.6	120.4	137.5	160.5	189.4	232.9	271.7	309.2
	4 Hours	3-D-φ	69.1	88.1	95.4	102.6	109.2	113.8	122.4	128.3	141.4	169.7	195.4	211.2
Acrylic	30 Minutes	3-E-α	151.3	547.9	609.1	634.1	652.5	671.0	682.8	697.9	715.7	727.5	730.2	734.1
	4 Hours	3-E-φ	41.4	85.5	93.4	102.0	105.9	109.9	113.1	119.1	127.6	130.2	130.9	130.9

Table C-4: Scaling Mass Loss Data for Mix Type 4 Specimens

Mix Type 4-Scaling Damage Accumulation per Cycle (g/m^2)													
Compound	**Application Time**	**Label**	**Cycles**										
			5	**10**	**15**	**20**	**25**	**30**	**35**	**40**	**45**	**50**	**55**	**60**
Wet Room	----	4-A	3.9	8.6	15.1	23.0	30.3	37.5	41.4	44.7	48.0	51.3	53.9	57.2
Linseed Oil	30 Minutes	4-B-α	8.6	22.4	76.3	251.9	332.2	381.5	421.7	461.8	498.6	527.6	563.7	609.1
	2 Hours	4-B-β	1.3	5.3	10.5	25.7	42.1	69.7	106.6	148.0	196.7	228.3	259.2	300.6
	4 Hours	4-B-φ	2.0	3.9	5.3	9.9	13.8	23.7	34.9	53.3	88.1	129.6	169.1	217.1
Wax	30 Minutes	4-C-α	46.0	102.6	118.4	122.4	127.0	139.5	153.3	159.2	168.4	171.0	176.9	178.9
	2 Hours	4-C-β	93.4	196.7	230.9	244.7	251.9	260.5	269.7	283.5	293.4	300.0	306.5	317.7
	4 Hours	4-C-φ	11.2	32.9	56.6	68.4	81.6	91.4	103.3	114.5	126.3	134.8	140.1	147.3
PAMS	30 Minutes	4-D-α	197.3	406.5	460.5	485.5	509.8	531.5	543.3	560.4	570.3	580.8	591.4	599.9
	2 Hours	4-D-β	118.4	290.7	348.0	370.3	409.2	444.0	465.7	503.2	525.6	547.9	569.0	591.4
	4 Hours	4-D-φ	32.9	118.4	155.2	175.0	203.3	246.7	281.5	330.9	355.9	382.2	409.8	426.9
Acrylic	30 Minutes	4-E-α	128.9	203.9	225.0	241.4	262.5	277.6	286.8	298.0	322.3	338.1	372.3	386.1
	4 Hours	4-E-φ	7.9	17.8	23.0	27.6	32.9	35.5	37.5	39.5	42.8	44.1	46.0	48.0

Table C-5: Scaling Mass Loss Data for Mix Type 5 Specimens

Mix Type 5-Scaling Damage Accumulation per Cycle (g/m^2)													
Compound	**Application Time**	**Label**	**Cycles**										
			5	**10**	**15**	**20**	**25**	**30**	**35**	**40**	**45**	**50**	**55**	**60**
Wet Room	----	5-A	19.1	44.1	57.9	66.4	77.0	90.1	97.4	111.2	125.0	140.8	173.7	202.6
Linseed Oil	30 Minutes	5-B-α	155.9	322.3	493.4	720.3	925.5	1001.8	1099.8	1162.3	1197.9	1234.7	1255.1	1295.2
	2 Hours	5-B-β	98.0	128.9	160.5	194.1	243.4	276.9	317.1	358.5	381.5	409.2	442.7	480.2
	4 Hours	5-B-φ	6.6	14.5	26.3	59.9	111.2	168.4	234.8	279.6	314.4	355.9	415.7	478.9
Wax	30 Minutes	5-C-α	436.8	755.2	814.4	845.9	865.0	881.5	900.5	910.4	922.9	959.1	1007.8	1082.1
	2 Hours	5-C-β	668.3	928.2	991.3	1030.1	1059.7	1078.8	1105.1	1132.1	1150.5	1203.1	1285.3	1427.4
	4 Hours	5-C-φ	483.5	814.4	915.0	949.2	987.4	1003.8	1035.4	1070.2	1092.6	1161.0	1262.3	1331.4
PAMS	30 Minutes	5-D-α	150.6	403.2	502.6	536.8	561.1	578.9	597.9	612.4	622.3	630.2	646.0	655.8
	2 Hours	5-D-β	238.1	756.5	878.2	919.6	940.7	959.1	974.9	991.3	1003.8	1020.2	1054.5	1074.8
	4 Hours	5-D-φ	194.1	565.1	646.6	668.3	680.2	691.3	709.1	720.3	732.1	745.3	770.9	791.3
Acrylic	30 Minutes	5-E-α	172.3	416.4	465.7	500.6	524.3	536.1	563.7	605.8	642.7	663.7	713.7	808.4
	4 Hours	5-E-φ	110.5	276.9	323.0	353.2	372.3	380.9	393.4	405.2	413.1	427.6	436.1	444.0

Table C-6: Scaling Mass Loss Data for Mix Type 6 Specimens

Mix Type 6-Scaling Damage Accumulation per Cycle (g/m^2)													
Compound	**Application Time**	**Label**	**Cycles**										
			5	**10**	**15**	**20**	**25**	**30**	**35**	**40**	**45**	**50**	**55**	**60**
Wet Room	----	6-A	5.3	42.1	67.1	83.5	109.9	125.6	134.8	150.6	180.9	213.8	280.9	312.5
Linseed Oil	30 Minutes	6-B-α	13.2	291.4	531.5	622.9	761.7	854.5	949.2	1014.3	1112.3	1208.4	1345.2	1461.6
	4 Hours	6-B-φ	1.3	2.6	25.0	33.5	111.2	176.3	234.2	313.1	490.7	576.9	672.3	726.2
Wax	30 Minutes	6-C-α	50.0	229.6	291.4	314.4	350.0	380.2	391.4	402.6	422.3	465.7	560.4	783.4
	4 Hours	6-C-φ	37.5	298.0	353.2	380.2	449.9	506.5	517.0	532.2	544.0	567.7	609.8	801.2
PAMS	30 Minutes	6-D-α	38.8	77.6	94.1	128.9	148.0	164.5	177.6	183.5	190.8	217.1	236.8	257.2
	4 Hours	6-D-φ	49.3	137.5	159.8	201.9	221.7	229.6	235.5	236.8	238.1	244.7	247.3	251.3
Acrylic	30 Minutes	6-E-α	39.5	1015.6	1234.0	1321.5	1416.9	1582.0	1629.4	1693.2	1776.7	1788.6	1905.6	1933.9
	4 Hours	6-E-φ	13.2	63.1	94.1	119.7	153.9	173.0	178.3	184.8	196.0	200.6	209.2	213.8

Appendix D Mix Designs

Table D-1: Mix Type 1 Designs

Mix Type 1-Limestone/OPC					
Mix	**Volume (ft^3)**	**Cement (lbs)**	**Fine Aggregate (lbs)**	**Coarse Aggregate (lbs)**	**Water (lbs)**
Butter	0.66	13.81	31.22	46.83	6.29
Batch 1: 9 Specimens	2.70	56.50	127.71	191.56	25.73

Table D-2: Mix Type 2 Designs

Mix Type 2-Limestone/Slag						
Mix	**Volume (ft^3)**	**Cement (lbs)**	**Slag Cement (lbs)**	**Fine Aggregate (lbs)**	**Coarse Aggregate (lbs)**	**Water (lbs)**
Butter	0.66	9.66	4.16	31.02	46.53	6.28
Batch 1: 9 Specimens	2.70	39.50	17.00	126.89	190.33	25.71

Table D-3: Mix Type 3 Designs

Mix Type 3-Limestone/Fly Ash						
Mix	**Volume (ft^3)**	**Cement (lbs)**	**Fly Ash (lbs)**	**Fine Aggregate (lbs)**	**Coarse Aggregate (lbs)**	**Water (lbs)**
Butter	0.66	9.66	4.16	31.02	46.23	6.28
Batch 1: 6 Specimens	2.00	29.26	12.59	93.38	140.08	19.03
Batch 2: 9 Specimens	2.7	39.5	17	126.07	189.1	25.69

Table D-4: Mix Type 4 Designs

Mix Type 4-Gravel/OPC					
Mix	**Volume (ft^3)**	**Cement (lbs)**	**Fine Aggregate (lbs)**	**Coarse Aggregate (lbs)**	**Water (lbs)**
Butter	0.66	13.81	30.85	46.27	6.02
Batch 1: 9 Specimens	2.70	56.50	126.19	189.28	24.62
Batch 1 with 0.41 w/c	2.7	56.50	126.19	189.28	25.44

Table D-5: Mix Type 5 Designs

Mix Type 5-Gravel/Slag						
Mix	**Volume (ft^3)**	**Cement (lbs)**	**Slag Cement (lbs)**	**Fine Aggregate (lbs)**	**Coarse Aggregate (lbs)**	**Water (lbs)**
Butter	0.66	9.66	4.16	30.65	45.97	6.01
Batch 1: 9 Specimens	2.70	39.50	17.00	125.38	188.07	24.60

Table D-6: Mix Type 6 Designs

Mix Type 6-Gravel/Fly Ash						
Mix	**Volume (ft^3)**	**Cement (lbs)**	**Fly Ash (lbs)**	**Fine Aggregate (lbs)**	**Coarse Aggregate (lbs)**	**Water (lbs)**
Butter	0.66	9.66	4.16	30.45	45.68	6.01
Batch 1: 6 Specimens	2.00	29.26	12.59	92.27	138.41	18.22
Batch 2: 9 Specimens	2.7	39.5	17	124.57	186.85	24.59

Appendix E Normality Assumption Derivation by Residuals

Normality can be assumed within samples of a larger population if the residuals of sample means are determined to be approximately normally distributed. A residual is the difference between a collected data point and the sample mean. The collected data points were the scaled damage amounts from individual ASTM C672 specimens, and the sample means were the average mass loss amounts after 60 cycles for a mix type-curing compound-application time set. These sample means were the average of three replicate specimens, so each sample mean had three residuals. A total of 198 residuals were calculated, corresponding to the 198 specimens within this study.

Figure E-1 is the histogram of the frequencies of the residuals using a bin size of approximately 5 g/m^2. The plot of the normal distribution scaled to the frequency data is superimposed upon the histogram. Because the residual frequency data appears to fit normal distribution, it is safe to assume that the data used to calculate the samples mean are normally distributed.

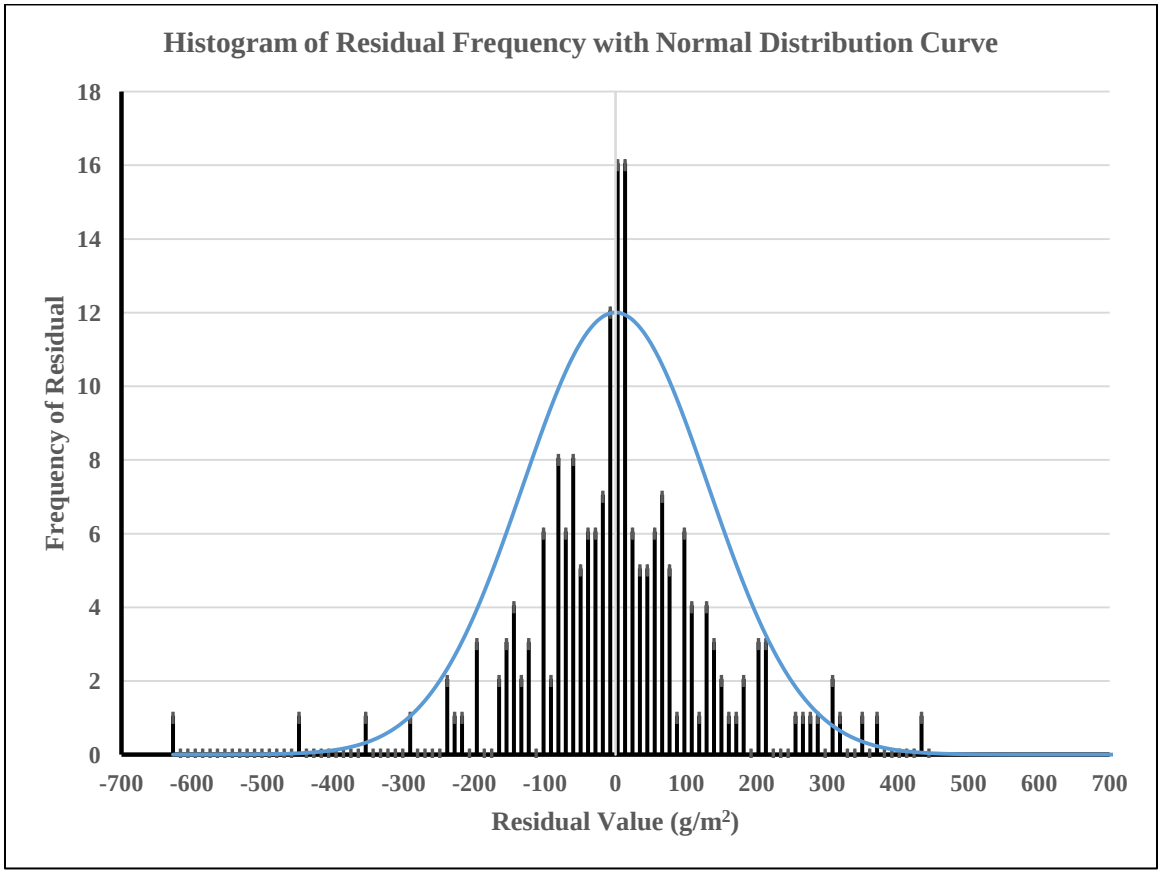

Figure E-1: Histogram of Residual Frequency with Superimposed Normal Distribution